TR-206

PERFORMANCE ANALYSIS OF SIGNAL PROCESSING AND TRACKING SYSTEMS FOR AIRBORNE ACOUSTIC ASW

FINAL REPORT

ALPHATECH, INC.
2 BURLINGTON EXECUTIVE CENTER
111 MIDDLESEX TURNPIKE
BURLINGTON, MA 01803
617-273-3388

TR-206

PERFORMANCE ANALYSIS OF SIGNAL PROCESSING AND TRACKING SYSTEMS FOR AIRBORNE ACOUSTIC ASW

FINAL REPORT

By

Dr. R.B. Washburn
Dr. D. Teneketzis
Dr. A.S. Willsky

July 1984

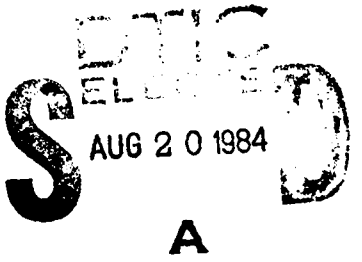

Submitted to:

Dr. Thomas Ballard
Naval Surface Weapons Center
White Oak Laboratory
Silver Springs, MD 20910

ALPHATECH Inc.
2 Burlington Executive Center
111 Middlesex Turnpike
Burlington, Massachusetts 01803
(617) 273-3388

UNCLASSIFIED

SECURITY CLASSIFICATION OF THIS PAGE *(When Data Entered)*

REPORT DOCUMENTATION PAGE	READ INSTRUCTIONS BEFORE COMPLETING FORM
1. REPORT NUMBER	2. GOVT ACCESSION NO. AD-A144 03 / 3. RECIPIENT'S CATALOG NUMBER
4. TITLE *(and Subtitle)* Performance Analysis of Signal Processing and Tracking Systems for Airborne Acoustic ASW	5. TYPE OF REPORT & PERIOD COVERED Final 30 May 1983- 30 June 1984
	6. PERFORMING ORG. REPORT NUMBER TR-206
7. AUTHOR(s) R. B. Washburn D. Teneketzis A. S. Willsky	8. CONTRACT OR GRANT NUMBER(s) N60921-83-C-0131
9. PERFORMING ORGANIZATION NAME AND ADDRESS ALPHATECH, INC. 111 Middlesex Turnpike Burlington, Massachusetts 01803	10. PROGRAM ELEMENT, PROJECT, TASK AREA & WORK UNIT NUMBERS 61153N WR01411 WR0141101 U34AA
11. CONTROLLING OFFICE NAME AND ADDRESS Naval Surface Weapons Center White Oak, Code U22 Silver Spring, MD 20910	12. REPORT DATE July 1984
	13. NUMBER OF PAGES 135
14. MONITORING AGENCY NAME & ADDRESS(if different from Controlling Office) Naval Surface Weapons Center White Oak, Code U22 Silver Spring, MD 20910	15. SECURITY CLASS. (of this report) Unclassified
	15a. DECLASSIFICATION/DOWNGRADING SCHEDULE

16. DISTRIBUTION STATEMENT *(of this Report)*

Approved for public release; distribution is unlimited.

17. DISTRIBUTION STATEMENT *(of the abstract entered in Block 20, if different from Report)*

18. SUPPLEMENTARY NOTES

19. KEY WORDS *(Continue on reverse side if necessary and identify by block number)*

Tracking
Rate Distortion
Acoustic
Cramer-Rao

20. ABSTRACT *(Continue on reverse side if necessary and identify by block number)*

Methods were investigated for predicting optimal mean square estimation error in nonlinear estimation problems associated with passive acoustic tracking. The objective was to develop performance prediction methods that are computationally efficient, applicable to realistic passive tracking models, and accurate. Previous work extended Cramer-Rao methods to obtain a method that was computationally efficient and applicable to a large class of realistic mathematical models. The present work reported here applied this method to study

DD FORM 1 JAN 73 1473 EDITION OF 1 NOV 65 IS OBSOLETE

S/N 0102-LF-014-6601

UNCLASSIFIED

SECURITY CLASSIFICATION OF THIS PAGE *(When Data Entered)*

the effect of an uncertain, unstable source frequency and the effect of a broadband source signal on passive tracking using omnidirectional and directional sonobuoys. In addition, the report describes work on developing performance prediction methods that are more accurate than Cramer-Rao methods in low signal-to-noise ratio cases. The method used is based on rate distortion theory.

ABSTRACT

The research described in this report has investigated methods for predicting optimal mean square estimation error in nonlinear estimation problems associated with passive acoustic tracking. The objective was to develop performance prediction methods that are computationally efficient, applicable to realistic passive tracking models, and accurate. Previous work extended Cramer-Rao methods to obtain a method that was computationally efficient and applicable to a large class of realistic mathematical models. The present work reported here applies this method to study the effect of an uncertain, unstable source frequency and the effect of a broadband source signal on passive tracking using omnidirectional and directional sonobuoys.

In addition, the report describes work on developing performance prediction methods that are more accurate than Cramer-Rao methods in low signal-to-noise ratio cases. One method is based on rate distortion theory and shows great promise. This method requires no simulation, it is analytically and efficiently computable for a large class of static nonlinear problems, and it is better than the Cramer-Rao method when signal-to-noise ratio is low. The work reported here also investigated a numerical method of performance prediction based on classical ambiguity analysis. This investigation obtained bounds on the error between the numerical prediction and the exact mean square error as a function of the size of the numerical computation.

CONTENTS

CONTENTS (continued)

A-1

FIGURES

TABLES

SECTION 1

INTRODUCTION

1.1 INTRODUCTION

The operational deployment and mission objective of airborne acoustic surveillance (passive sonobuoys monitored by aircraft) create a special acoustic environment and restrict the information processing capabilities in respects which differ from other passive acoustic surveillance methods (towed arrays, hull-mounted arrays, bottom-anchored arrays). But the currently operational and planned next generation of airborne signal processing systems have an architecture similar to other passive acoustic systems. That is, the processing system consists of (1) a "front-end" which performs spectral analysis of the raw signal from each sonobuoy to extract frequency and bearing information about the target and (2) a "back-end" which uses the front-end output to detect, locate, or track the target. Much work has been done on improving the design of the individual modules, but there appears to have been little work on evaluating and designing the overall signal processing-tracking system.

The research described in this report addresses the problem of evaluating the potential performance that might be achieved by improving the design of the overall signal processing and tracking system. Specifically, our research problem is to develop mathematical methods and numerical algorithms to estimate the optimal tracking performance possible with given mathematical-physical models of acoustic signals and sensors. Our objective has been to develop

performance prediction methods that are computationally efficient, applicable to realistic passive tracking models, and accurate. In our previous work [1]* we developed a Cramer-Rao method to obtain a method that was computationally efficient and applicable to a large class of mathematical models. In Section 2 of this report we have shown that this method is easy to apply to more realistic models than the ones used in [1]. Specifically, we have used the method to study the effect of uncertain, unstable source frequency and the effect of the presence of a broadband source component on tracking accuracy.

In some nonlinear estimation problems of low signal-to-noise ratio, Cramer-Rao methods may predict performance much better than the optimal processing algorithm can actually achieve. This disadvant[illegible]f Cramer-Rao methods motivated us to investigate performance prediction methods which would be more accurate when the signal-to-noise ratio was low, but which are still efficiently computable for a large class of realistic models. Sections 3 and 4 focused on this problem.

Section 3 investigated an analytical (i.e., not requiring simulation) method based on rate distortion theory [4]. This method shows great promise because it is efficient to compute for a large class of nonlinear problems and it is better than the Cramer-Rao method when signal-to-noise ratio is low. However, the method requires further development to make it applicable to realistic dynamic problems.

Section 5 investigated a numerical method of performance prediction often described as ambiguity analysis [7],[15]. This method is essentially based on numerical computations rather than on analytical formulas. The method can

*References are indicated by numbers in square brackets, the list appears at the end of the main body of this report.

give an accurate performance prediction provided sufficient computational resources are available. Our investigation studied the relationship between prediction accuracy and computational complexity for this method. Further work remains to determine the precise effect of signal-to-noise ratio on the relationship between prediction accuracy and computational complexity.

In the remainder of this section we present a summary of the research detailed in Sections 2, 3, and 4.

1.2 CRAMER-RAO PERFORMANCE ANALYSIS OF FREQUENCY UNCERTAINTY AND BROADBAND SIGNALS

In our previous work [1] we refined available Cramer-Rao performance analysis methods to exploit special features of the airborne acoustic signal processing and tracking problem. In particular, it was possible to obtain an efficient, recursive computation, and to avoid completely Monte-Carlo simulation despite the presence of nonlinear measurements. A finite dimensional stochastic differential equation [2] was used to model a constant velocity target radiating acoustic signals to passive omnidirectional and directional sonobuoys. In [1] we found that such models of airborne acoustic tracking problems have the following structural property: all nonlinearties of the state equations are functions only of the source kinematic states (position and velocity). The other state variables, modeling such quantities as source frequencies, broadband component, received signal phase, etc. occur linearly in the state equations. Because of this structure of the mathematical model, we were able to derive an efficient Cramer-Rao type lower bound that treats the source kinematic variables as unknown parameters and all other state variables as random, normally distributed parameters.

In the work of Section 2 we have illustrated further the utility of this approach by analyzing two effects not studied in [1]: the effect of an initially uncertain and randomly unstable source frequency, and the effect of a broadband component of the source frequency. The random frequency was parameterized by two variables, initial root-mean-square uncertainty and rate of variation. The rate of variation (studied for .01 to 1.0 Hz/min) appeared to have negligible effect on both position and velocity tracking error. Initial uncertainty had little effect on position tracking error, but it did have a significant effect on velocity tracking error. When the initial source frequency uncertainty reaches 1 Hz, the initial velocity tracking error is not substantially reduced until the source passes through the sonobuoy field. This indicates that initial uncertainty concerning source frequency can make the velocity tracking performance sensitive to source-sensor geometry (i.e., good velocity tracking will depend more crucially on good geometry).

The broadband source component was modeled as a simple stationary first-order Markov process. The bandwidth of this process was fixed at 200 Hz and the ratio of broadband to narrowband power was varied from 10^{-5} to 10^{4}. Increasing this ratio increases the total source power, and the position and velocity tracking error decrease as a consequence. The decrease in tracking error is comparable to the decrease in error with increased narrowband source signal power studied in [1]. This indicates that broadband source energy is comparable in value to narrowband source energy, and that the broadband component of the source signal can be profitably exploited by an acoustic signal processing system.

Many other realistic models can be analyzed using the methods of Section 2. However, before analyzing the performance of other realistic models of

passive acoustic tracking problems, we need to determine the degree of optimism inherent in the performance prediction of Section 2. Sections 3 and 4 present one approach to doing this, namely by trying to develop more accurate performance predictions with which to compare the methods of Section 2. It is also desirable to compare these performance predictions to the performance of actual algorithms. The methods of Section 2 suggest a processing algorithm architecture that might realize the performance prediction in some cases (see [1] for discussion).

1.3 RATE DISTORTION PERFORMANCE ANALYSIS

Communication theory provides a useful interpretation of tracking problems different from the more conventional statistical estimation theory point of view. Messages are generated by a source and coded by an encoder. The encoded messages are transmitted through a channel, decoded by a decoder, and received by a user. In communication problems the source, channel, and user are specified, and the problem is to design encoder and decoder so that messages received by the user are accurate reproductions of the messages generated by the source.

One can interpret a tracking system as a type of communication system in the following way. In this interpretation the message generated by the source is a set of target parameters (e.g., positions and velocities at a given time). The encoder for passive tracking problems does nothing to code the source message. In active tracking we can control the encoder to some extent (e.g., increase signal strength). The encoder and channel for the tracking problem represent the transformation between target parameters and sensor outputs. One might also include preprocessing of sensor outputs as part of the channel if that preprocessing is already specified. Finally, the decoder

for the tracking problem is the tracking algorithm which provides estimates of target parameters to a user. In tracking problems the source (target model), encoder and channel (measurement model), and user are specified, and the problem is to design a decoder (tracking algorithm) so that estimates received by the user are accurate reproductions of the parameters generated by the source.

The communication theory viewpoint is useful because it allows us to apply to the tracking problem techniques of information theory which do not exist in statistical estimation theory. The techniques relevant to tracking performance analysis involve rate distortion theory [4] first developed by Shannon [5],[6]. Distortion is a measure of the average error between the message generated by the source and the decoded message received by the user. In a tracking problem it could be the mean square error in the tracking algorithm's target parameter estimation.

Using rate distortion techniques and some simple extensions of them in Section 3, we showed how to compute analytically rate distortion lower bounds of mean square error for static nonlinear estimation problems with additive Gaussian noise. Specifically, we obtained a lower bound of the mean square estimation error for any specified component of the state vector. We showed that the rate distortion bound is asymptotically tighter than the Cramer-Rao bound in the limit of low signal-to-noise ratio.

Based on present results, the rate distortion bound offers a better approximation of mean square performance in the high measurement noise regime than the Cramer-Rao bound. Furthermore, the rate distortion bound requires little, if any, more computation than the Cramer-Rao bound. Thus, the rate distortion bound appears to complement the Cramer-Rao method in the nonlinear,

high noise regime where the latter bound is known to give overly optimistic approximations of the true mean square error. However, in order to make the rate distortion theory useful for the dynamic nonlinear estimation problems of tracking, we must develop our current results in two significant ways:

1. it is necessary to obtain a simple rate distortion bound in the case of a vector state and a general vector measurement;

2. it is necessary to derive a recursively computable bound for dynamic estimation problems.

Other directions for further investigation exist beside these two necessary extensions. One direction would extend the bounds to problems for which the state is an unknown, non-random parameter (or a mixture of random and non-random parameters). In [1] we found that a large class of tracking problems can be modeled by a state process which consists of an unknown deterministic component and an unknown, Gaussian distributed random component. Rate distortion theory for nonstatistical sources (ε - entropy methods [4]) may allow us to derive such results.

Another direction is to study the effect of architecture constraints, such as preprocessing of measurements, on tracking estimation performance. We investigated this problem in [1] using Cramer-Rao methods. A rate distortion approach, based as it is on information theory, would provide a more general, more accurate method of analyzing architectural constraints.

1.4 AMBIGUITY PERFORMANCE ANALYSIS

Ambiguity analysis ([7],[15] Chapter 10) is an attempt to understand the global nature of a parameter estimation problem. This is in contrast to Cramer-Rao methods which provide a more local analysis of estimation performance. The Cramer-Rao lower bound on mean square estimation error will be an accurate

estimate of true optimal performance provided that it is possible to acquire or maintain an estimate near the unknown parameter at all. The local problem (addressed by the Cramer-Rao method) is to analyze accuracy given acquisition; the global problem (addressed by ambiguity analysis) is to analyze the acquisition performance.

The ambiguity method approximates the mean square error of the maximum likelihood estimator by forming a weighted sum of the Cramer-Rao lower bound with a finite number of discrete errors. The weights are probabilities associated with the finite hypothesis testing problem of choosing one of a finite number of regions in the parameter space. The regions were selected so that one large region (proportional to $N^{-1/2}$ in size) contained the true parameter. The rest of parameter space was divided into smaller regions (proportional to N^{-1} in size). We showed that this method is different from the exact mean square error by a term proportional to N^{-1}. Thus, the method converges to the exact mean square error as the number of regions increases, and the error of the approximation is inversely proportional to the number of regions.

Further work is required to determine how the magnitude of the measurement noise (or equivalently, the signal-to-noise ratio) enters into the approximation error. This result will clarify how large the number of regions needs to be for a given signal-to-noise ratio. The convergence analysis also needs to be extended to the general case of vector states and measurements and to the case where a measurement process is observed. The order of the approximation error is expected to remain the same in these generalizations but a more precise idea of the size of this error would help us understand the computational feasibility of applying the ambiguity analysis method to analyze the performance of complex estimation problems.

SECTION 2

CRAMER-RAO PERFORMANCE ANALYSIS OF FREQUENCY INSTABILITY AND BROADBAND SIGNALS

2.1 INTRODUCTION

In our previous work [1] we refined available Cramer-Rao performance analysis methods to exploit special features of the airborne acoustic signal processing and tracking problem. In particular, it was possible to obtain an efficient, recursive computation, and to avoid completely Monte-Carlo approximation despite the presence of nonlinear measurements. In this section we illustrate further the utility of this approach by analyzing the effects of unstable and unknown source frequency and of broadband source signals on the predicted optimal tracking performance. We describe the mathematical model we have used in subsection 2.2. Subsection 2.3 presents the results of numerical runs and subsection 2.4 presents conclusions based on these results.

2.2 MATHEMATICAL MODEL WITH FREQUENCY INSTABILITY AND BROADBAND SOURCE

A finite dimensional stochastic differential equation [2] was used to model a constant velocity target radiating direct path acoustic signals to passive omnidirectional and directional sonobuoys. This model has the general form

$$dx = f(x)dt + G\,dw \tag{2-1}$$

$$dy = h(x)dt + dv \tag{2-2}$$

where x is the finite dimensional state vector and y is the finite dimensional vector of measurements. The state noise and measurement noise were assumed to be independent Gaussian white noise processes. Note that f and h were nonlinear functions of x and G was a constant matrix.

The state vector x used in the model consisted of the following components.

$$x = \begin{bmatrix} \vec{x}_1 \\ \vec{x}_2 \\ \vec{v}_1 \\ \vec{v}_2 \\ \phi_1 \\ \vdots \\ \phi_{Nb} \\ f \\ s_1 \\ \vdots \\ s_{Nb} \end{bmatrix} \qquad (2\text{-}3)$$

In Eq. 2-3 the expressions $\vec{x}_1$, $\vec{x}_2$ denote the two orthogonal components of the position of the target relative to some fixed position (the origin at 0,0). The expressions $\vec{v}_1$, $\vec{v}_2$ similarly denote the components of the target velocity.

The expression ϕ_k denotes the phase of the narrowband component of the received acoustic signal at buoy number k. Similarly, s_k denotes the broadband component of the received acoustic signal. The expression f denotes the transmitted source frequency. There are N total sonobuoys.

The measurement vector y consisted of the following components.

$$y = \begin{bmatrix} y_1 \\ y_2 \\ \cdot \\ \cdot \\ \cdot \\ y_{Nb} \end{bmatrix} \tag{2-4}$$

where for each k the expression y_k denotes either

$$y_k = y_{k,om} \tag{2-5}$$

if sonobuoy k is an omnidirectional buoy, and

$$y_k = \begin{bmatrix} y_{k,om} \\ y_{k,d1} \\ y_{k,d2} \end{bmatrix} \tag{2-6}$$

if sonobuoy k is a directional buoy. In any case $y_{k,om}$ denotes the omnidirectional channel signal and $y_{k,d1}$, $y_{k,d2}$ denote the two directional channel signals.

The target model assumed constant velocity motion, namely

$$\begin{aligned} d\vec{x}_1 &= \vec{v}_1\, dt \\ d\vec{x}_2 &= \vec{v}_2\, dt \\ d\vec{v}_1 &= 0 \\ d\vec{v}_2 &= 0 \end{aligned} \qquad (2\text{-}7)$$

Note that Eq. 2-7 contains no driving noise on the right-hand side. This was important in developing an efficient method to compute performance as described in [1]. The initial position components $\vec{x}_1(0)$, $\vec{x}_2(0)$ and the initial velocity components $\vec{v}_1(0)$, $\vec{v}_2(0)$ were treated as unknown parameters rather than as random variables. This is in contrast to the treatment of f, ϕ_k and s_k as random parameters.

The acoustic signal radiated by the target was assumed to consist of two parts: a narrowband component and a broadband component. The narrowband component was modeled as follows. The source frequency f satisfied the stochastic differential equation

$$df = -\alpha_f(f - \bar{f})dt + dw_f \qquad (2\text{-}8)$$

where $\alpha_f > 0$, $\bar{f}$ and the variance σ_f^2 associated with w_f were known constants. The initial variance of f(0) was assumed to be the steady state variance given by

$$\overline{(f(0) - \overline{f(0)})^2} = \frac{\sigma_f^2}{2\alpha_f} \qquad (2\text{-}9)$$

where the overbars ($\overline{}$) denote mathematical expectations. The physical meaning of Eq. 2-8 is that the source frequency f(t) at time t is an unknown random variable that varies randomly about the constant nominal value $\bar{f}$

($\bar{f}$ = 100 Hz in our numerical examples). Note that the average variation of f per time constant is of order

$$\sigma_f \cdot \sqrt{\alpha_f} \quad . \tag{2-10}$$

That is, Eq. 2-10 gives the average speed of variation of the source frequency (it has units Hz/min in our numerical examples).

The source frequency f is Doppler-shifted and drives a random phase equation given by

$$d\phi_k = f \cdot \left(1 + \frac{\vec{v}_1 \cdot (\vec{x}_1 - z_{k,1}) + \vec{v}_2 \cdot (\vec{x}_2 - z_{k,2})}{c\sqrt{(\vec{x}_1 - z_{k,1})^2 + (\vec{x}_2 - z_{k,2})^2}} \right)^{-1} dt$$

$$+ dw_{\phi,k} \quad . \tag{2-11}$$

In Eq. 2-11 $z_{k,1}$ and $z_{k,2}$ denote the coordinates of the position of sonobuoy k, and c is the assumed constant speed of sound. The noise processes $w_{\phi,k}$ were assumed to have the same variance, σ_ϕ^2, associated with all of them. The model also allowed the possibility of correlation between $w_{\phi,k}$ and $w_{\phi,j}$ for $k \neq j$. A constant correlation coefficient ρ ($0 \leq \rho \leq 1$) was assumed for all such cases.

The physical interpretation of Eq. 2-11 is obtained as follows. Consider a signal y(t) with phase $\phi_k(t)$, specifically

$$y(t) = \sin \phi_k(t) \tag{2-12}$$

If one assumes that the phase is initially unknown (i.e., distributed uniformly over 360 degrees), then y(t) is a wide sense stationary process [3] with total power 1/2 and two-sided power spectral density at frequency ω given by

$$\frac{\sigma_\phi^2}{4\pi} \cdot \frac{\frac{\sigma_\phi^4}{4} + f_D^2 + \omega^2}{\left[\frac{\sigma_\phi^4}{4} + (f_D - \omega)^2\right]\left[\frac{\sigma_\phi^4}{4} + (f_D + \omega)^2\right]} \quad . \tag{2-13}$$

This result assumes that the Doppler-shifted frequency is fixed or varies slowly relative to the phase variation. The expression in Eq. 2-13 represents a spectrum with peak at frequency f_D and width of order σ_ϕ^2.

The broadband component of the received signal is modeled by the stochastic differential equation

$$ds_k = - \alpha_s \cdot s_k \, dt + dw_{s,k} \tag{2-14}$$

where $\alpha_s > 0$ and the variance σ_s^2 associated with $w_{s,k}$ are known constants. The signal $s_k(t)$ is a stationary process with two-sided power spectral density at frequency ω given by

$$\frac{1}{2\pi} \frac{\sigma_s^2}{(\alpha_s^2 + \omega^2)} \quad , \tag{2-15}$$

total power $\sigma_s^2/2\alpha_s$ and bandwidth of order α_s.

The processes ϕ_k and s_k are combined to form the received signal process as follows. The omnidirectional channel process $y_{k,om}$ satisfies the equation

$$dy_{k,om} = (s_k + A \sin \phi_k)dt + dv_{k,om} \tag{2-16}$$

where the constant A and the variance $\sigma_{k,om}^2$ associated with $v_{k,om}$ are assumed known. Note that the total power of the narrowband component of $y_{k,om}$ is $A^2/2$ compared to the broadband component power $\sigma_s^2/2\alpha_s$ and the noise component power spectral density $\sigma_{k,om}^2/2\pi$ (the white noise $dv_{k,om}$ has infinite total power of course).

The directional channel signals $y_{k,d1}$ and $y_{k,d2}$ satisfy similar equations given by the following.

$$dy_{k,d1} = (s_k + A \sin \phi_k) \cdot \frac{(\vec{x}_1 - z_{k,1})}{\left[(\vec{x}_1 - z_{k,1})^2 + (\vec{x}_2 - z_{k,2})^2\right]^{1/2}} dt + dv_{k,d1} \tag{2-17}$$

$$dy_{k,d2} = (s_k + A \sin \phi_k) \cdot \frac{(\vec{x}_2 - z_{k,2})}{\left[(\vec{x}_1 - z_{k,1})^2 + (\vec{x}_2 - z_{k,2})^2\right]^{1/2}} dt + dv_{k,d2} \tag{2-18}$$

2.3 NUMERICAL EXAMPLES

This section describes the numerical examples we computed to study the effects of unknown, unstable source frequency and the effects of a broadband source signal on predicted optimal tracking performance. Tracking performance was measured by the root-mean-square (rms) errors in position and in velocity versus time after initial contact. The target-sensor geometry assumed in each example is shown in Fig. 2-1; nominal test parameters are shown in Table 2-1. Note that the measurement noise for omnidirectional channels was chosen so that a single directional buoy within 5 kft of the source could determine source frequency to within .2 Hz and bearing to within 4 degrees based on 1 minute worth of raw data. Figures 2-2 and 2-3 show respectively the position and velocity tracking performance for the nominal test parameters. Note that the rms error is plotted on a logarithmic scale in these figures.

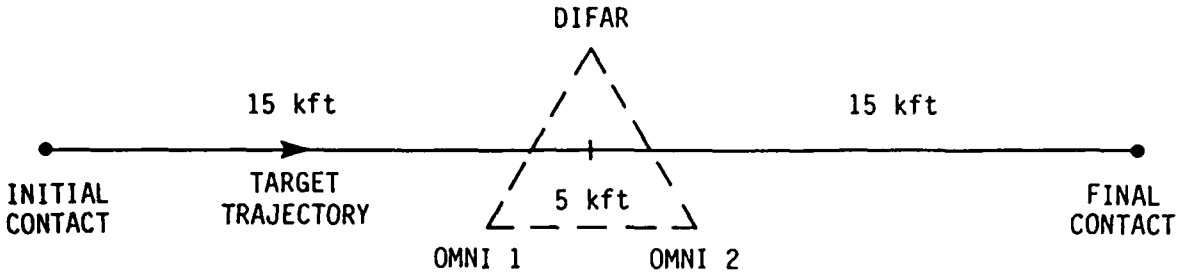

Figure 2-1. Target Sensor Geometry

TABLE 2-1. NOMINAL TEST PARAMETER VALUES

TARGET	
Initial x position	-15 kft
Initial y position	0 kft
Initial x velocity	1.2 kft/min (approx. 10 kt)
Initial y velocity	0 kft/min
Initial position uncertainty	30 kft
Initial velocity uncertainty	1.5 kft/min
Total time of contact	25 min
SOURCE SIGNAL	
Narrowband center frequency	100 Hz
Initial uncertainty of frequency	.01 Hz
Frequency variation rate	.01 Hz/min
Narrowband component line width	.1 Hz
Broadband bandwidth	200 Hz
Broadband:narrowband power ratio	10^{-5}
SENSOR	
Number of directional buoys	1
Number of omnidirectional buoys	2
Interbuoy distance	5 kft
Buoy phase correlation coefficient	0
Omnidirectional channel noise	.11
Directional channel noise	.03

Table 2-2 shows the cases computed to study the effects of frequency uncertainty and frequency instability. As shown in Table 2-2, two parameters measuring initial source frequency uncertainty (given by Eq. 2-9) and average rate of variation (given by Eq. 2-10) were varied independently. The effect on tracking position error is shown in Figs. 2-4 through 2-15; the effect on tracking velocity error is shown in Figs. 2-16 through 2-27.

Table 2-3 shows the cases computed to study the effect of a broadband source component. One parameter, the ratio of total broadband to total narrowband power, was varied. This ratio is given by

$$\frac{\sigma_s^2}{\alpha_s A^2} \tag{2-19}$$

The effect on tracking position error is shown in Figs. 2-28 through 2-32; the effect on tracking velocity error is shown in Figs. 2-33 through 2-37.

2.4 CONCLUSIONS

Table 2-4 shows the effect of source frequency uncertainty and instability on the minimum tracking position error achieved during contact and the velocity error given at the same time. In Figs. 2-4 through 2-15 this error is the minimum of the position error curves. Note that the position error minimum occurs at 14 minutes after initial contact; the closest point of approach occurs at 12.5 minutes after initial contact. As Figs. 2-4 through 2-15 and Table 2-4 indicate, the initial uncertainty in source frequency has a small effect on position tracking error; the rate of source frequency variation appears to have virtually no effect. Table 2-4 indicates that the rate of source frequency variation has no effect on velocity tracking error; but

the initial source frequency uncertainty has a greater effect on velocity error than it has on position error. The effect of initial source frequency uncertainty on velocity error is shown in Figs. 2-16 through 2-27 where the initial uncertainty varies from .01 Hz to 10 Hz. These figures show that the initial velocity uncertainty (1.5 kft/min) is reduced very little until the source passes through the sonobuoy field when initial frequency uncertainty is high. This indicates that initial frequency uncertainty could make the velocity tracking performance sensitive to target-sensor geometry (i.e., good performance will depend more crucially on good geometry).

Table 2-5 shows the effect of a broadband source signal component on the minimum tracking position error achieved during contact and the velocity error given at the same time. In Figs. 2-28 through 2-32 this error is the minimum of the position error curves. As before, the minimum occurs at 14 minutes after initial contact. Increasing the ratio of total broadband to total narrowband power decreases position and velocity error as indicated in Table 2-5. However, this effect is the expected consequence of the total increase in signal power relative to the background noise level. That is, the total narrowband power and the background noise levels are held constant in the examples described here. The decrease in tracking error with increased broadband source signal power is comparable to the decrease in tracking error with increased narrowband source signal power studied in [1]. This indicates that broadband source energy is comparable in value to narrowband source energy, and that the broadband component of the source signal might be profitably exploited by an acoustic signal processing system.

TABLE 2-2. FREQUENCY EFFECT CASES STUDIED

Variation Rate (Hz/min) \ Initial Uncertainty (Hz)	.01	.1	1	10
.01	Fig. 2-4* Fig. 2-16**	Fig. 2-5 Fig. 2-17	Fig. 2-6 Fig. 2-18	Fig. 2-7 Fig. 2-19
.1	Fig. 2-8 Fig. 2-20	Fig. 2-9 Fig. 2-21	Fig. 2-10 Fig. 2-22	Fig. 2-11 Fig. 2-23
1	Fig. 2-12 Fig. 2-24	Fig. 2-13 Fig. 2-25	Fig. 2-14 Fig. 2-26	Fig. 2-15 Fig. 2-27

TABLE 2-3. BROADBAND EFFECT CASES STUDIED

Broadband to Narrowband Power Ratio				
10^{-5}	10^{-2}	1	10^{2}	10^{4}
Fig. 2-28* Fig. 2-33**	Fig. 2-29 Fig. 2-34	Fig. 2-30 Fig. 2-35	Fig. 2-31 Fig. 2-36	Fig. 2-32 Fig. 2-37

* position error versus time

** velocity error versus time

TABLE 2-4. FREQUENCY EFFECT ON MINIMUM TRACKING ERROR

Variation Rate (Hz/min) \ Initial Uncertainty (Hz)	.01	.1	1	10
.01	.40 kft* .08 kft/min**	.41 kft .11 kft/min	.42 kft .14 kft/min	.43 kft .15 kft/min
.1	.40 kft .08 kft/min	.41 kft .10 kft/min	.43 kft .15 kft/min	.43 kft .15 kft/min
1	.40 kft .08 kft/min	.41 kft .08 kft/min	.43 kft .15 kft/min	.43 kft .15 kft/min

TABLE 2-5. BROADBAND EFFECT ON MINIMUM TRACKING ERROR

Broadband to Narrowband Power Ratio

10^{-5}	10^{-2}	1	10^{2}	10^{4}
.40 kft* .08 kft/min**	.40 kft .08 kft/min	.36 kft .07 kft/min	.22 kft .04 kft/min	.12 kft .04 kft/min

* minimum position error

** velocity error at time of minimum position error

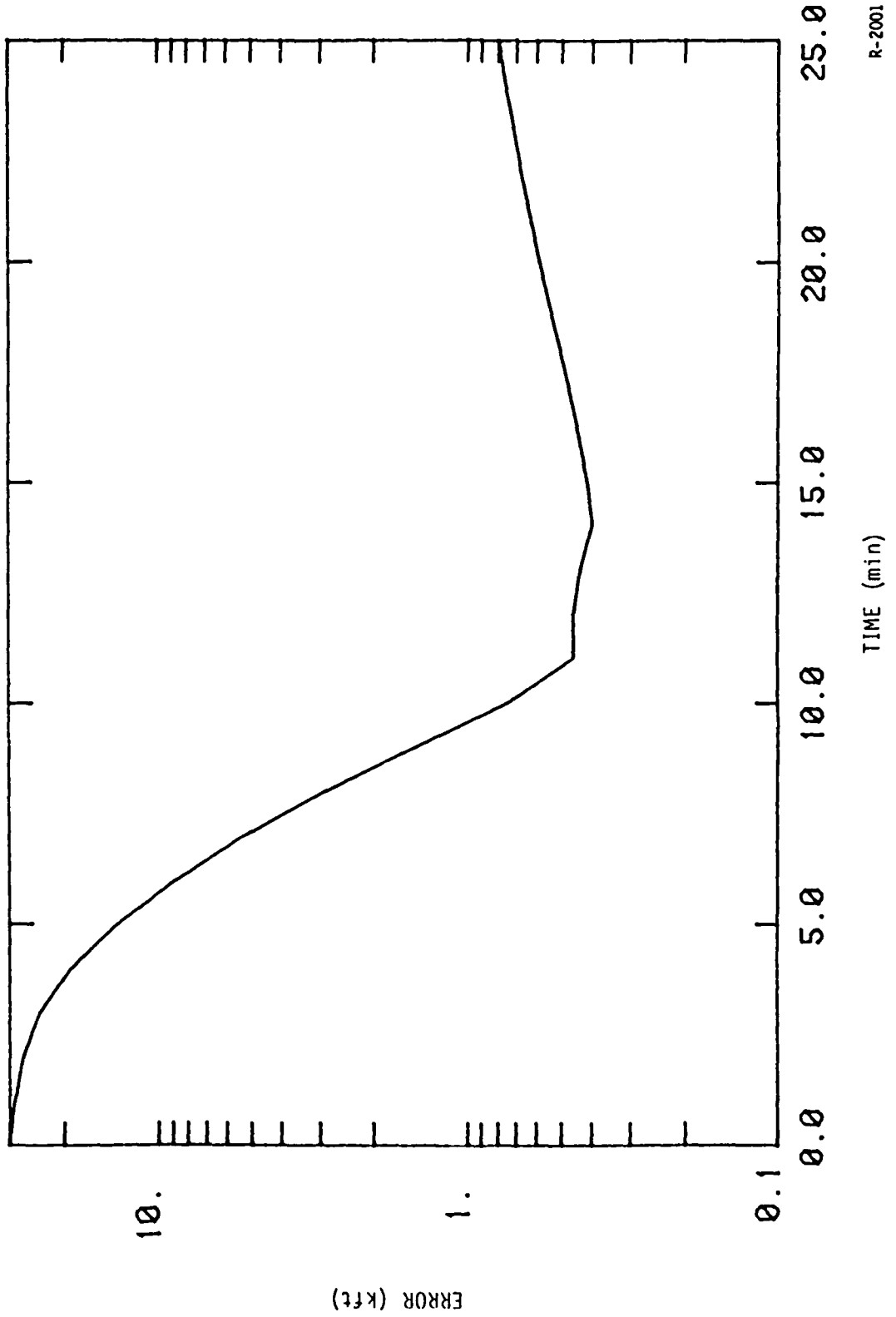

Figure 2-2. Position Error for Nominal Case

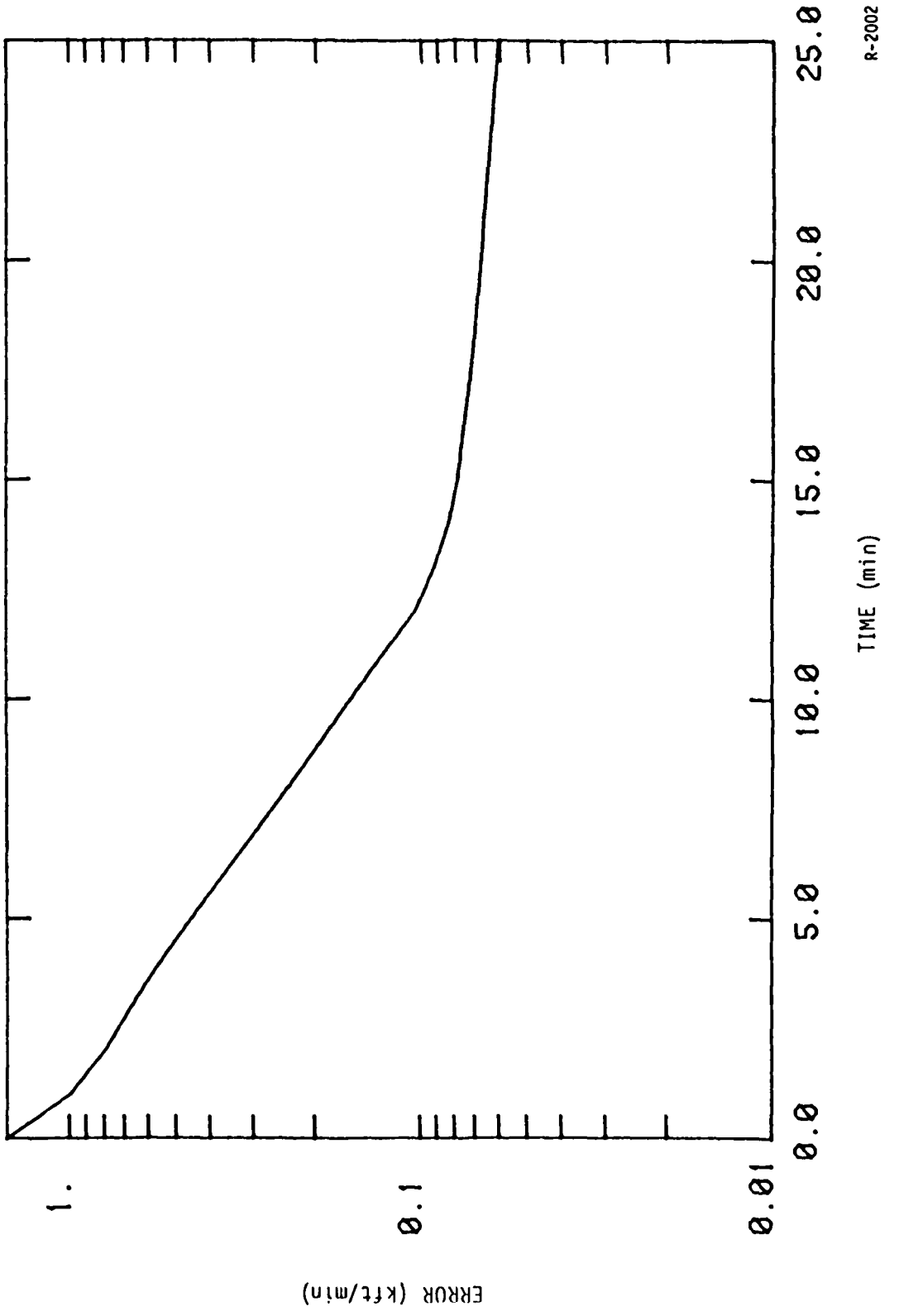

Figure 2-3. Velocity Error for Nominal Case

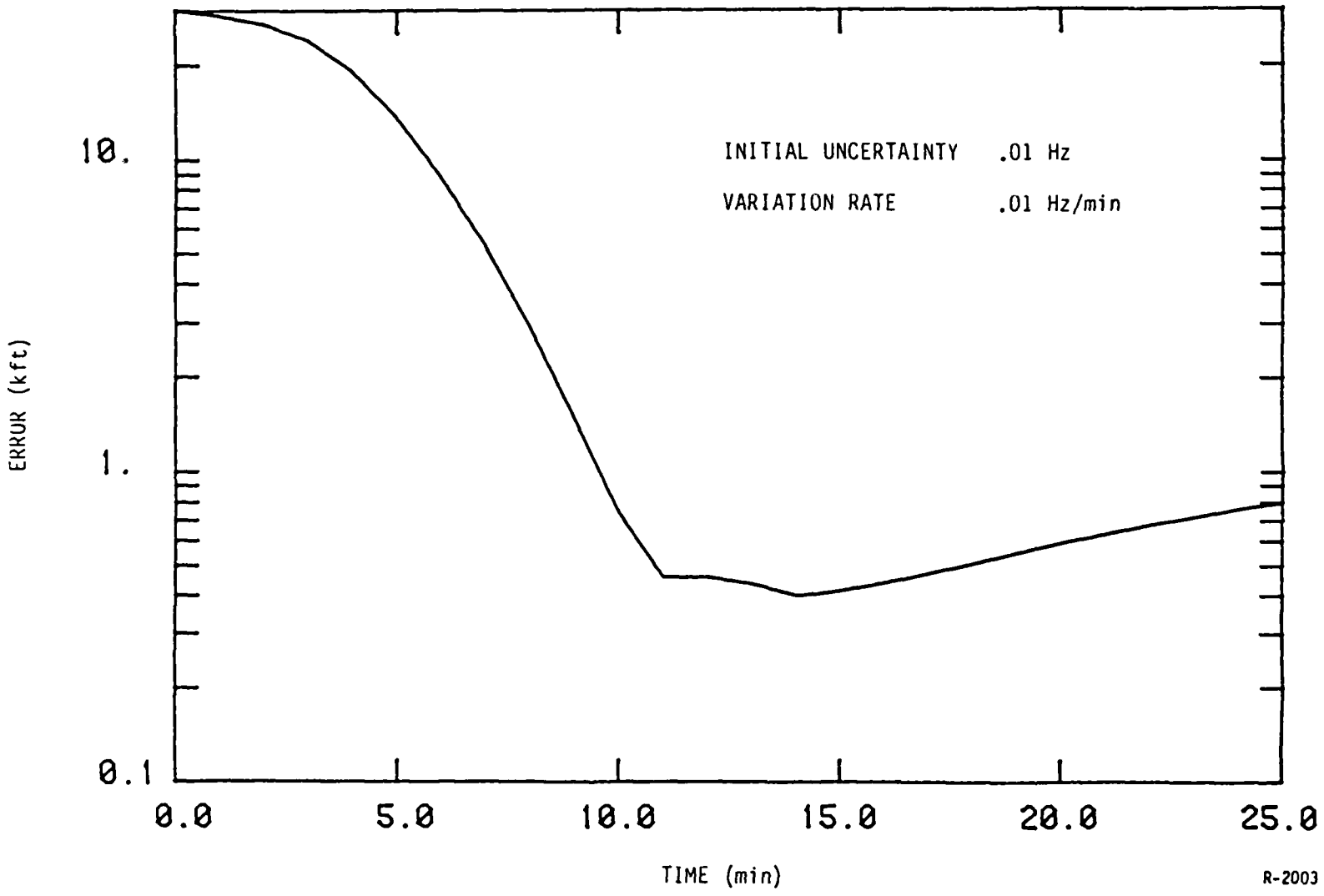

Figure 2-4. Frequency Effect on Position Error

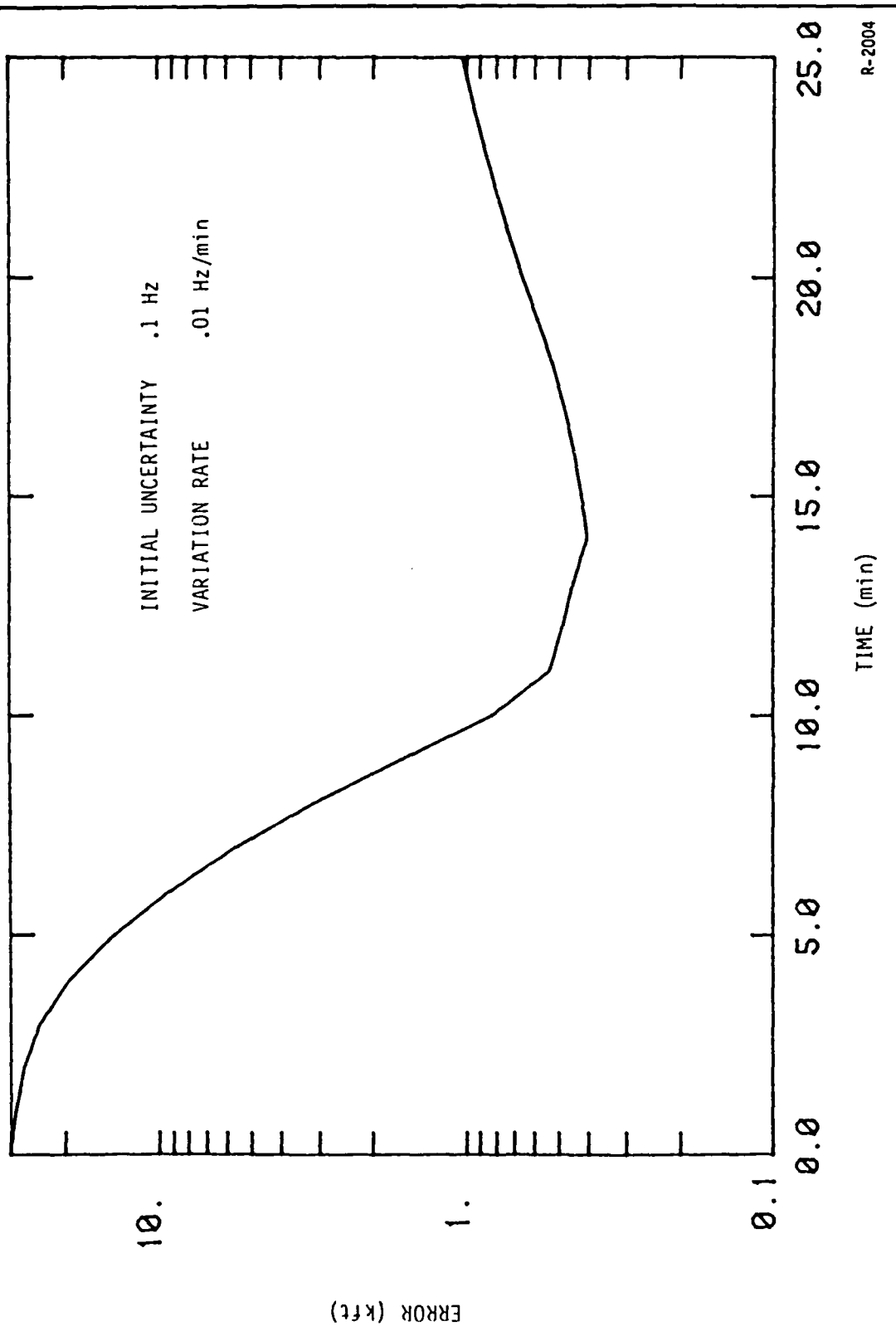

Figure 2-5. Frequency Effect on Position Error

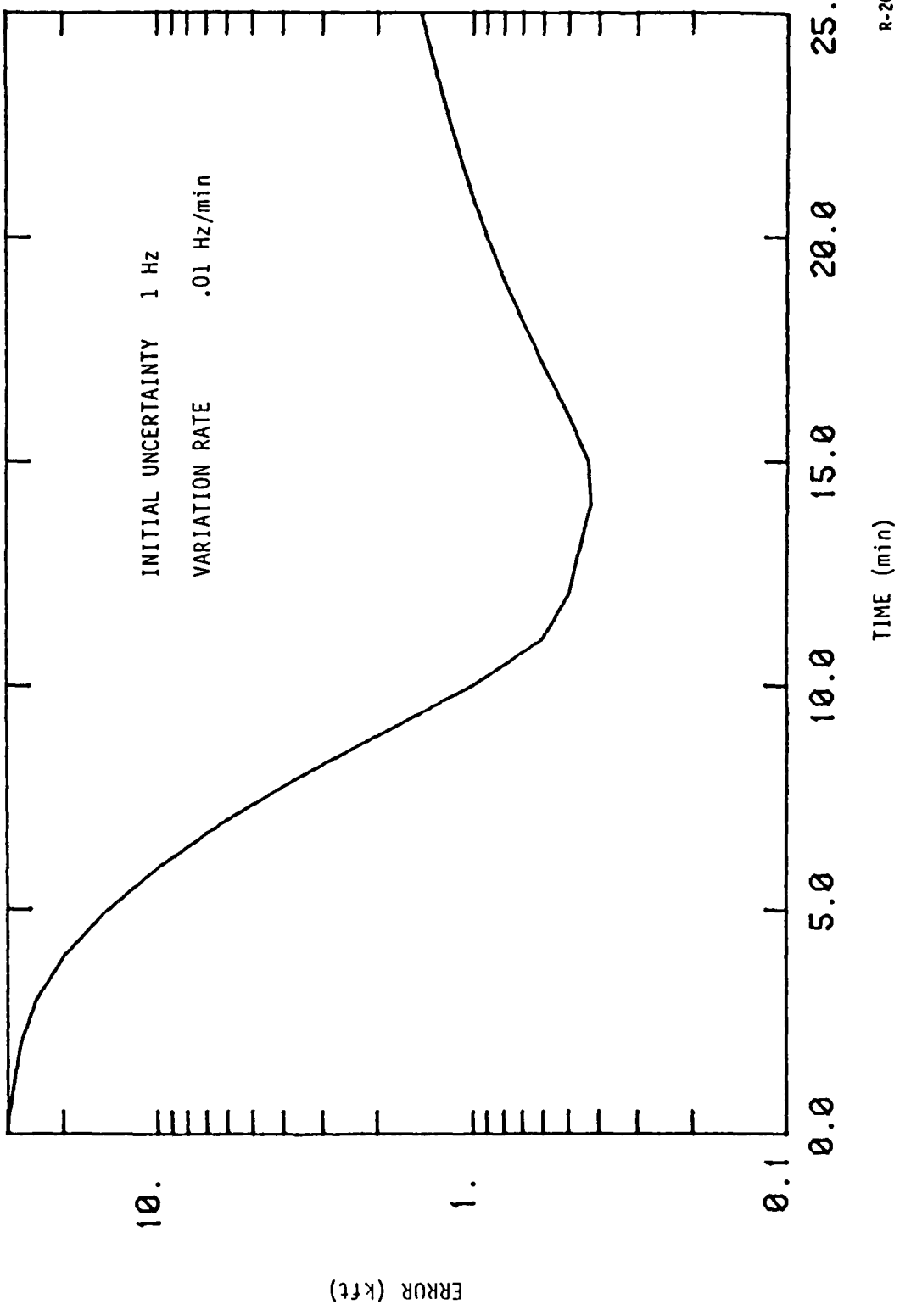

Figure 2-6. Frequency Effect on Position Error

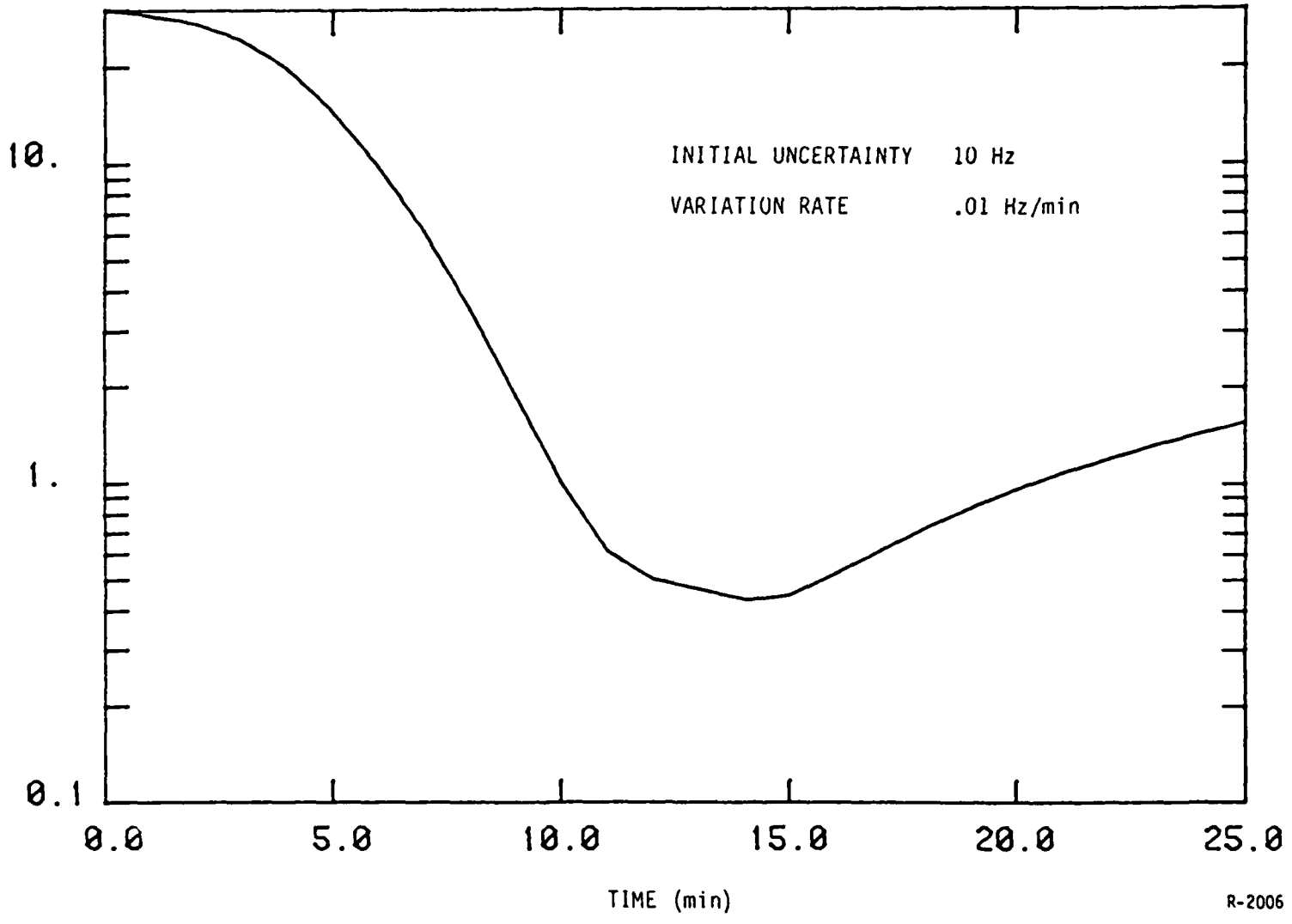

Figure 2-7. Frequency Effect on Position Error

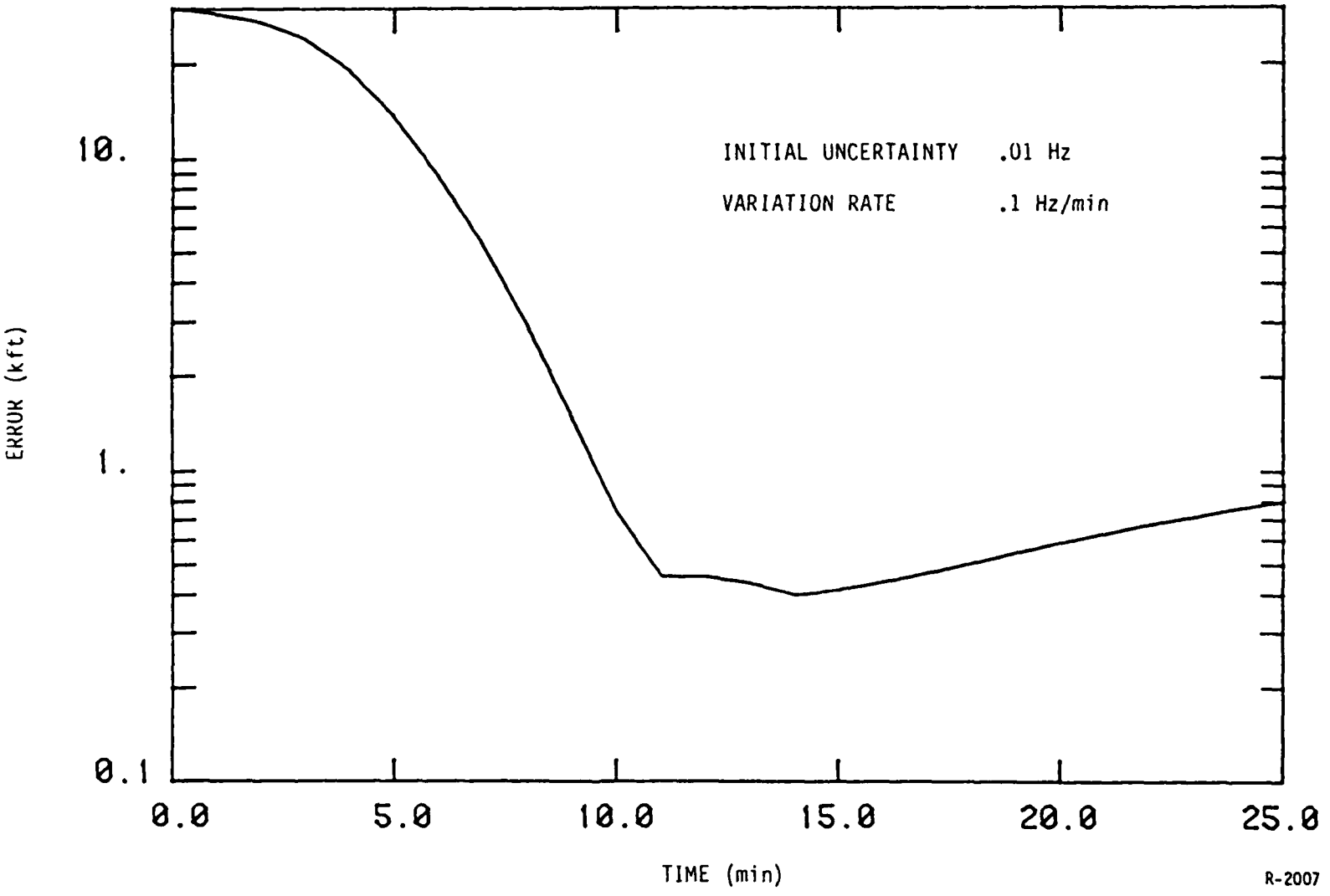

Figure 2-8. Frequency Effect on Position Error

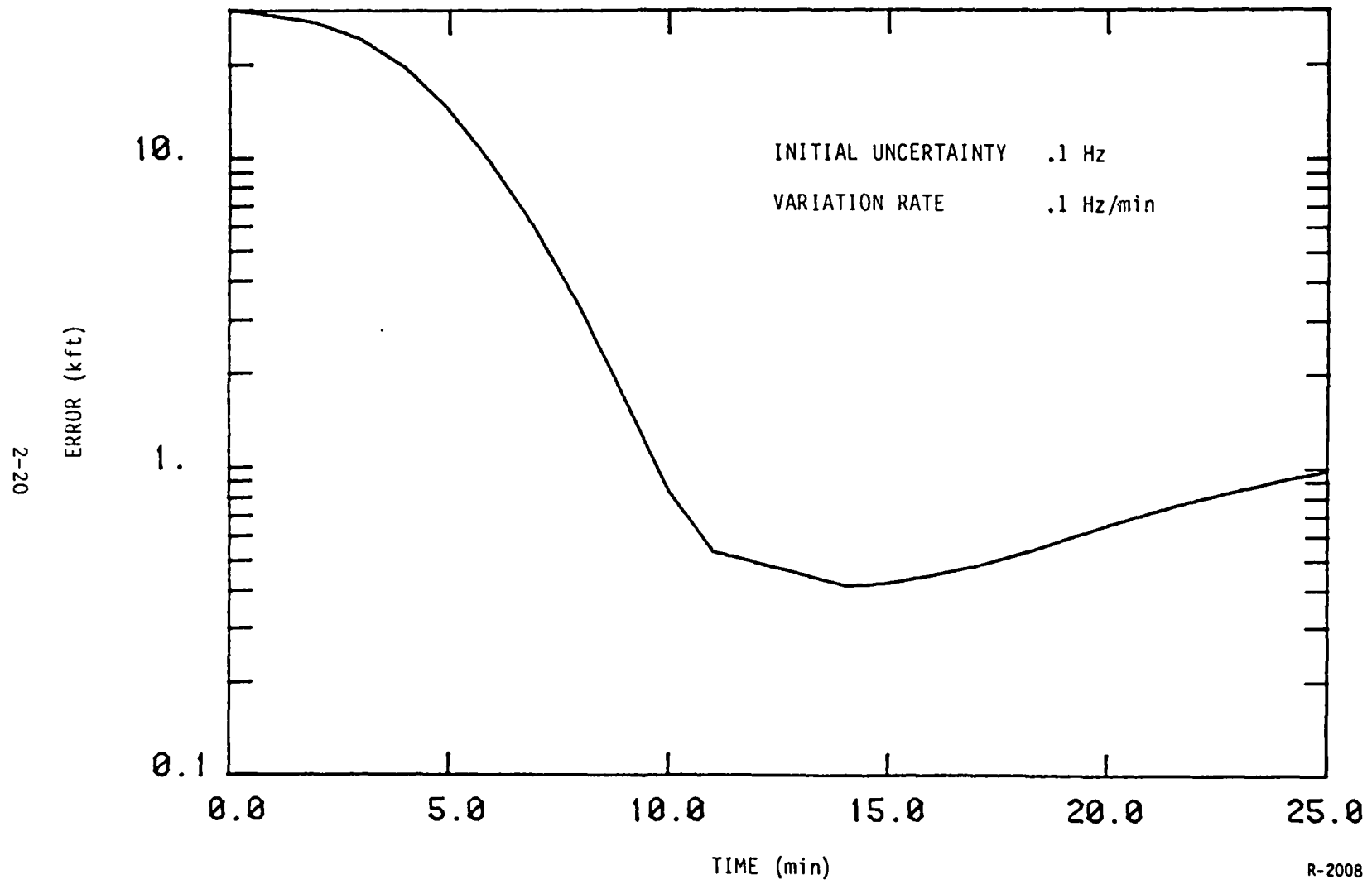

Figure 2-9. Frequency Effect on Position Error

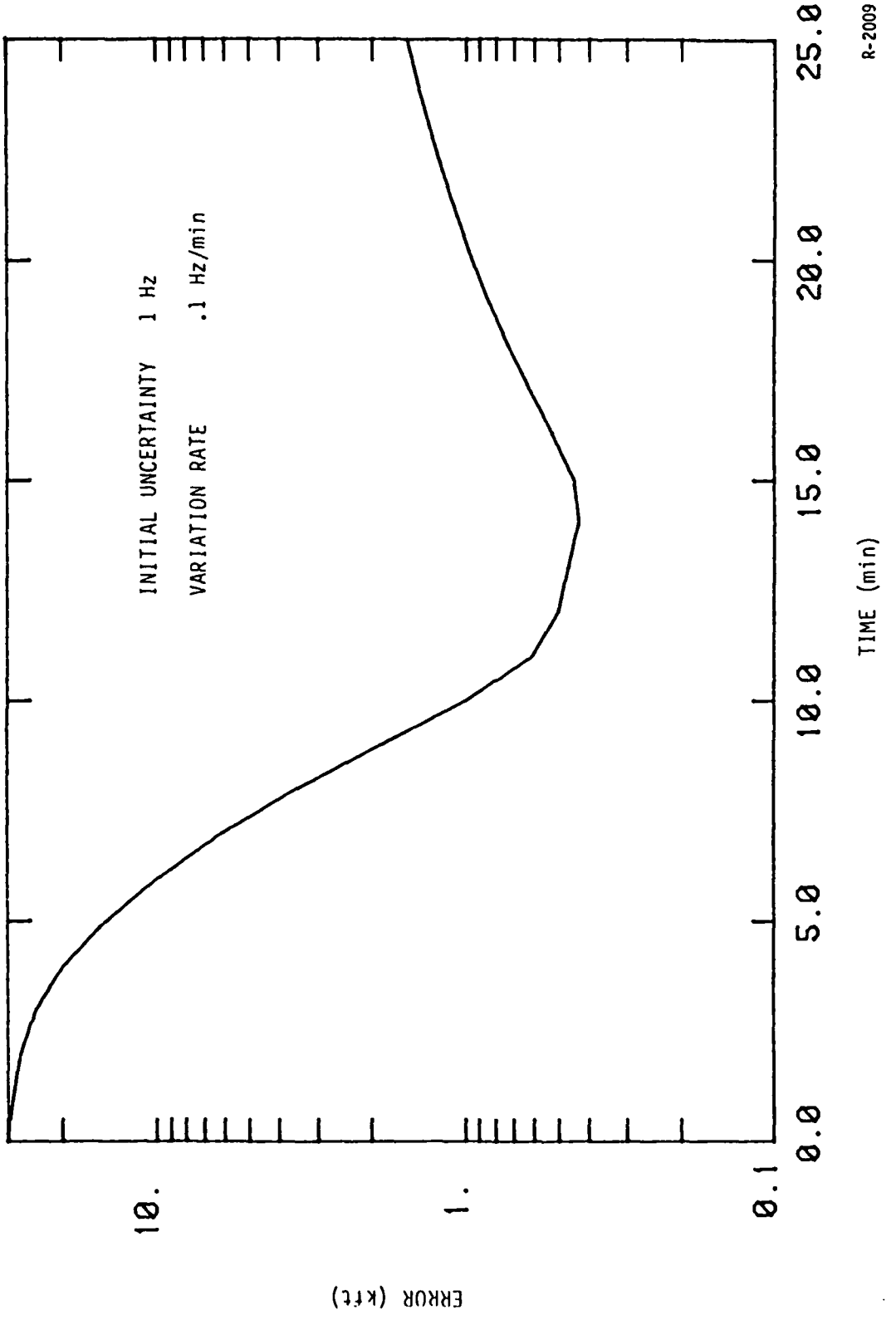

Figure 2-10. Frequency Effect on Position Error

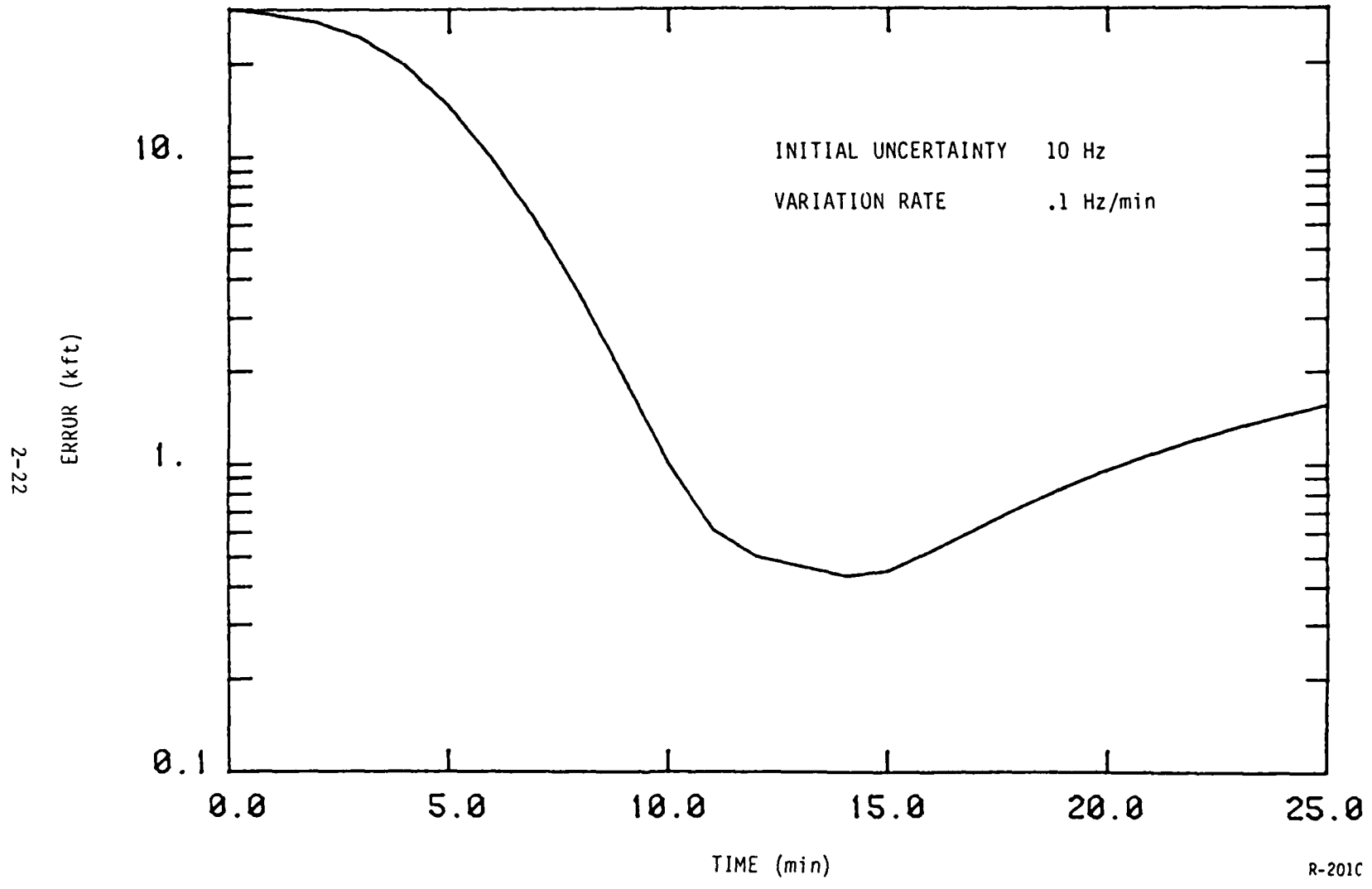

Figure 2-11. Frequency Effect on Position Error

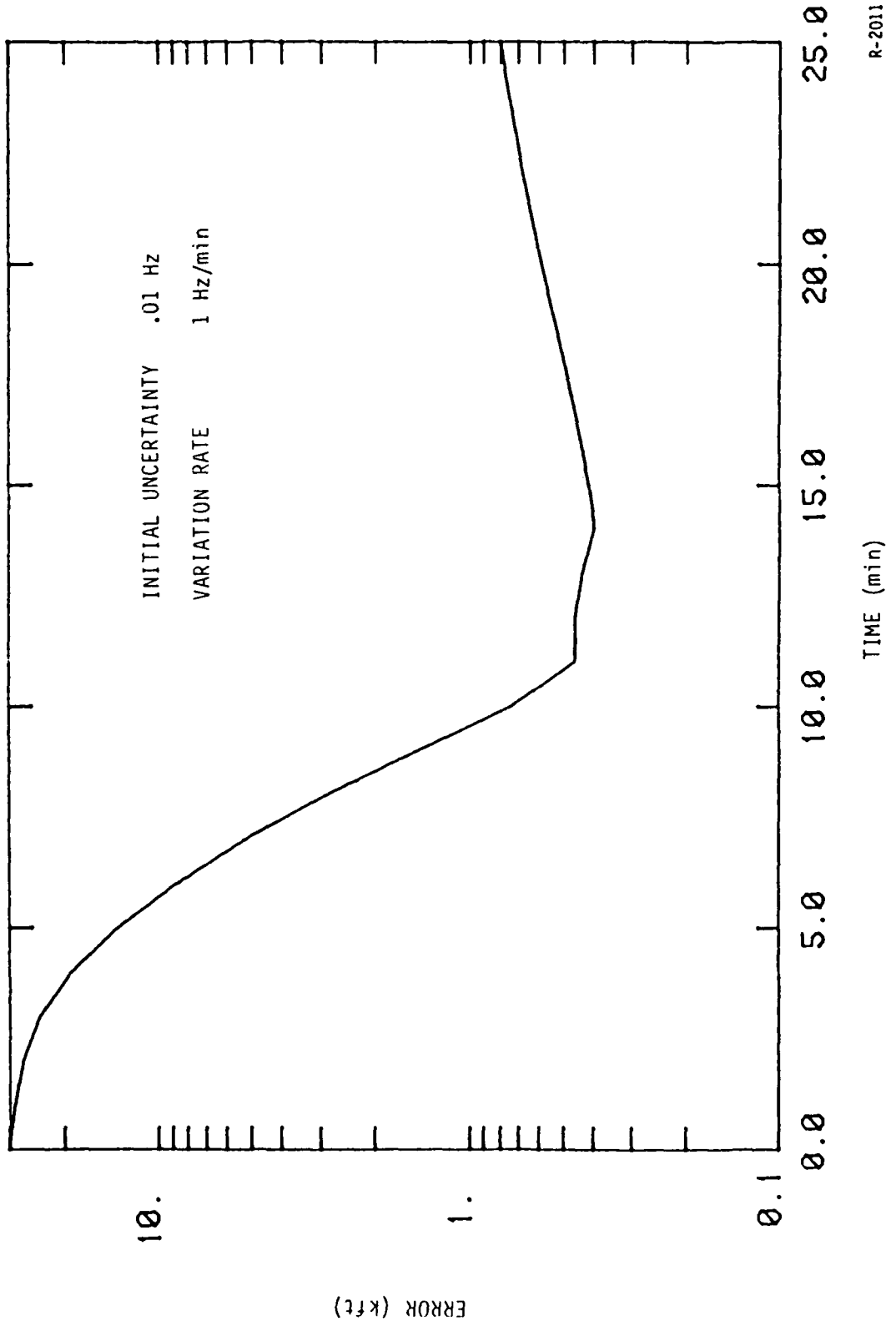

Figure 2-12. Frequency Effect on Position Error

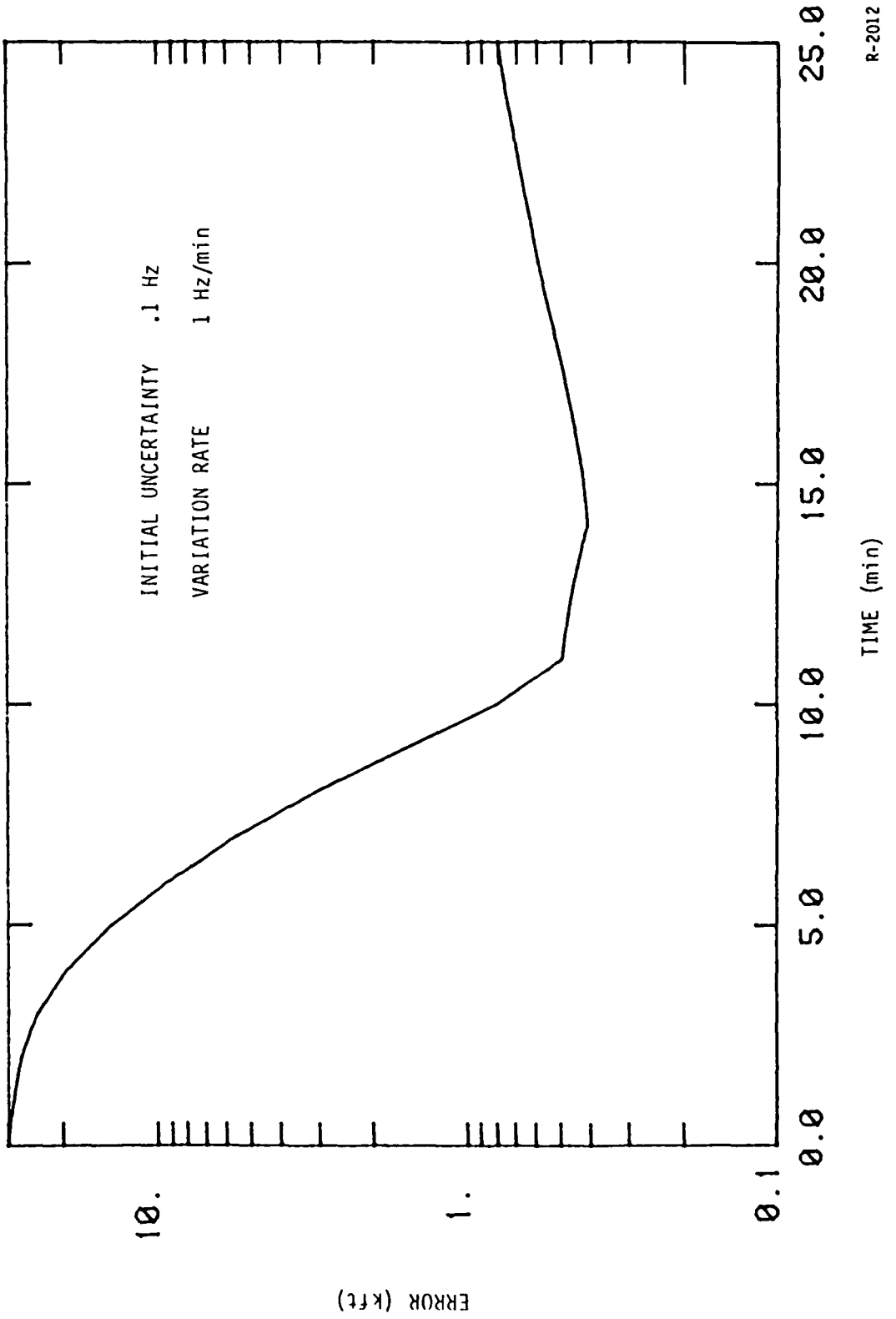

Figure 2-13. Frequency Effect on Position Error

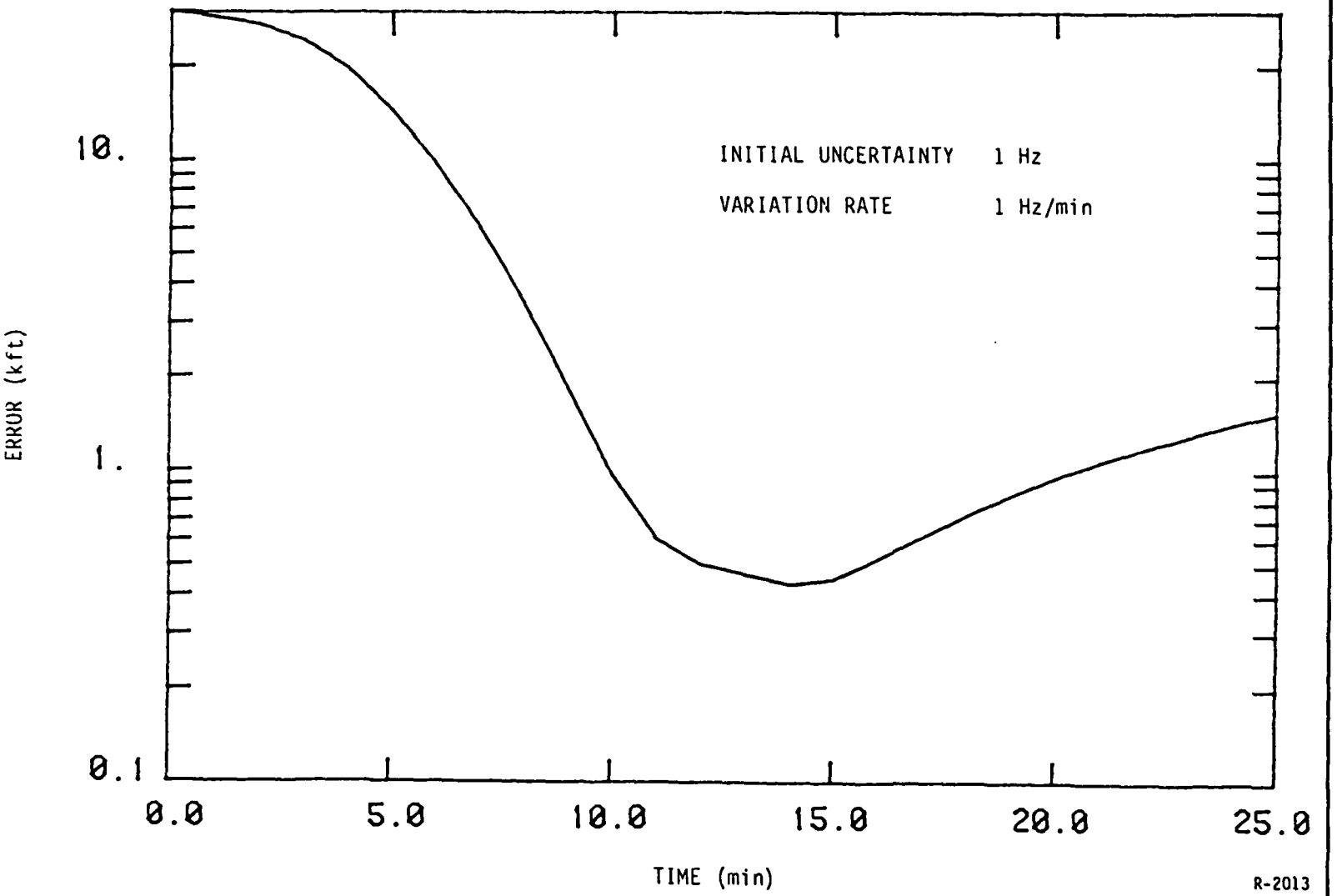

ALPHATECH, INC.

Figure 2-14. Frequency Effect on Position Error

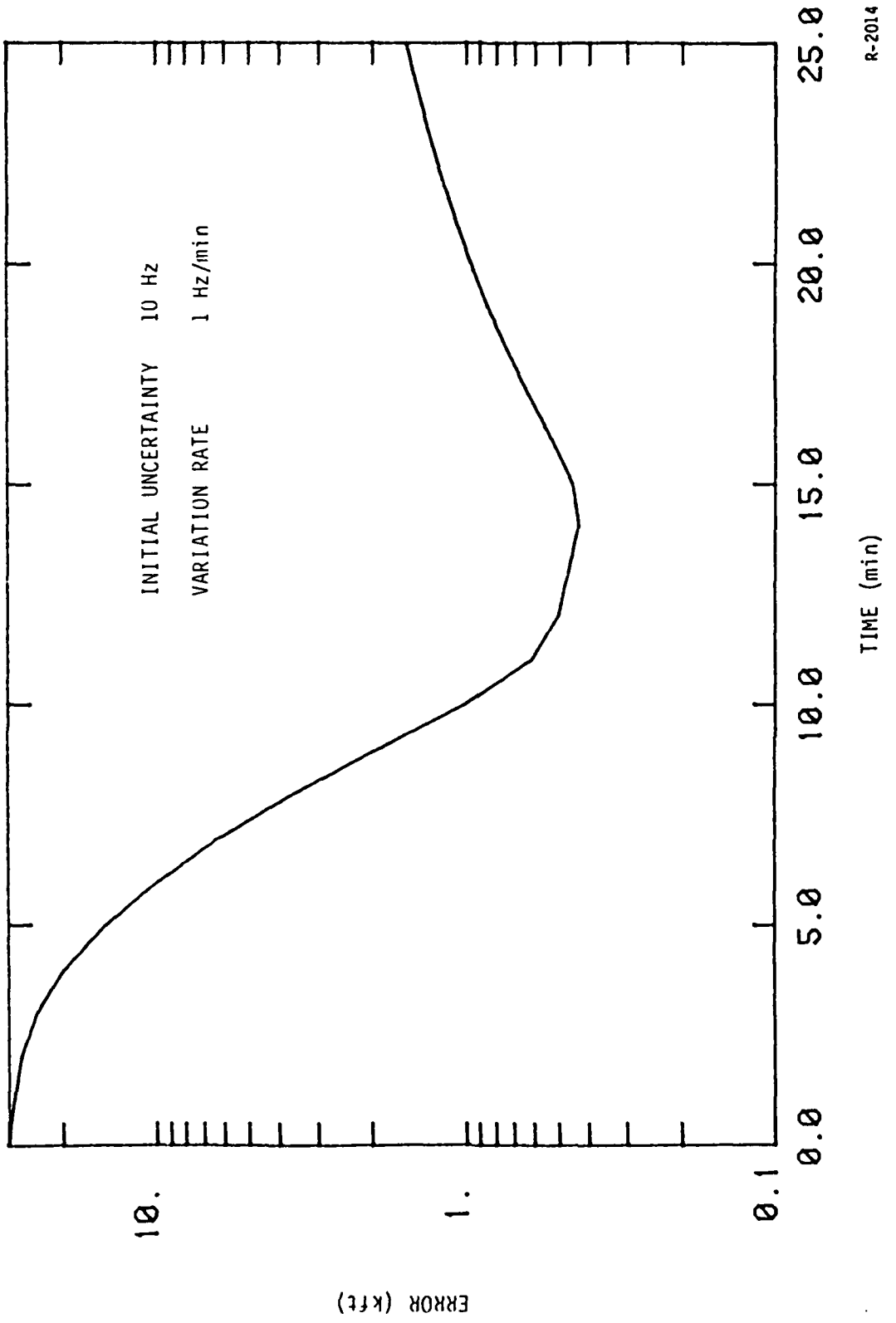

Figure 2-15. Frequency Effect on Position Error

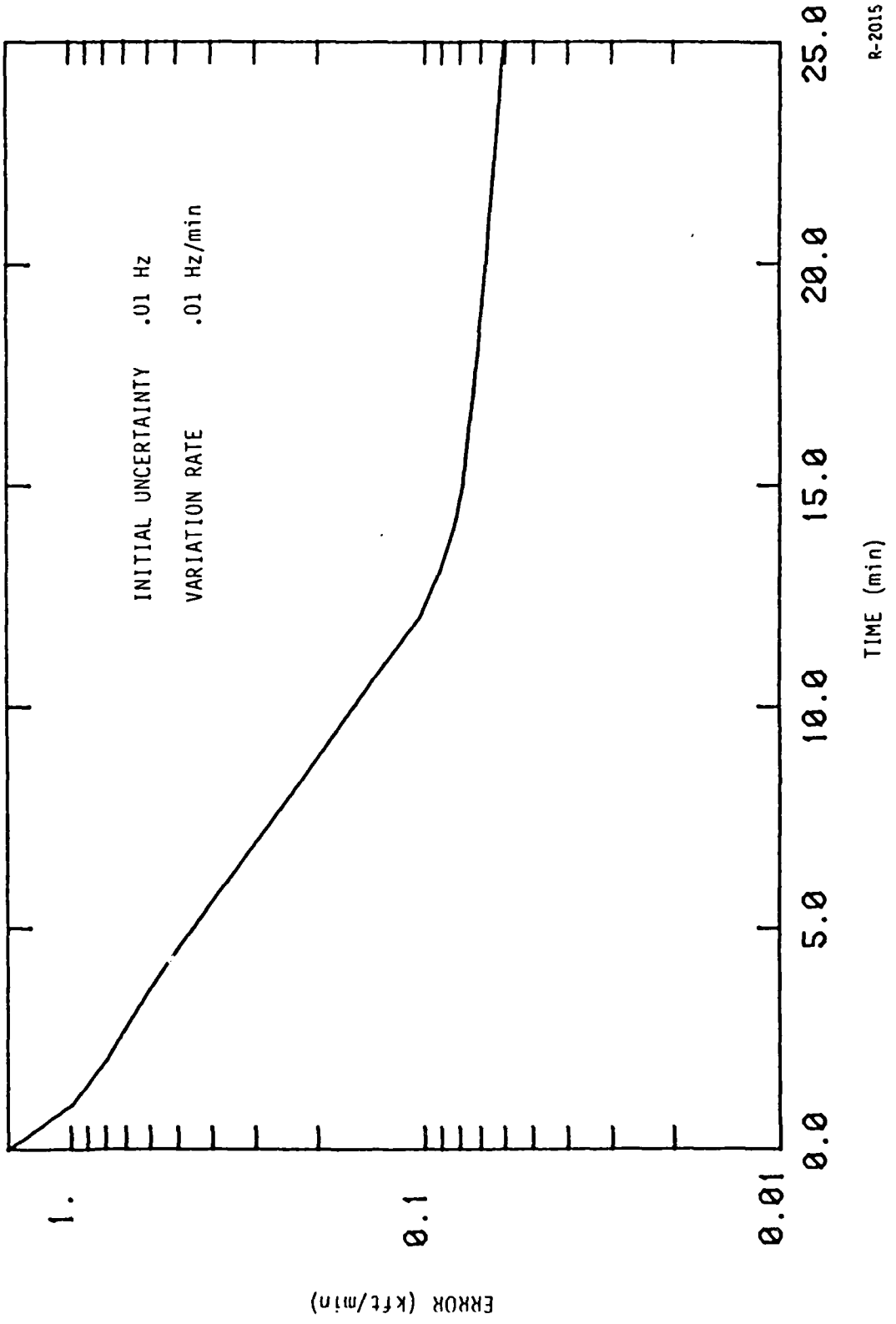

Figure 2-16. Frequency Effect on Velocity Error

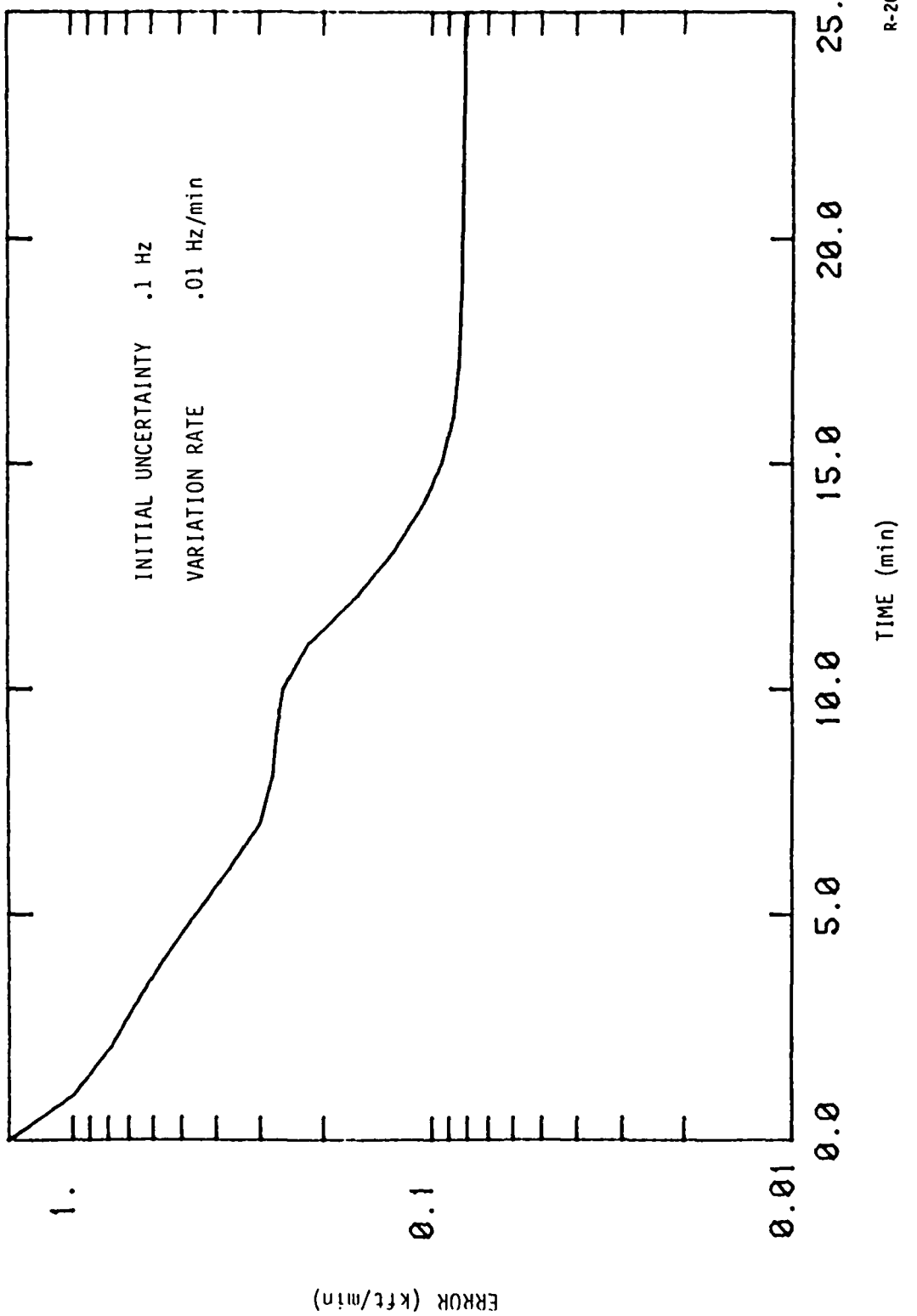

Figure 2-17. Frequency Effect on Velocity Error

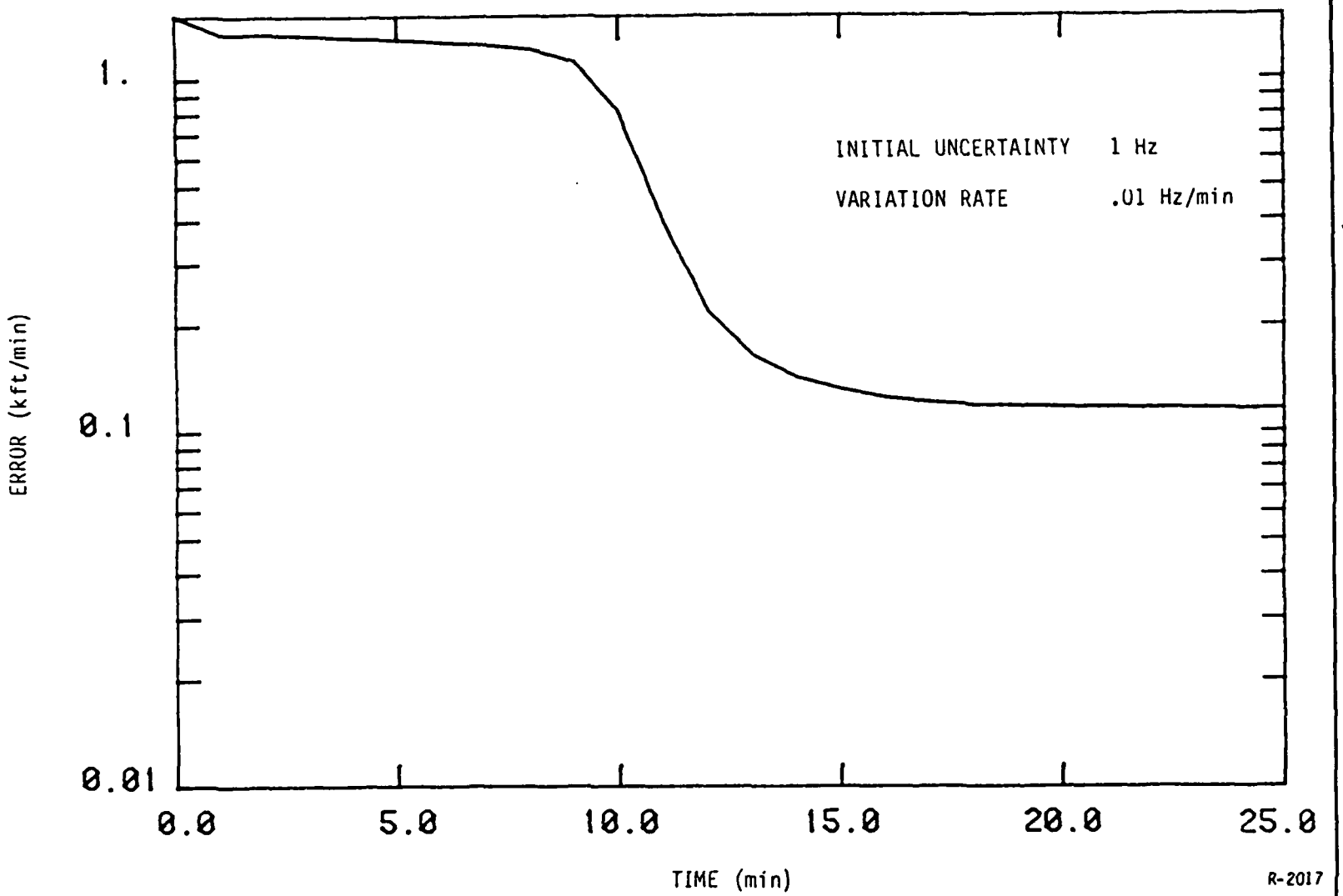

Figure 2-18. Frequency Effect on Velocity Error

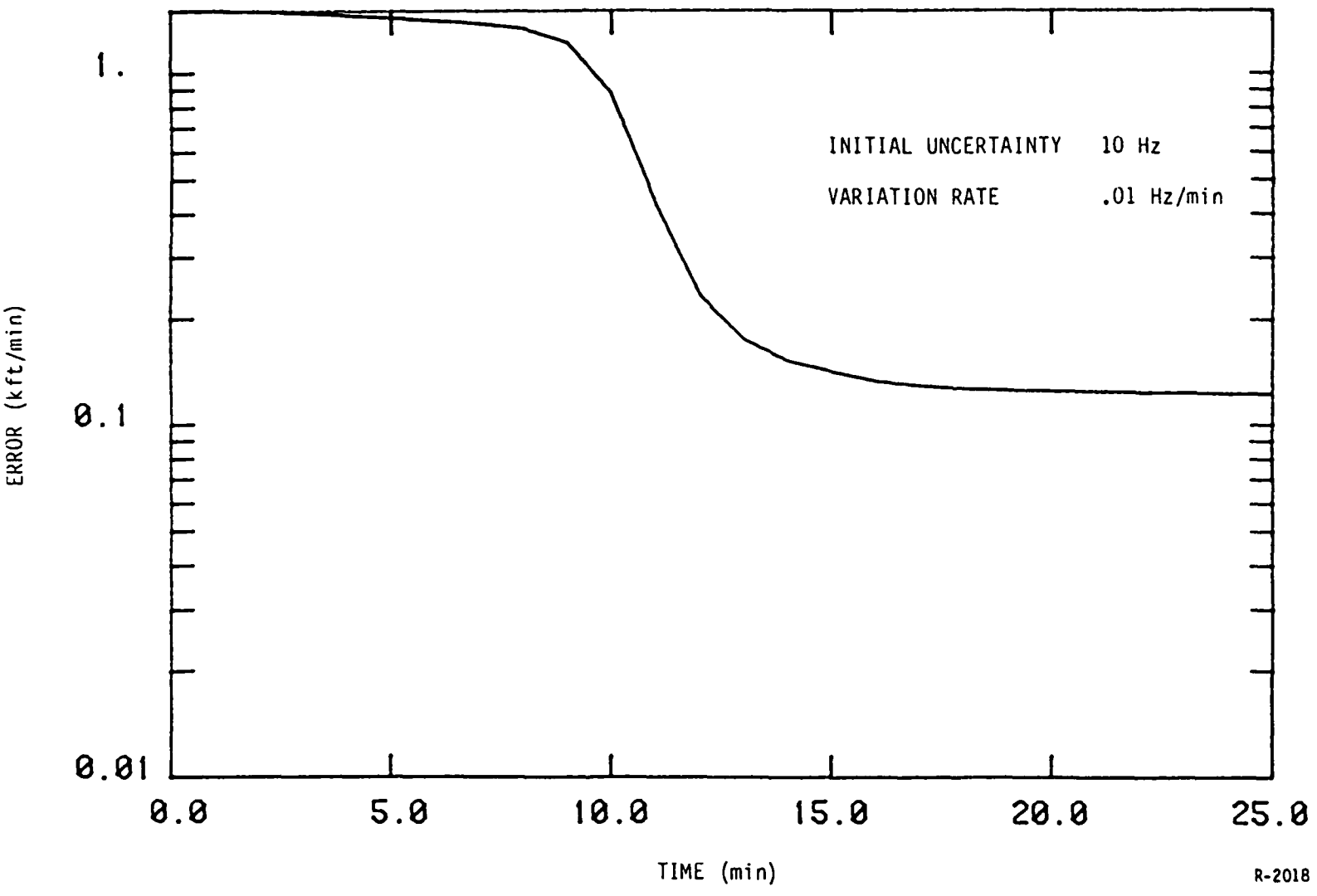

Figure 2-19. Frequency Effect on Velocity Error

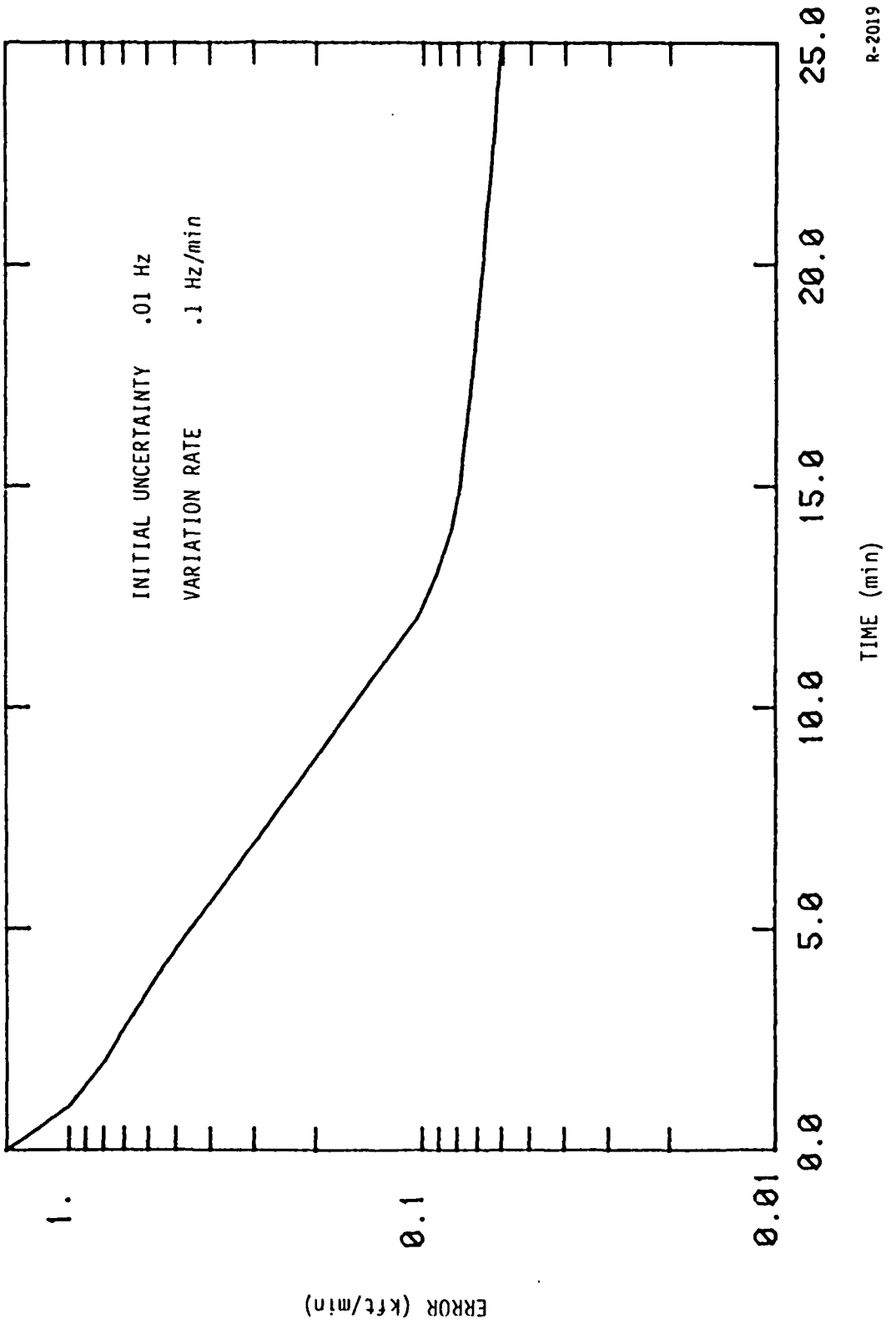

Figure 2-20. Frequency Effect on Velocity Error

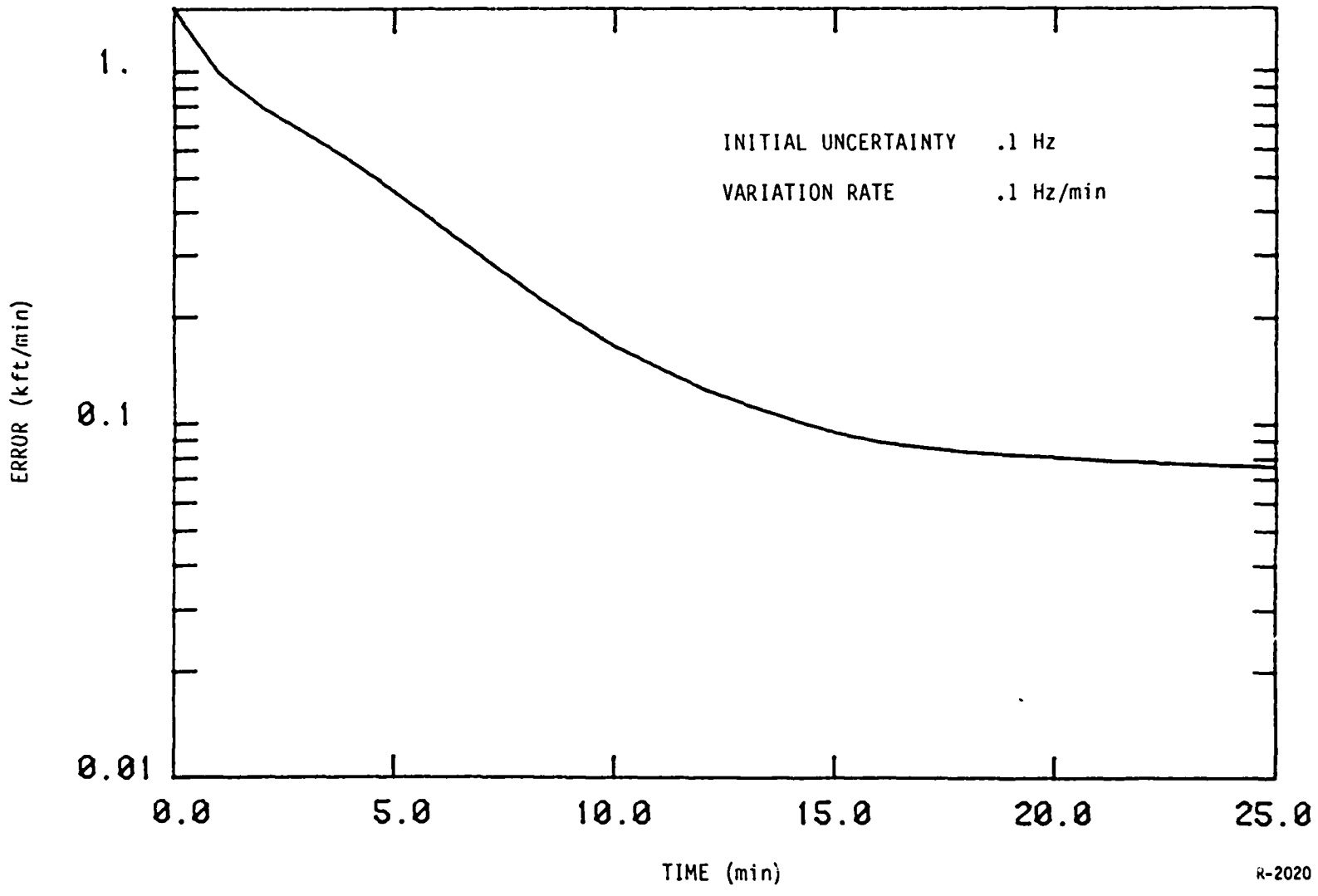

Figure 2-21. Frequency Effect on Velocity Error

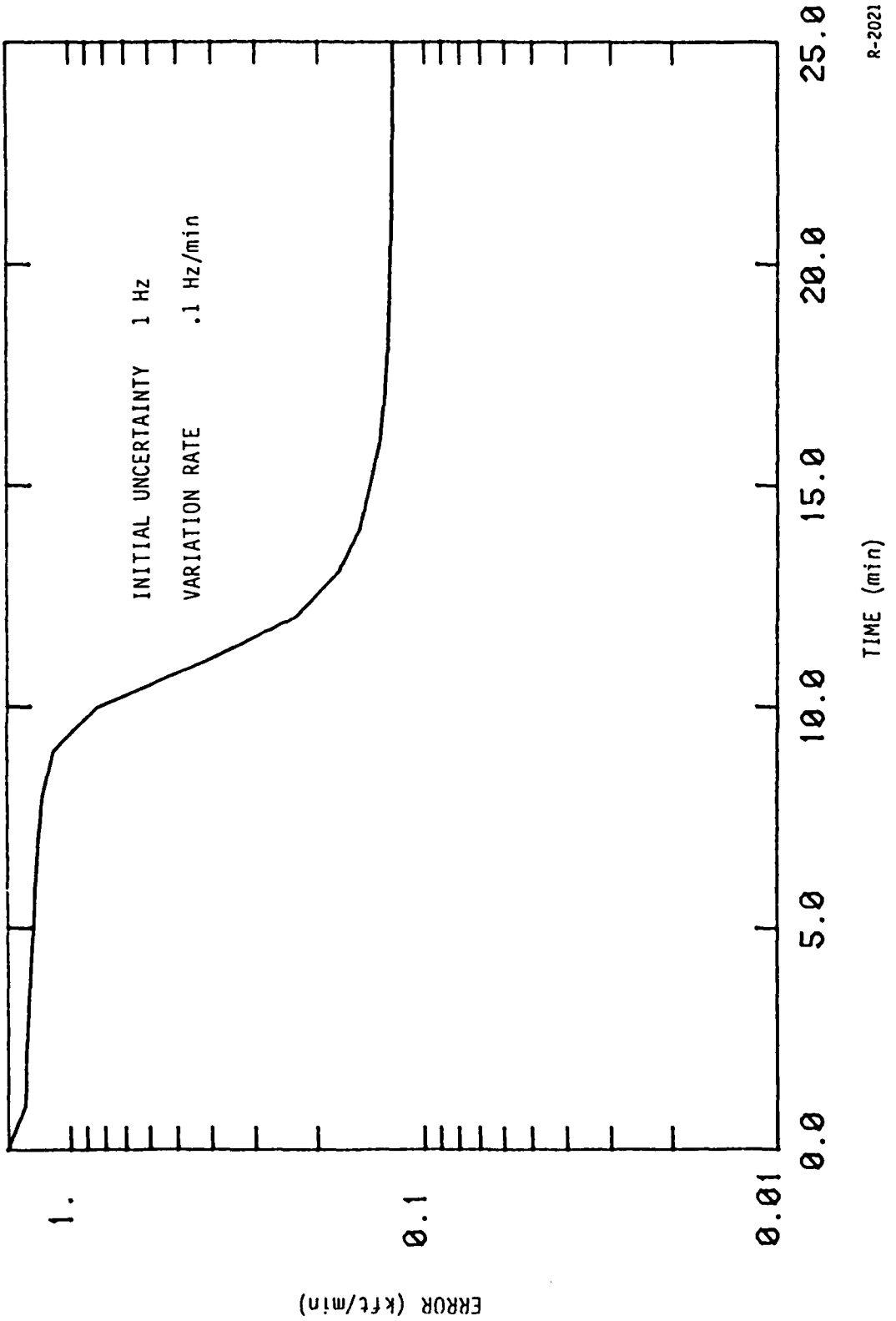

Figure 2-22. Frequency Effect on Velocity Error

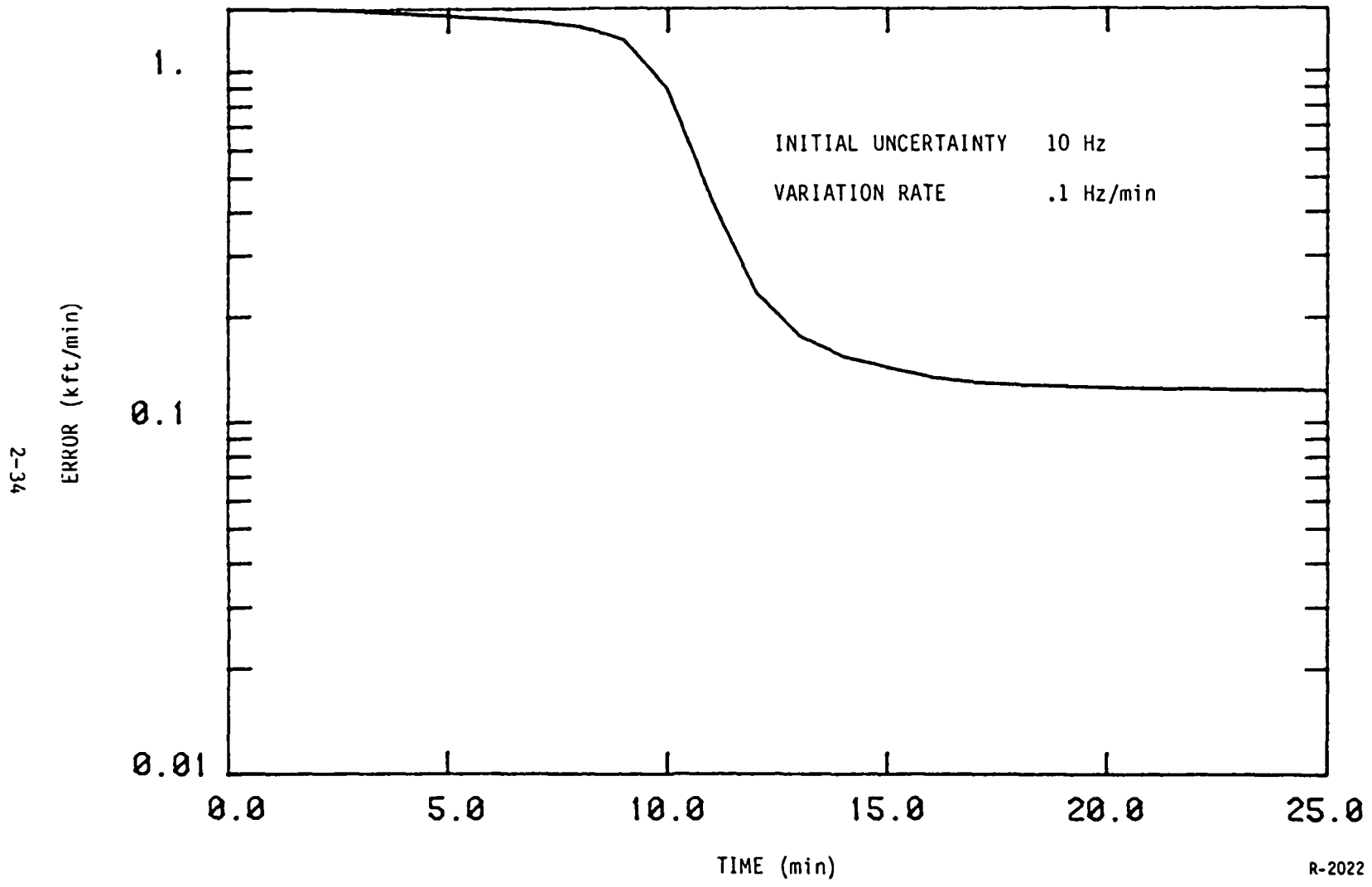

ALPHATECH, INC.

Figure 2-23. Frequency Effect on Velocity Error

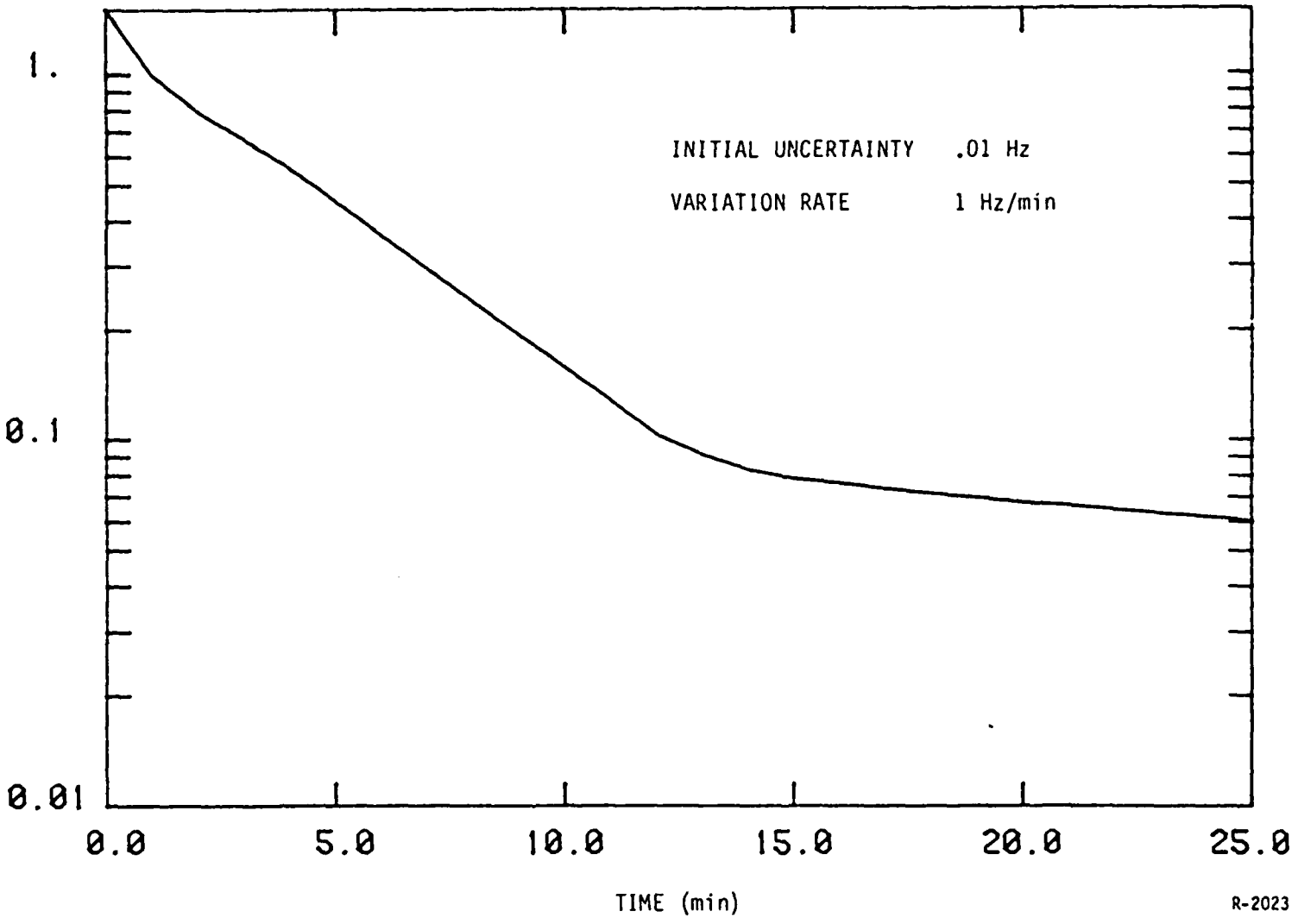

Figure 2-24. Frequency Effect on Velocity Error

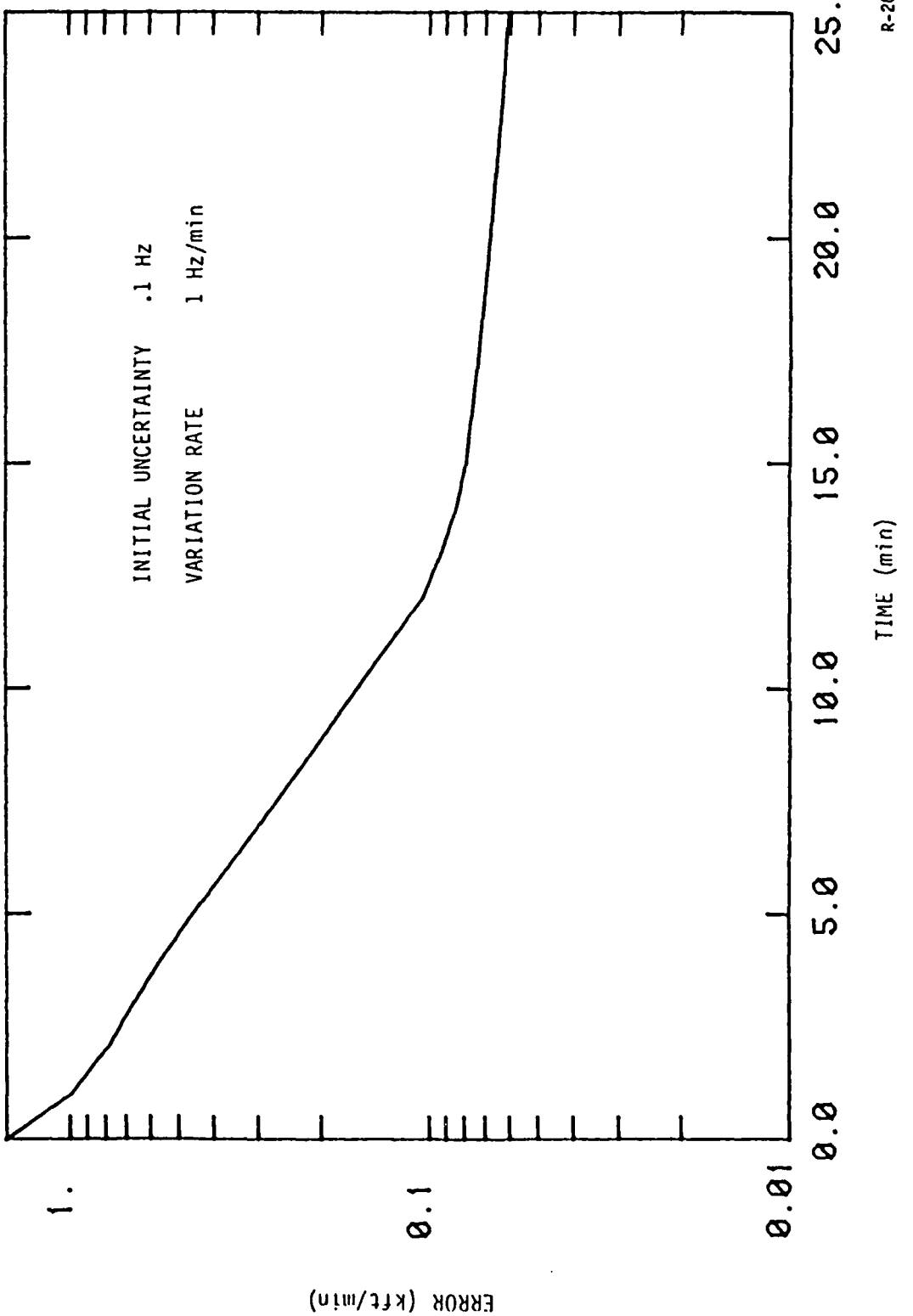

Figure 2-25. Frequency Effect on Velocity Error

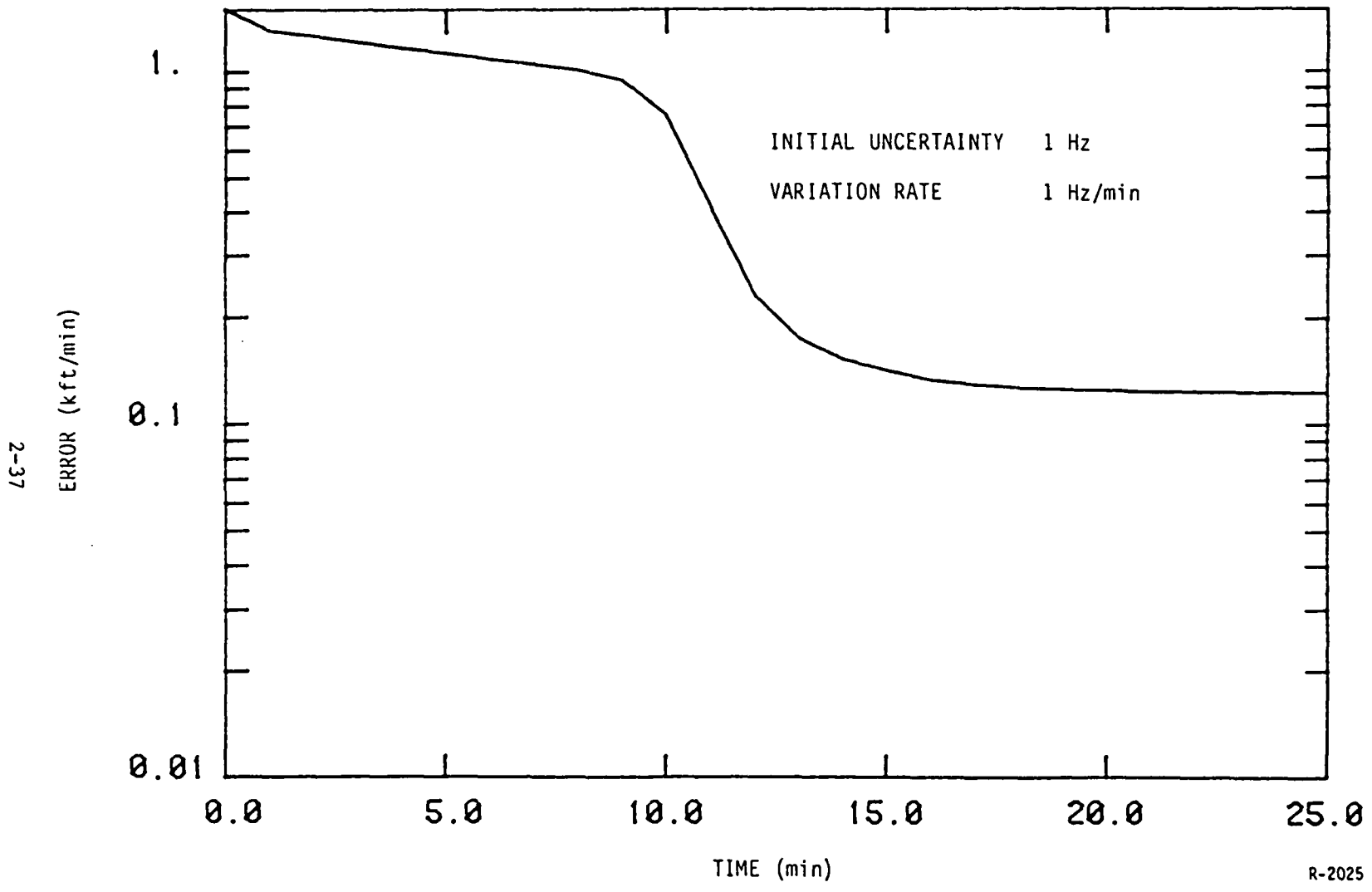

Figure 2-26. Frequency Effect on Velocity Error

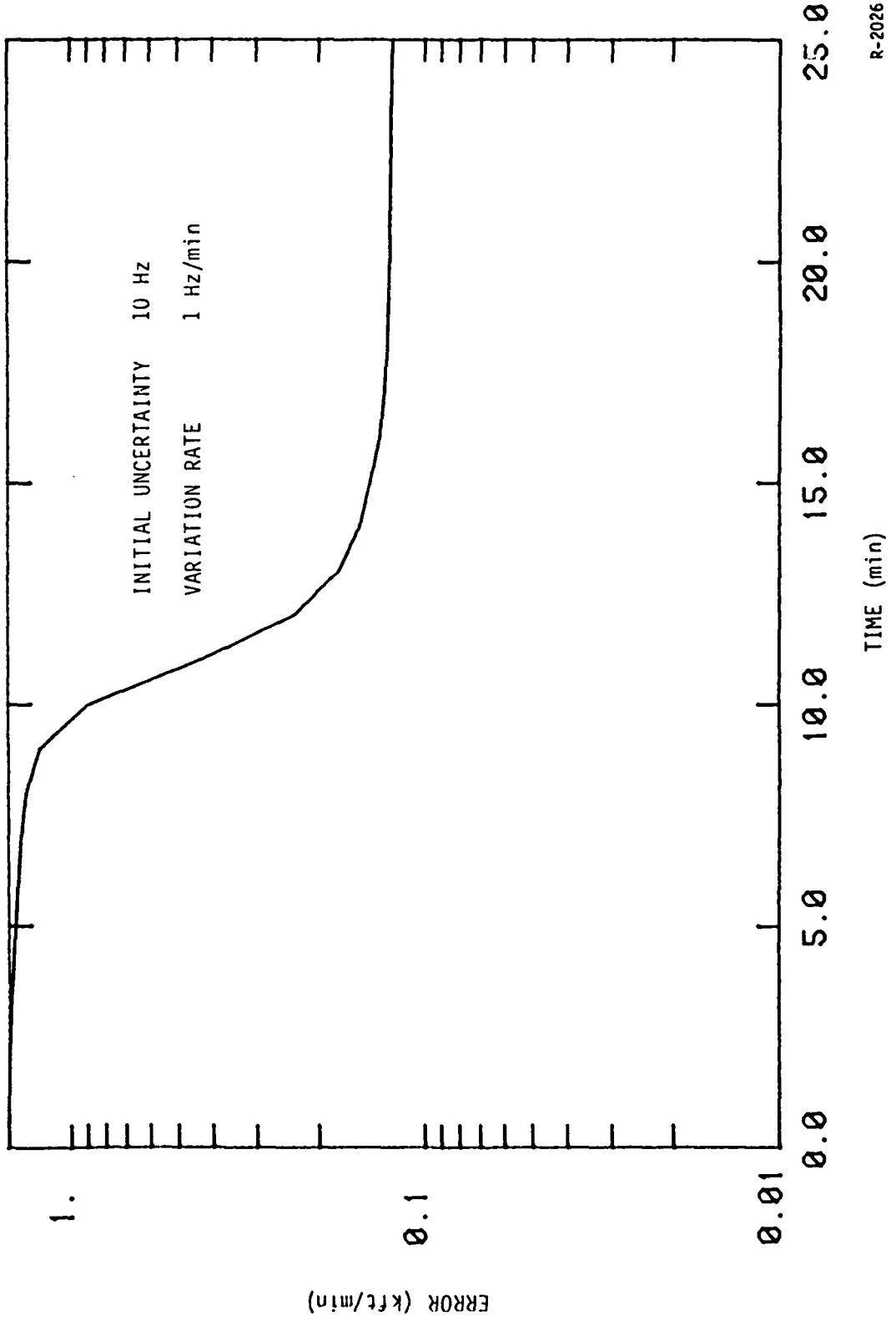

Figure 2-27. Frequency Effect on Velocity Error

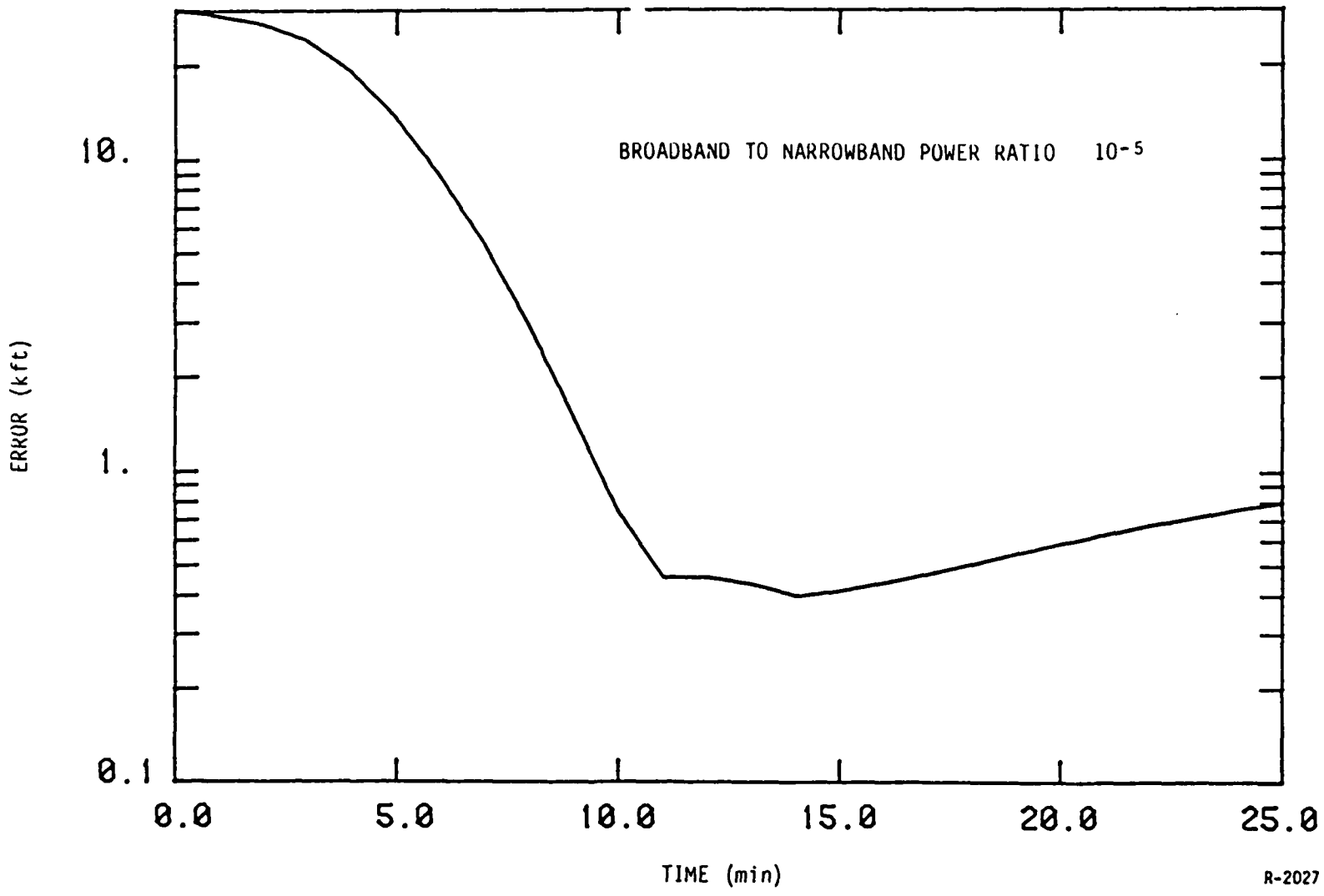

Figure 2-28. Broadband Effect on Position Error

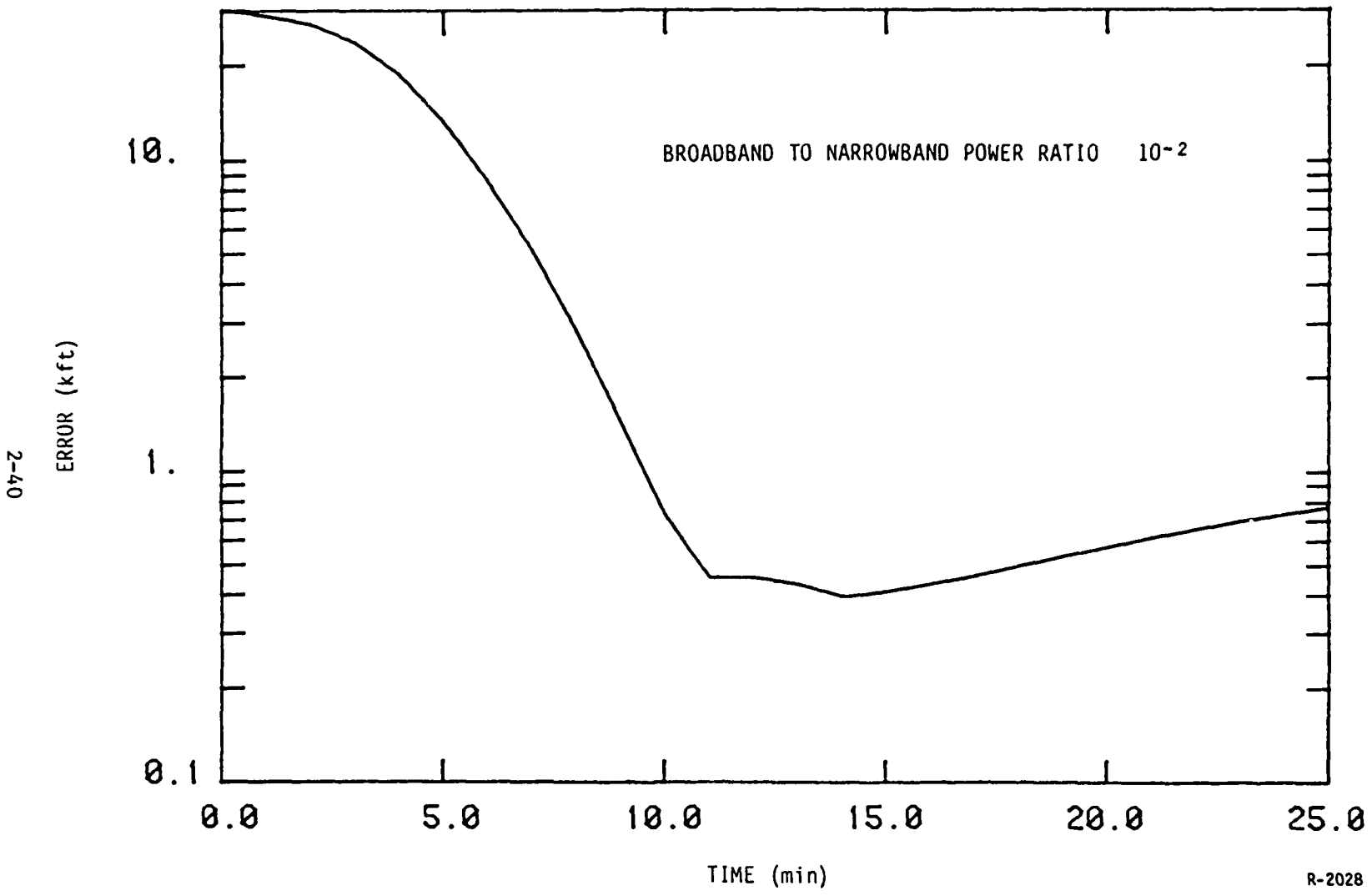

Figure 2-29. Broadband Effect on Position Error

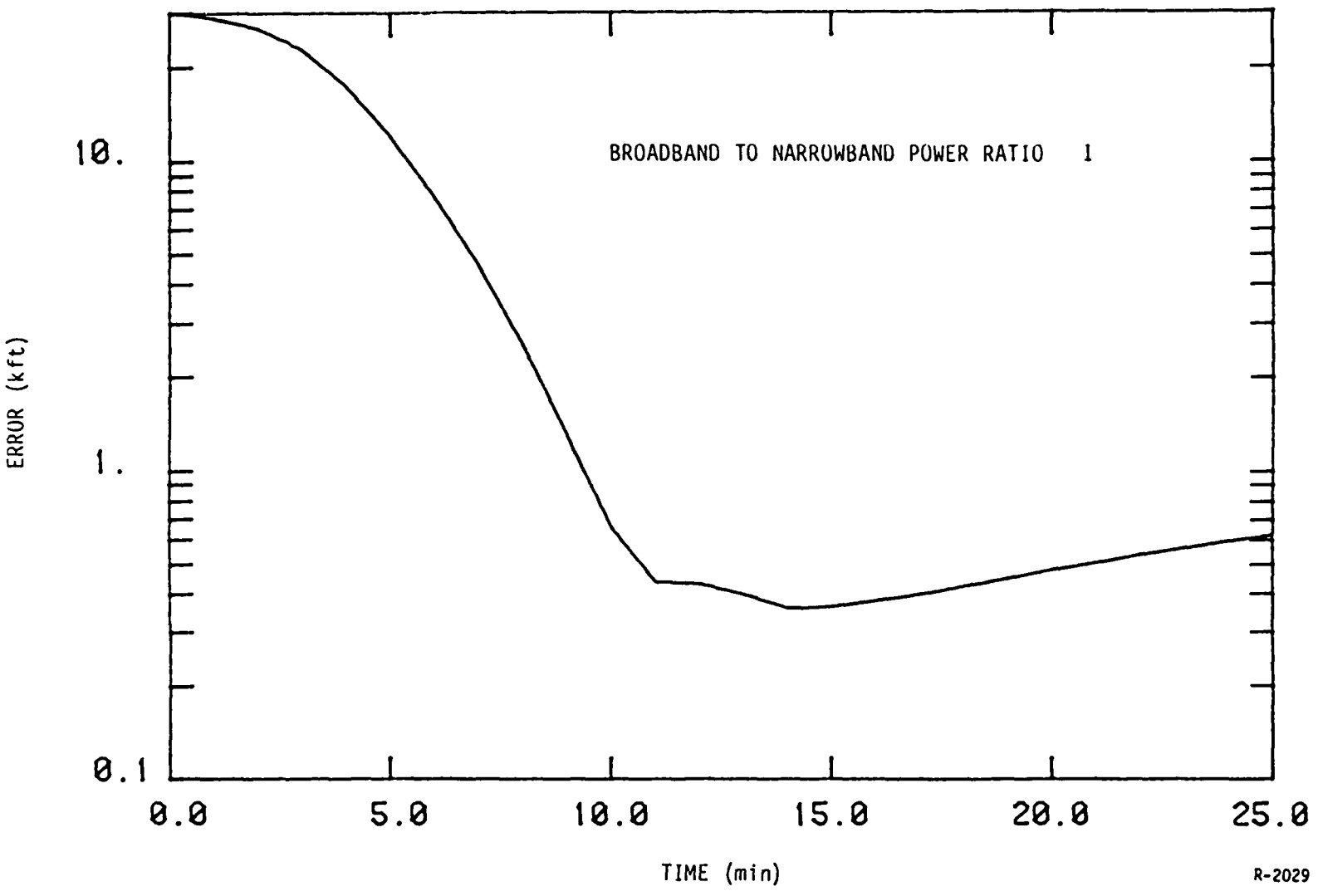

Figure 2-30. Broadband Effect on Position Error

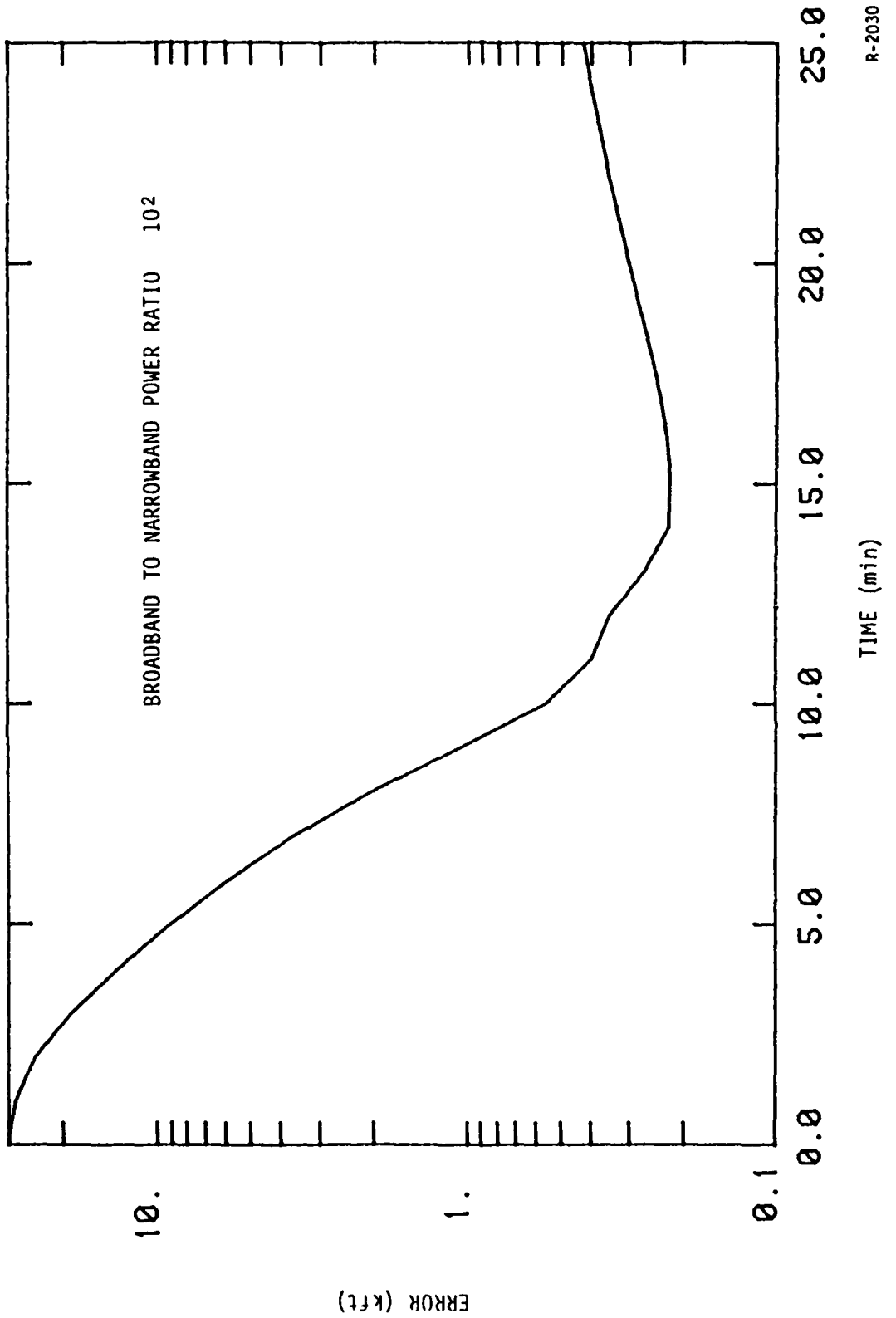

Figure 2-31. Broadband Effect on Position Error

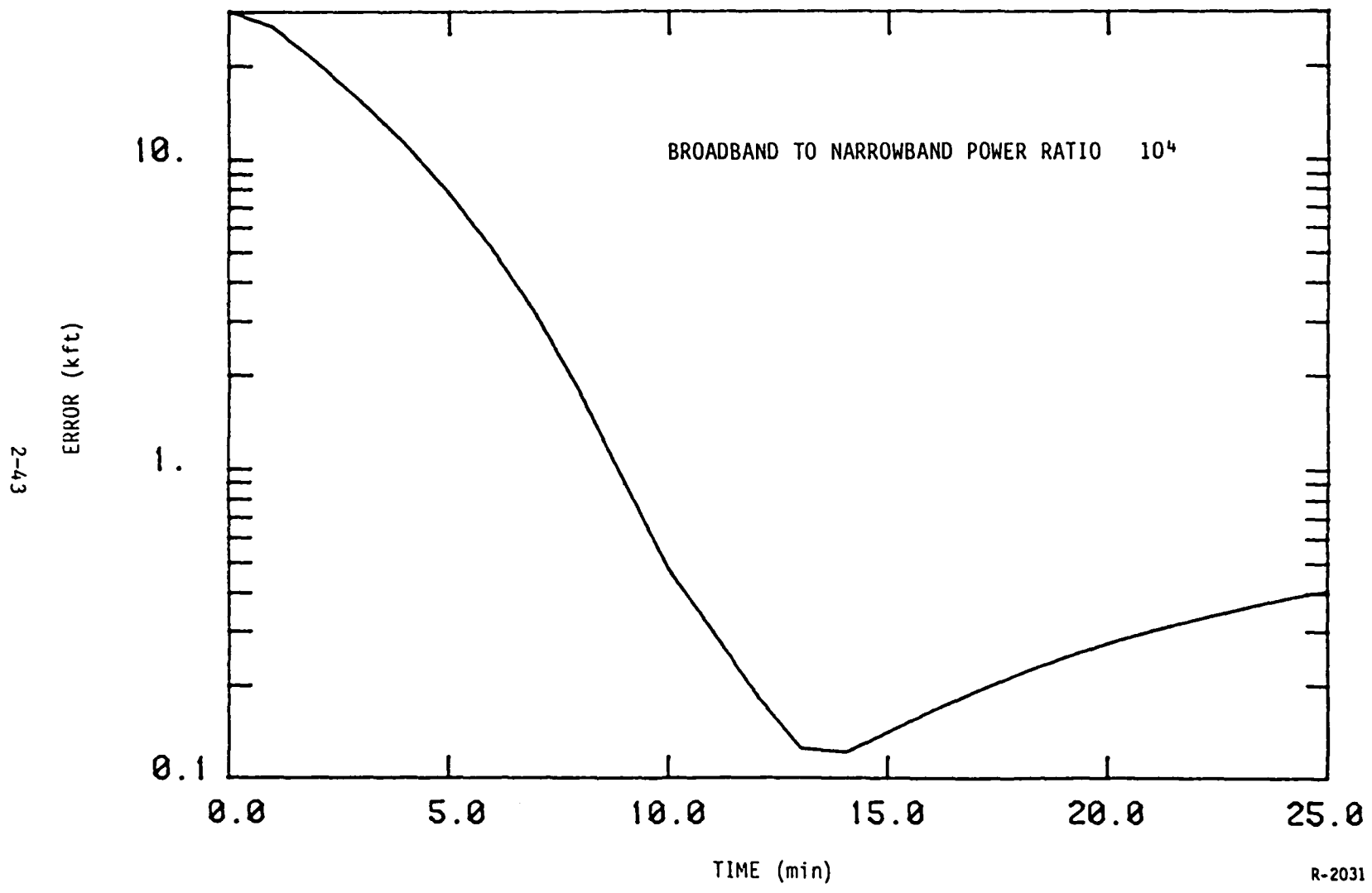

Figure 2-32. Broadband Effect on Position Error

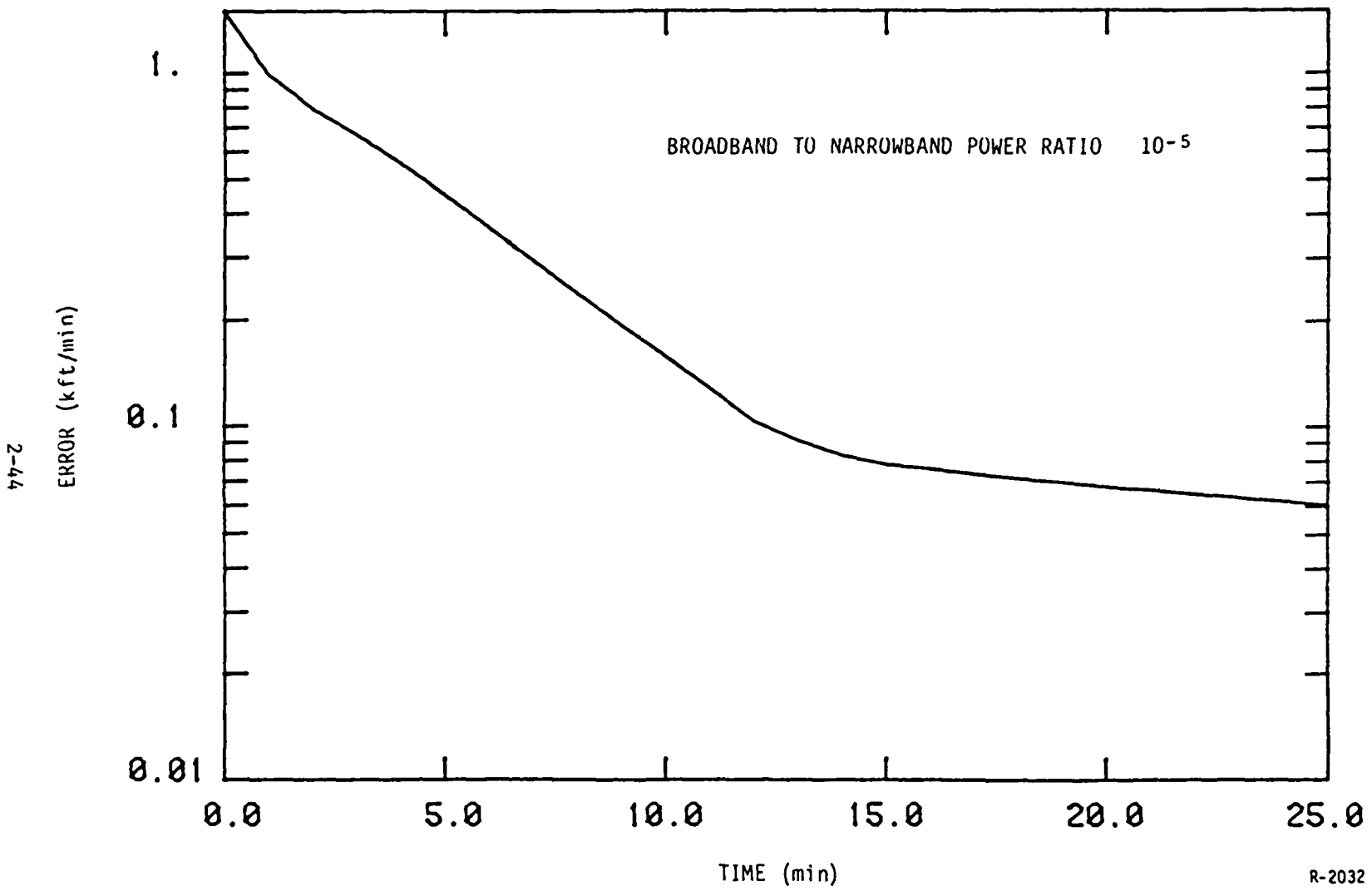

Figure 2-33. Broadband Effect on Velocity Error

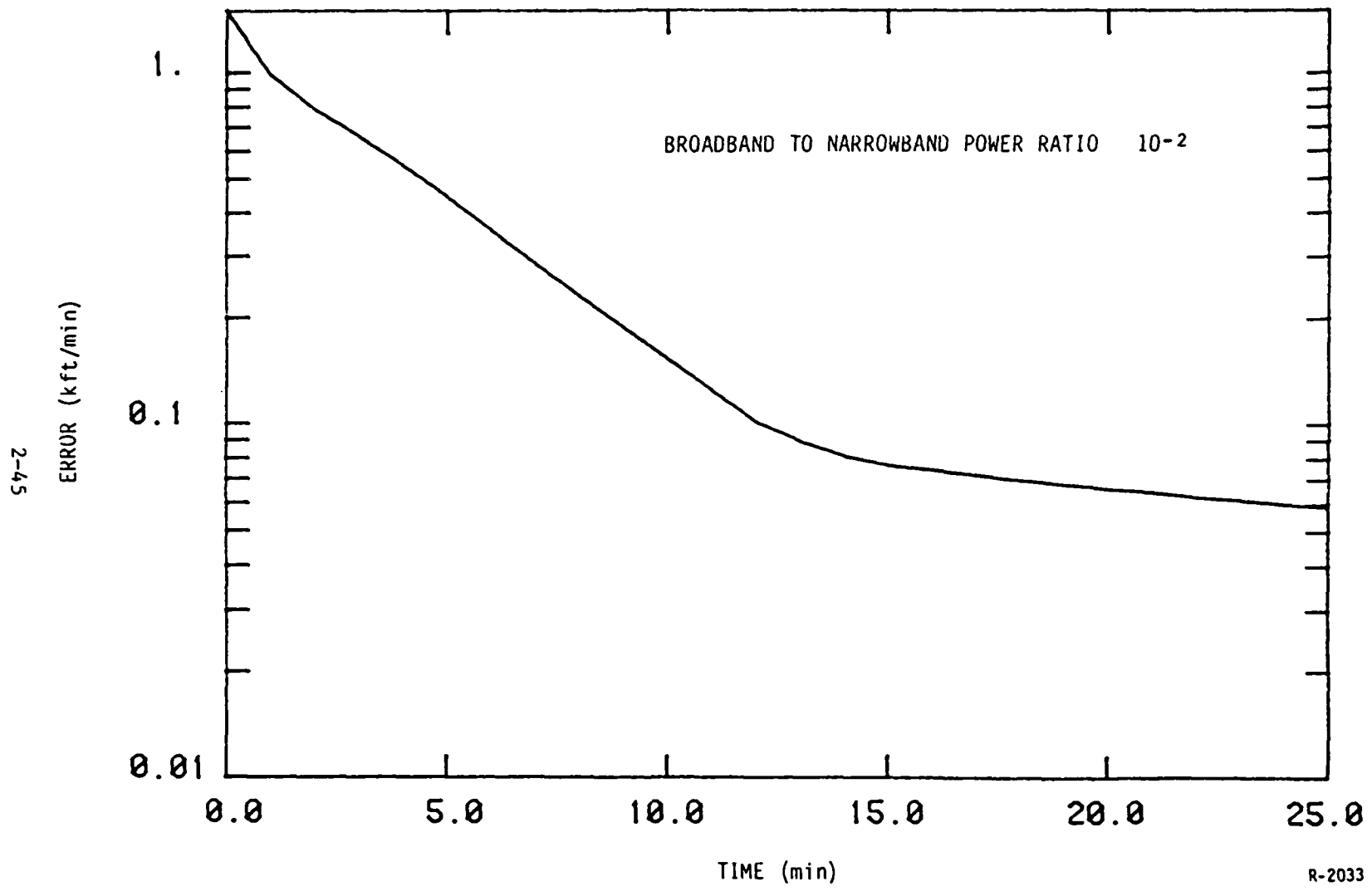

Figure 2-34. Broadband Effect on Velocity Error

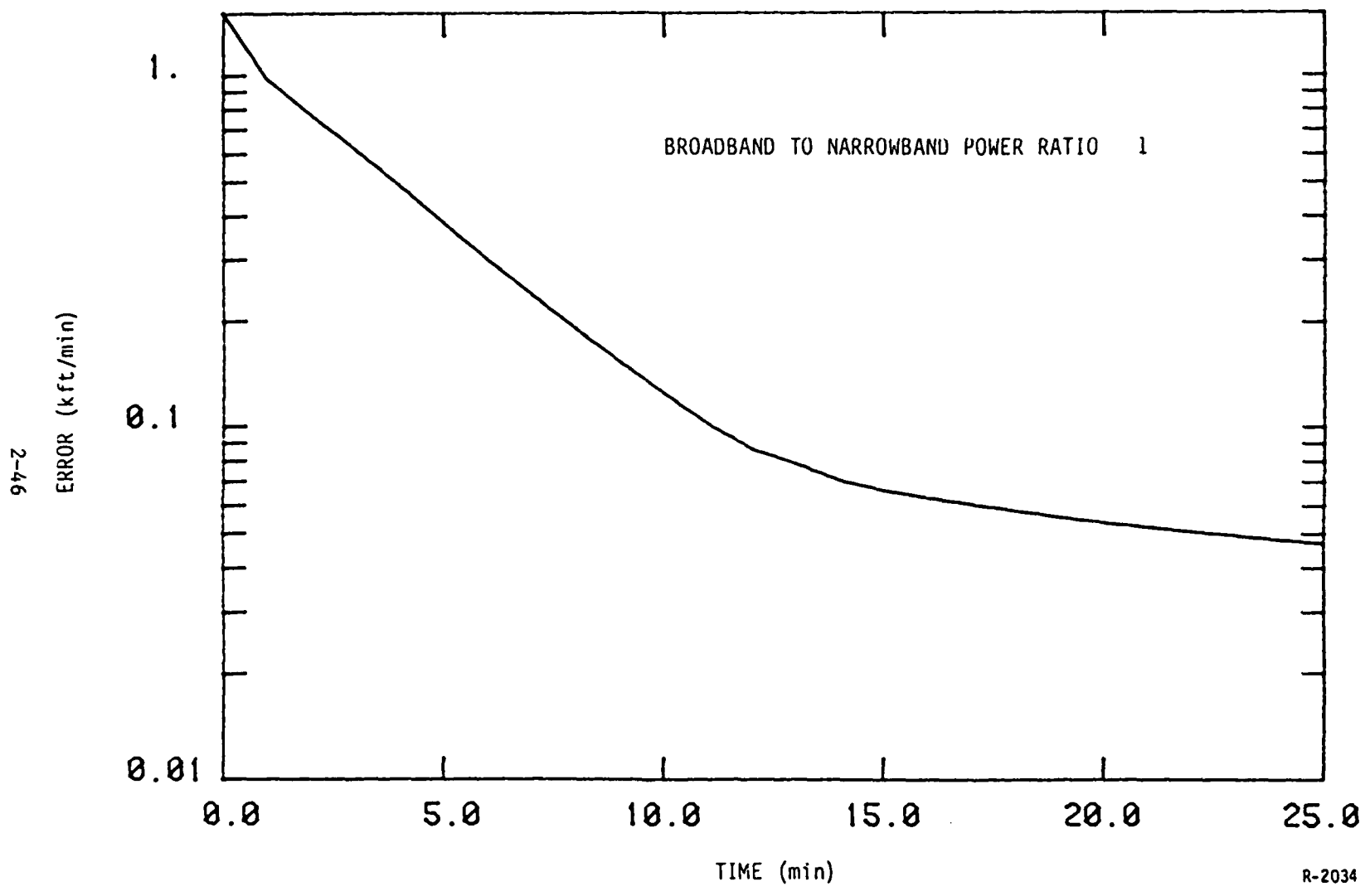

Figure 2-35. Broadband Effect on Velocity Error

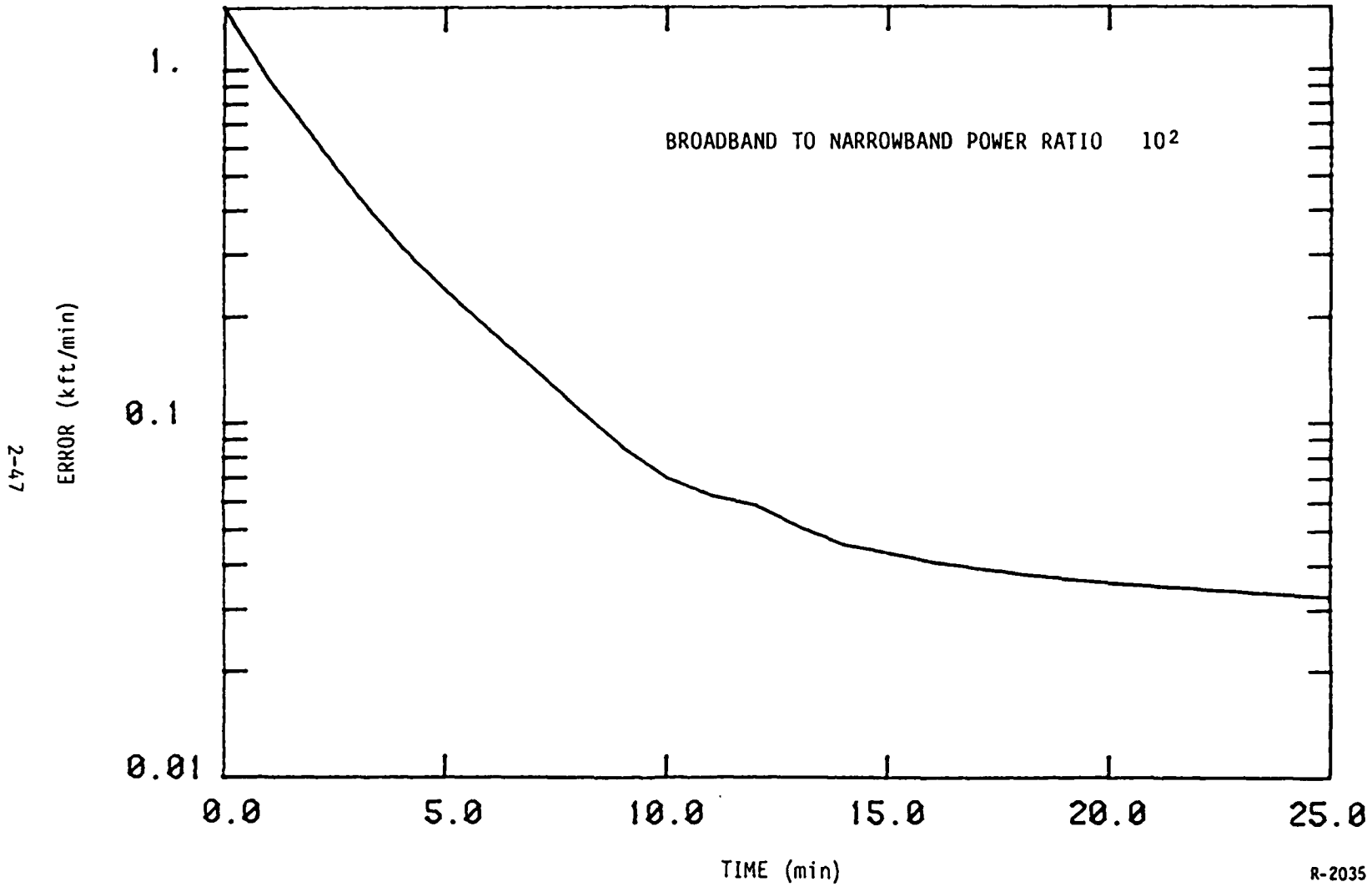

Figure 2-36. Broadband Effect on Velocity Error

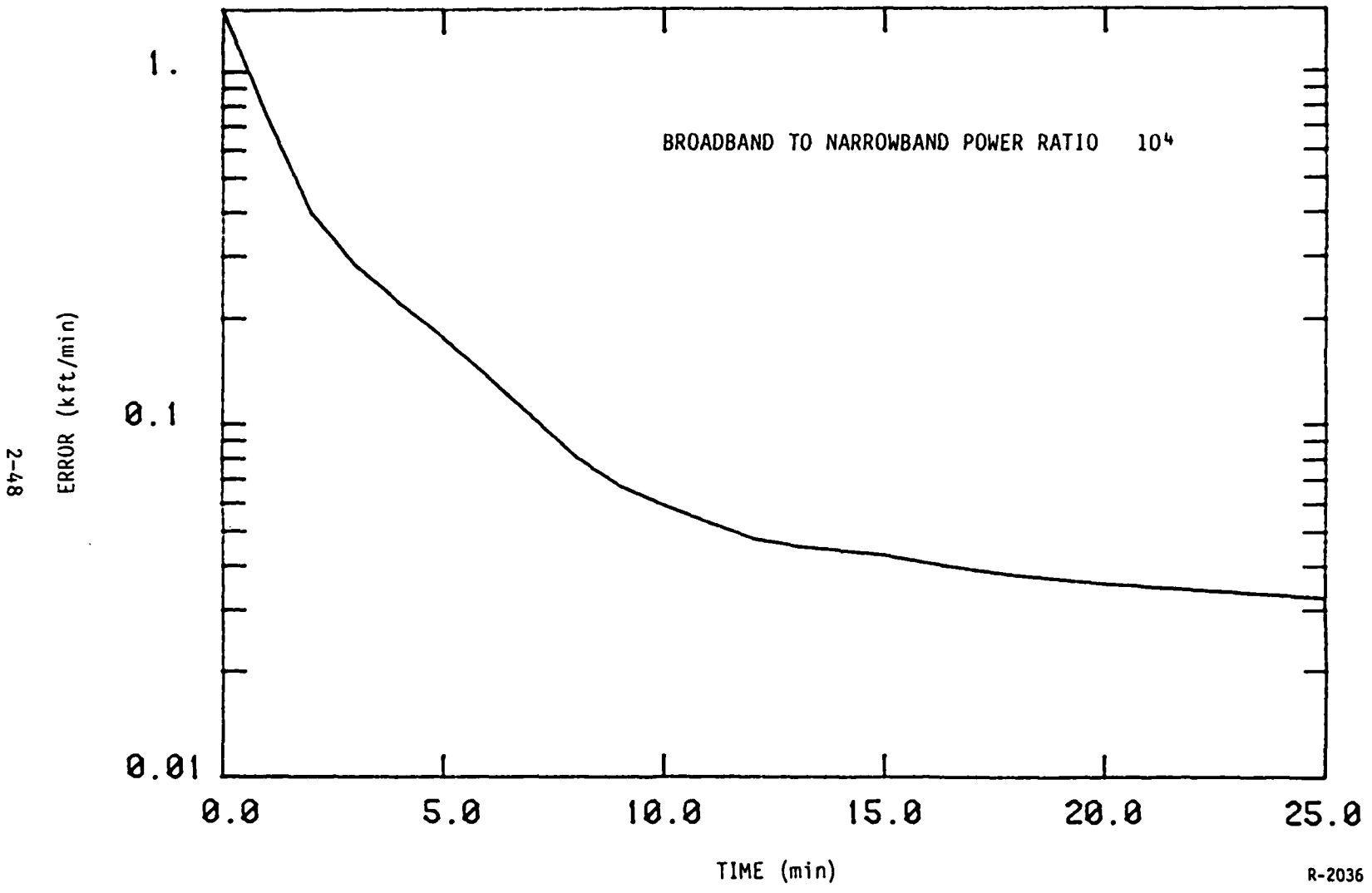

Figure 2-37. Broadband Effect on Velocity Error

SECTION 3

RATE DISTORTION PERFORMANCE ANALYSIS

3.1 INTRODUCTION

This section discusses the rate distortion theory approach to analyze mean square error in statistical nonlinear estimation problems. We present here preliminary results for static estimation problems and compare the rate distortion and Cramer-Rao-Van Trees approaches. Based on preliminary results, the rate distortion method gives a computable lower bound which is tighter than the Cramer-Rao-Van Trees lower bound in the regime of low signal-to-noise ratio.

This section is organized as follows. Subsection 3.2 presents the necessary background in communication and rate distortion theory. It also sketches the communication system approach to statistical estimation problems. Subsection 3.3 investigates the static estimation problem with a scalar state. Subsection 3.4 extends this to the vector state case.

Finally, subsection 3.5 concludes the section, discussing other work and directions for further investigation.

3.2 INFORMATION THEORY BACKGROUND

3.2.1 Communication Theory Point of View

Communication theory provides a useful interpretation of tracking problems different from the more conventional statistical estimation theory point of view. The block diagram of a communication system is shown in Fig. 3-1.

Messages are generated by a source and coded by an encoder. The encoded messages are transmitted through a channel, decoded by a decoder, and received by a user. In communication problems the source, channel, and user are specified, and the problem is to design encoder and decoder so that messages received by the user are accurate reproductions of the messages generated by the source.

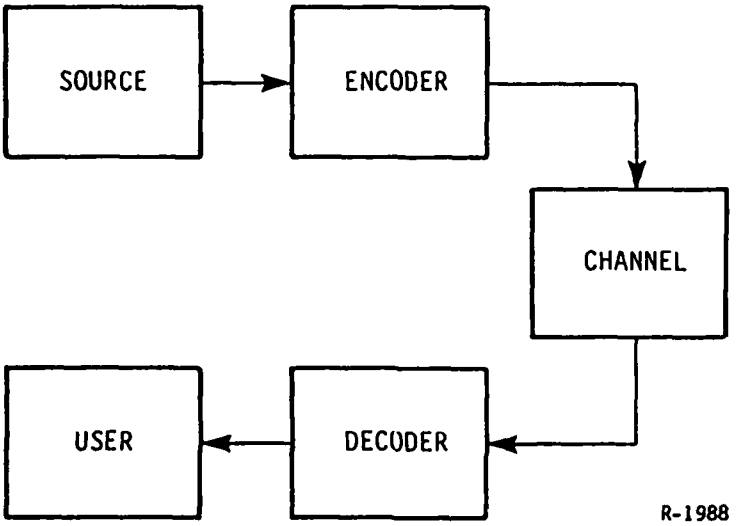

Figure 3-1. Communication System Block Diagram

Figure 3-2 shows how one can interpret a tracking system as a type of communication system. In this interpretation the message generated by the source is a set of target parameters (e.g., positions and velocities at a given time). The encoder for passive tracking problems does nothing to code the source message. In active tracking we can control the encoder to some extent (e.g., increase signal strength). The encoder and channel for the tracking problem represent the transformation between target parameters and sensor outputs.

One might also include preprocessing of sensor outputs as part of the channel if that preprocessing is already specified. Finally, the decoder for the tracking problem is the tracking algorithm which provides estimates of target parameters to a user. In tracking problems the source (target model), encoder and channel (measurement model), and user are specified, and the problem is to design a decoder (tracking algorithm) so that estimates received by the user are accurate reproductions of the parameters generated by the source.

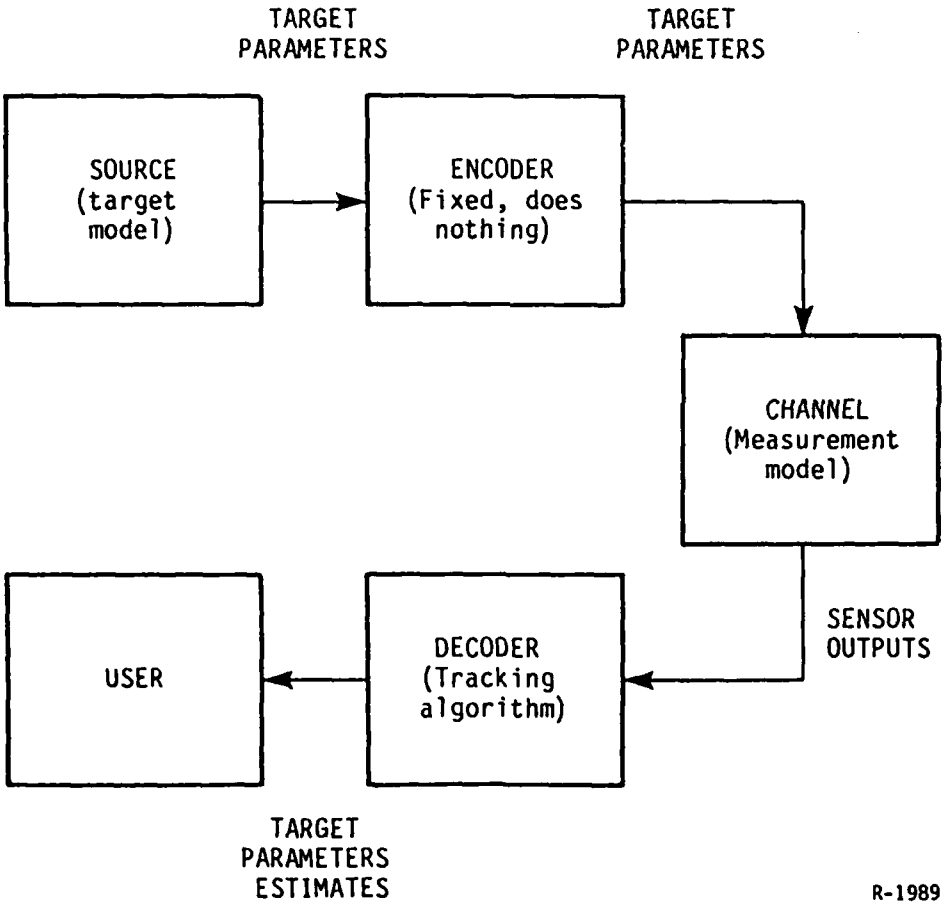

Figure 3-2. Communication System Interpretation of Tracking System

The communication theory viewpoint is useful because it allows us to apply to the tracking problem techniques of information theory which do not exist in statistical estimation theory. The techniques relevant to tracking performance analysis involve rate distortion theory [4] first developed by Shannon [5],[6]. Distortion is a measure of the average error between the message generated by the source and the decoded message received by the user. In a tracking problem it could be the mean square error in the tracking algorithm's target parameter estimates. An important question about a communication problem is: given a source, channel, and user, under what conditions is it possible to design an encoder and decoder that reproduce the source output for the user with an average distortion that does not exceed some specified upper limit D? This question is the analog of the tracking performance analysis problem we are interested in: given target and measurement model, under what conditions is it possible to design a tracking system that estimates target parameters with an average error that does not exceed some specified upper limit D?

Rate distortion theory is able to answer the communication system question in a precise and relatively simple way. Associated with the source and user is a function R(D) of D, called the rate distortion function. Associated with the channel is a quantity C called its capacity. One can achieve average distortion D if and only if channel capacity exceeds R(D). A typical rate distortion function is shown in Fig. 3-3. To apply rate distortion theory to the tracking problem we need to find the rate distortion function R(D) associated with the target model and the user-defined error criterion, and find the capacity C associated with the measurement model. These quantities will tell us that an average tracking error smaller than D can be achieved only if

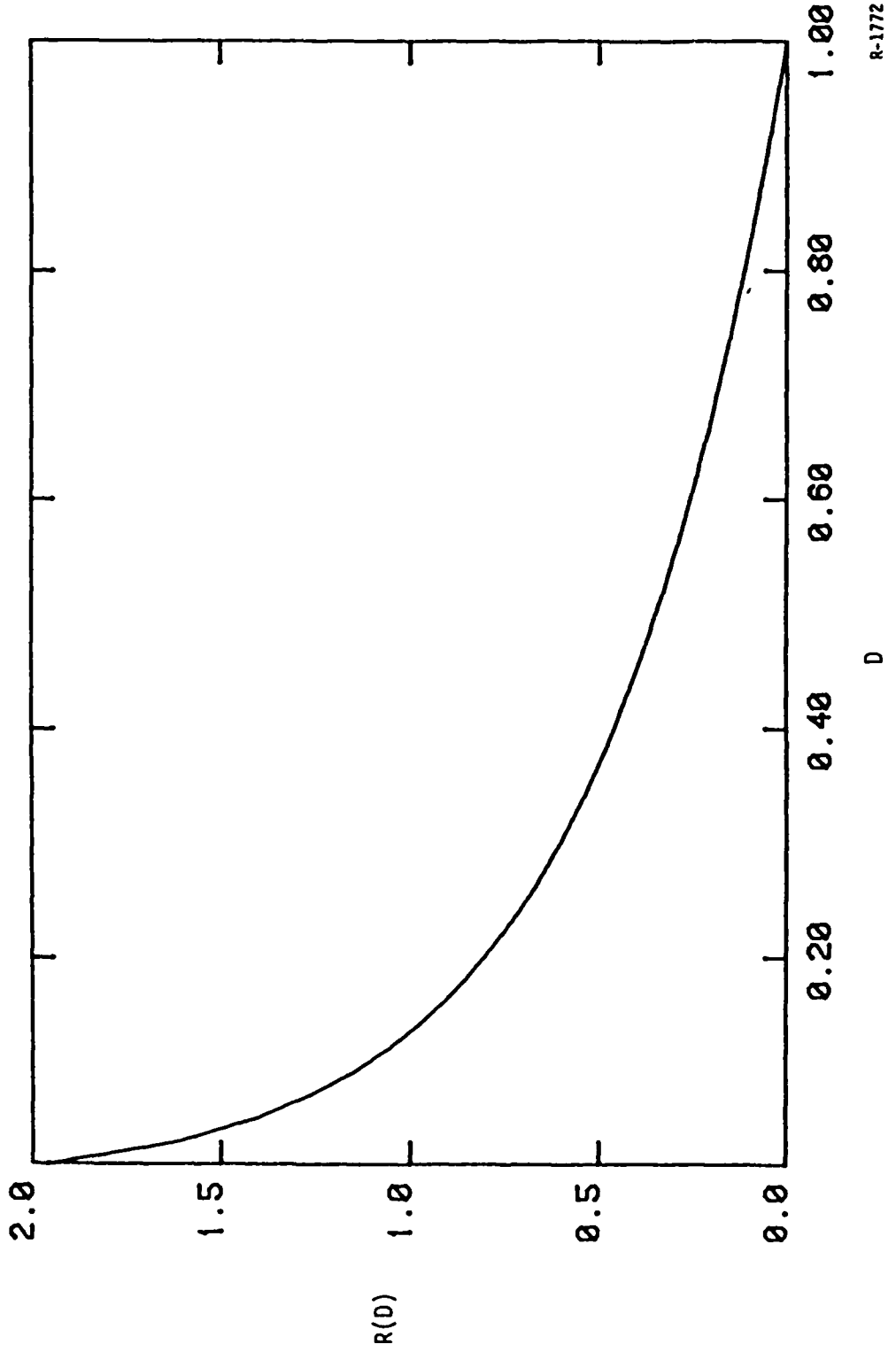

Figure 3-3. A Typical Rate Distortion Function

$R(D) < C$. Note that the converse statement, that $R(D) < C$ implies we can achieve average error of D, is not true in tracking because we cannot control the encoder as one does in conventional communication systems.* Thus, the inequality $R(D) < C$ imposes a lower bound on the average distortion, lower than which we cannot achieve with the given target model and measurement model. However, it may be possible that no tracking algorithm is able to achieve this lower limit. Thus, rate distortion theory will give us lower bounds on tracking error, and we will need to study the tightness of these lower bounds as a separate issue.

Rate distortion theory provides techniques for computing or approximating R(D) and C for general classes of sources, users (i.e., fidelity criteria), and channels. We will describe some of the fundamental results of rate distortion theory in the next subsection and apply these results to tracking performance analysis in subsequent subsections.

3.2.2 Rate Distortion Theory Fundamentals and Estimation Problems

We are interested in tracking problems which can be formulated as the following type of statistical estimation problem.

$$x(t+1) = Ax(t) + w(t) \tag{3-1}$$

$$y(t) = h(x(t)) + v(t) \tag{3-2}$$

In Eqs. 3-1 and 3-2, the variable x(t) is the state at time t we desire to estimate given measurements up to that time. Note that the state evolves linearly (Eq. 3-1), and we assume w(t) and v(t) are zero mean Gaussian random vectors. The performance analysis problem is to approximate the mean square

*For very special systems (e.g., linear Gaussian ones), this is true.

error of an optimal estimator. In previous work [1] we found that many tracking problems can be formulated as above, and this particular mathematical structure simplifies the computation of the Cramer-Rao-Van Trees performance bound [1],[7],[8],[9]. We wish to see here whether similar simplifications occur for rate distortion theory performance bounds.

Before attempting to tackle the dynamic problem formulated in Eqs. 3-1 and 3-2 we will study the static problem

$$y = h(x) + v \tag{3-3}$$

where x, v are assumed to be Gaussian random vectors and h is a nonlinear function of x. Our approach is to understand the general static problem of Eq. 3-3 first. We can then write the dynamic problem of Eqs. 3-1 and 3-2 as a large static problem and try to exploit the recursive structure of this special type of static problem to obtain an efficient, recursive approximation of the minimum mean square estimation error. In this report we will consider only static problems; we will discuss dynamic problems in a subsequent report.

The rate distortion function of a memoryless scalar Gaussian source of mean $\bar{x}$ and variance Q with respect to the squared-error criterion is [4, p.99]

$$R(D) = \frac{1}{2} \log \left(\frac{Q}{D} \right) . \tag{3-4}$$

The capacity C of a channel defined by

$$y = h(x) + v \tag{3-5}$$

where v is zero mean Gaussian with covariance matrix R and dimension m is given by the mutual information I(y;x) between y and x.

$$C = I(y;x) \tag{3-6}$$

We cannot compute I(y;x) for general nonlinear h, but we can approximate it as follows.

$$I(y;x) = H(y) - H(y|x) \tag{3-7}$$

Equation 3-7 gives the mutual information in terms of the differential entropy H(y) and the conditional differential entropy H(y|x). Now we can compute H(y|x) exactly:

$$H(y|x) = H(v) = \frac{m}{2} \log(2\pi e \, [\det R]^{\frac{1}{m}}) \tag{3-8}$$

We cannot compute H(y) in general, but we can bound it as follows [4].

$$H(y) \leq \frac{m}{2} \log \, (2\pi e \, [\det \Lambda]^{\frac{1}{m}}) \tag{3-9}$$

In Eq. 3-8 the mxm matrix Λ is the covariance of y:

$$\Lambda = E([y - E(y)] \, [y - E(y)]^T) \tag{3-10}$$

where E(.) denotes mathematical expectation and T denotes matrix or vector transposition.

If D is the minimum mean square error

$$D = \min_{\hat{x}} E((x - \hat{x}(y))^2) \tag{3-11}$$

where the mimimum is taken over all estimators $\hat{x}$ based on the measurement y, then rate distortion theory [4] tells us that

$$R(D) \leq C \quad . \tag{3-12}$$

From Eqs. 3-8 and 3-9 we see that

$$C \leq \frac{1}{2} \log\left(\frac{\det \Lambda}{\det R}\right) \tag{3-13}$$

Combining Eqs. 3-4, 3-12 and 3-13 gives

$$\frac{1}{2} \log\left(\frac{Q}{D}\right) \leq \frac{1}{2} \log\left(\frac{\det \Lambda}{\det R}\right) \tag{3-14}$$

or equivalently,

$$D \geq \frac{Q \det R}{\det \Lambda} \quad . \tag{3-15}$$

Thus, from Eq. 3-11 we see that

$$E((x - \hat{x}(y))^2) \geq \frac{Q \det R}{\det \Lambda} \tag{3-16}$$

for any estimate of x based only on y. Note that in this problem the covariance of y can be written

$$\Lambda = \Gamma + R \tag{3-17}$$

where

$$\Gamma = E([h(x) - E(h(x))]\,[h(x) - E(h(x))]^T) \quad . \tag{3-18}$$

Thus, we have

$$E(x - \hat{x}(y))^2) \geq \frac{Q \det R}{\det\,(\Gamma + R)} \quad . \tag{3-19}$$

This is the basic result of rate distortion theory we will use in the following subsections to analyze the minimum mean square error in static estimation problems.

3.3 SCALAR STATE

3.3.1 Computation of the Rate Distortion Bound

In this subsection we consider the problem of estimating a scalar Gaussian state x with mean $\bar{x}$ and variance Q given the vector measurement

$$y = h(x) + v \tag{3-20}$$

where v is a Gaussian random vector with dimension m, 0-mean, and covariance R. In subsection 3.2 we found the basic rate distortion bound (RDB) of mean square error:

$$E((x - \hat{x}(y))^2) \geq \frac{Q \cdot \det R}{\det (\Gamma + R)} \tag{3-21}$$

where

$$\Gamma = E([h(x) - E(h(x))]\ [h(x) - E(h(x))]^T) \tag{3-22}$$

To compute the RDB requires computing Γ, or equivalently, computing

$$E(h(x)) \tag{3-23}$$

and

$$E(h(x)h(x)^T) \quad . \tag{3-24}$$

The expectations Eqs. 3-23 and 3-24 are taken with respect to a Gaussian distribution and can be computed in closed form for a large class of nonlinear h. Note that we utilized this fact in earlier work [1] to compute Cramer-Rao-Van Trees bounds. Indeed, if h(x) is a sum of products of polynomials, exponential, and sine or cosine functions, then we can compute the expectations in Eqs. 3-23 and Eq. 3-24 in closed form. This is true also if x is a vector.

The computation of such expectations derives from the basic formula

$$E(\Phi(u,x)) = \Psi(u) \tag{3-25}$$

where

$$\Phi(u,x) = \exp(u^T x)$$

$$\Psi(u) = \exp(u^T \bar{x} + \frac{1}{2} u^T Q u) \tag{3-26}$$

where $u = (u_1, u_2, \ldots u_n)^T$ is a vector of complex numbers, and x is a Gaussian random vector of dimension n, mean $\bar{x}$, and covariance Q. Consider the scalar case n=1 for example. If n is a real number we find

$$E(e^{ux}) = e^{u\bar{x} + \frac{1}{2} u^2 Q} \quad . \tag{3-27}$$

If u = i (imaginary number $\sqrt{-1}$), we obtain

$$E(e^{ix}) = e^{ix}\, e^{\frac{-1}{2} Q} \tag{3-28}$$

which gives the two results

$$E(\sin x) = \sin \bar{x} \cdot e^{\frac{-1}{2} Q} \tag{3-29}$$

$$E(\cos x) = \cos \bar{x}\, e^{\frac{-1}{2} Q} \quad . \tag{3-30}$$

Taking derivatives of Eq. 3-26 with respect to u gives us an expression for $E(x^n)$:

$$E(x^n) = \frac{d^n}{du^n} \left[e^{u\bar{x} + \frac{1}{2} u^2 Q} \right]_{u=0} \quad . \tag{3-31}$$

We can obtain other expectations by combining these operations.

In general, we consider the class A_n of all functions f(x) which can be written

$$f(x) = \sum_{k=1}^{p} c_k \cdot D_k \phi(u_k, x) \tag{3-32}$$

where c_k are complex constants, u_k are constant complex vectors, and D_k are differential operators of the general form

$$D_k = \left(\frac{\partial}{\partial u_1}\right)^{k(1)} \cdot \left(\frac{\partial}{\partial u_2}\right)^{k(2)} \cdots \left(\frac{\partial}{\partial u_n}\right)^{k(n)} \cdot \tag{3-33}$$

For example, in the scalar n=1 case

$$x^n = \left(\frac{\partial}{\partial_n}\right)^n \cdot \phi(0,x) \quad . \tag{3-34}$$

Note that if f_1 and f_2 are in A_n, then so are $f_1 \cdot f_2$ and $f_1 + f_2$. The class A_n also contains all constant functions.

If f(x) is given by Eq. 3-32, then

$$E(f(x)) = \sum_{k=1}^{p} c_k \, D_k \Psi(u_k) \tag{3-35}$$

is the closed form expression for the expectation.

Thus, we see that if each component function of h(x) is in A_n, then each component of $h(x)\, h(x)^T$ is also in A_n and we can compute the expectations in Eqs. 3-23 and 3-24 in closed form. Furthermore, we can approximate any non-linear function h using functions in A_n; and this gives us a method for approximating the expectations in Eqs. 3-23 and 3-24 for general h. In the next subsection we will use this approach to compute the rate distortion bound in some examples.

3.3.2 Examples of the Rate Distortion Bound

3.3.2.1 Linear Measurements

Suppose that $h(x) = h \cdot x$ is linear. Let us compute the RDB for

$$y = h \cdot x + v \quad . \tag{3-36}$$

The bound for Eq. 3-36 will be the same as for

$$\tilde{y} = \tilde{h} \cdot x + \tilde{v} \tag{3-37}$$

where

$$\tilde{h} = \sqrt{R}^{-1} \cdot h \tag{3-38}$$

$$\tilde{v} = \sqrt{R}^{-1} v \tag{3-39}$$

The second version will simplify computation because the covariance of $\tilde{v}$ is just the mxm identity matrix I_m. The main quantity to compute is

$$\det (\tilde{\Gamma} + I_m) = \det (\tilde{h}\, \tilde{h}^T \cdot Q + I_m) \tag{3-40}$$

This is easy if one notes that the determinant of a matrix is the product of its eigenvalues. The matrix

$$\tilde{h}\, \tilde{h}^T \cdot Q + I_m \tag{3-41}$$

has one eigenvalue

$$\tilde{h}^T \tilde{h} \cdot Q + 1 \tag{3-42}$$

and m-1 eigenvalues 1. Thus, the RDB is

$$\text{RDB} = \frac{Q}{\tilde{h}^T \tilde{h} \cdot Q + 1} \tag{3-43}$$

In terms of h and R this is just

$$RDB = (h^T R^{-1} h + Q^{-1})^{-1} \tag{3-44}$$

which is in fact the minimum mean square error for the linear problem.

3.3.2.2 Scalar Nonlinear Measurements

Let us assume that y and v are scalar random variables, and let us consider examples of nonlinear h(x). For simplicity, we will assume $\bar{x} = 0$ in this set of examples.

$h(x) = x^n$

The RDB in this case is

$$RDB = (B_n \cdot Q^{n-1} R^{-1} + Q^{-1})^{-1} \tag{3-45}$$

where

$$B_n = \frac{(2n)!}{2^n \cdot n!} - \frac{(n!)^2}{2^n \left[\left(\frac{n}{2}\right)!\right]^2} \tag{3-46}$$

for even n = 2, 4, 6,... and

$$B_n = \frac{(2n)!}{2^n \cdot n!} \tag{3-47}$$

for odd n = 1, 3, 5,... . Figure 3-4 shows the dependence of this bound on R for fixed Q = 1.0 and n = 1, 2, 3.

$h(x) = \sin x$ and $h(x) = x - x^3/6$

The bound for sin x is

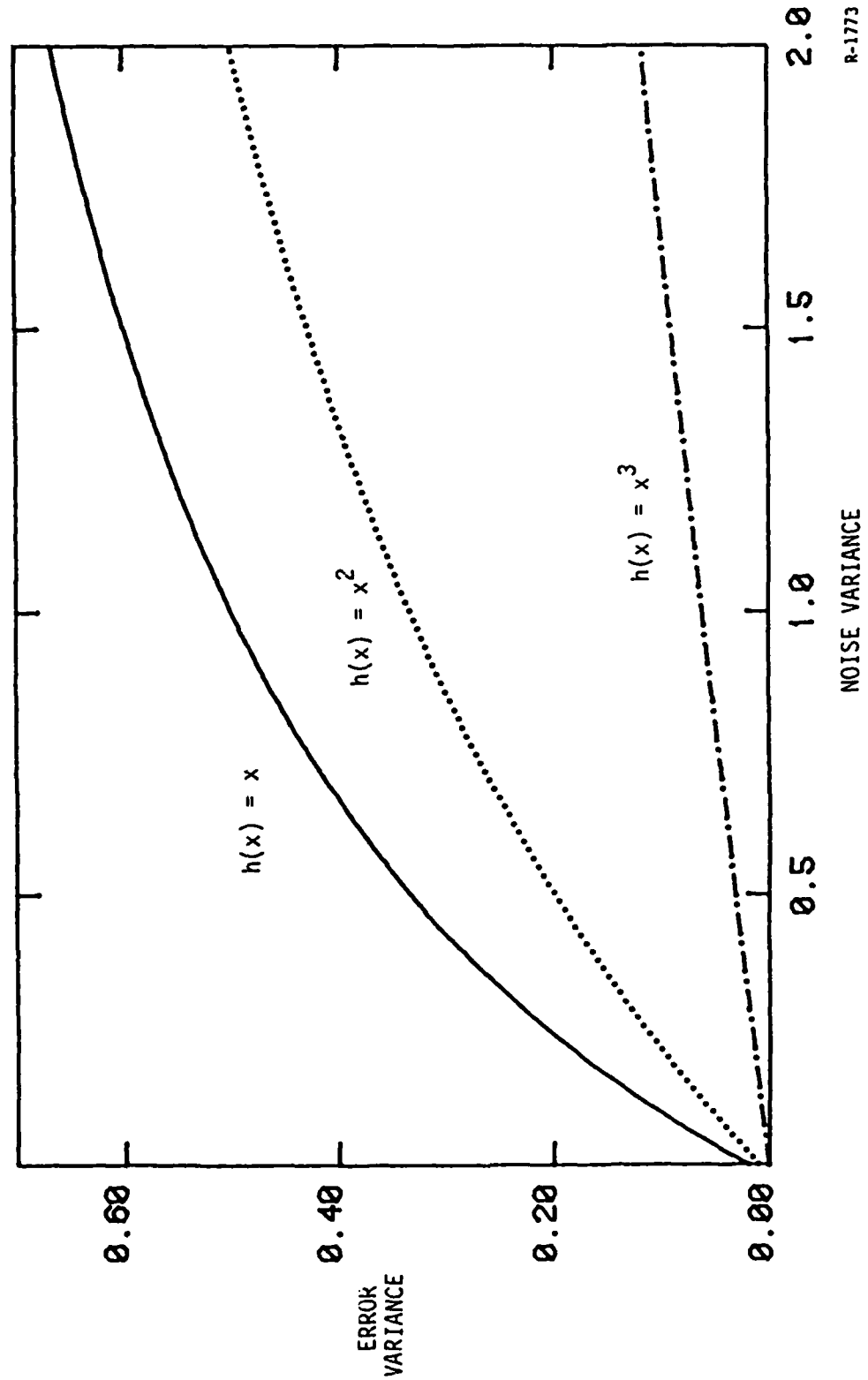

Figure 3-4. Rate Distortion Bounds for $h(x) = x, x^2, x^3$

$$RDB = (\frac{1}{2}\,[1 - e^{-2Q}]\; Q^{-1}R^{-1} + Q^{-1})^{-1} \qquad (3\text{-}48)$$

The bound for the third order expansion of sin x, namely $x - \frac{x^3}{6}$ is

$$RDB = ([1 - Q + \frac{5}{12} \cdot Q^2]R^{-1} + Q^{-1})^{-1} \quad . \qquad (3\text{-}49)$$

Figure 3-5 shows these bounds together with that for h(x) = x versus R for Q =1.0.

3.3.2.3 Identically Distributed Conditionally Independent Scalar Measurements

Suppose that we take N measurements

$$y(t) = h(x) + v(t) \qquad (3\text{-}50)$$

such that v(t) are independent, scalar Gaussian random variables of variance R. Let

$$\Gamma = E([h(x) - E(h(x))]^2) \quad . \qquad (3\text{-}51)$$

Then we can compute the RDB for Eq. 3-50 in terms of Q, Γ, R and N. The static vector measurement problem equivalent to Eq. 3-50 has the RDB given by

$$\frac{Q \cdot \det\,(R \cdot I_N)}{\det\,(\Gamma_N + R \cdot I_N)} \qquad (3\text{-}52)$$

where I_N is the NXN identity matrix and Γ_N is the NXN matrix which has all of its elements equal to Γ. Reasoning as in subsection 3.3.2.1 we can compute the determinant in the denominator of Eq. 3-52. Note that Γ_N is a rank 1 matrix with only one nonzero eigenvalue, namely

$$Tr\;\Gamma_N = N \cdot \Gamma \quad , \qquad (3\text{-}53)$$

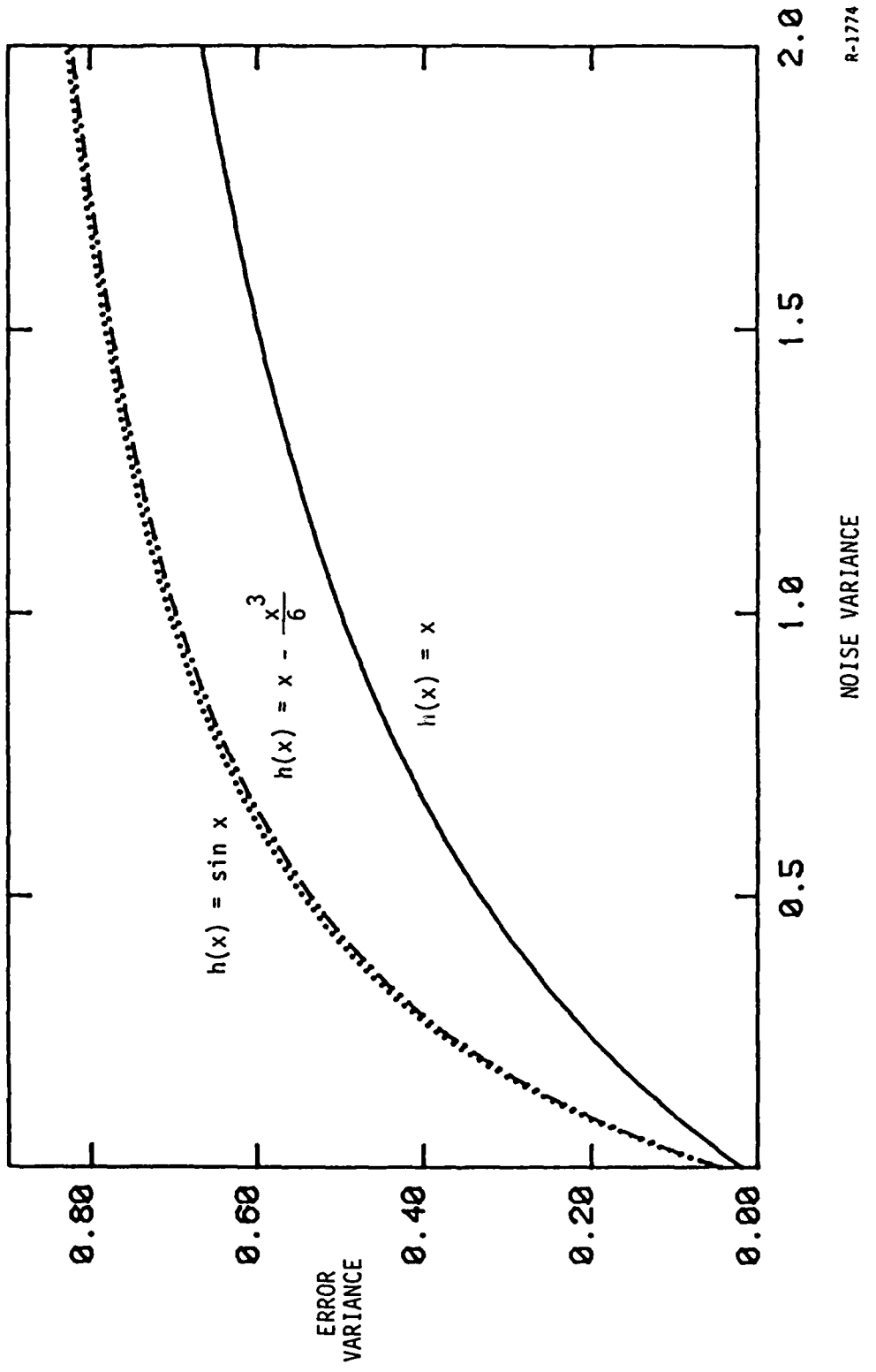

Figure 3-5. Rate Distortion Bounds for $h(x) = \sin x$, $h(x) = x - \frac{x^3}{6}$ and $h(x) = x$

where Tr denotes the trace of a matrix. Consequently, $\Gamma_N + R \cdot I_N$ has one eigenvalue equal to $N \cdot \Gamma + R$ and $N - 1$ eigenvalues equal to R. Thus, the determinant is $(N \cdot \Gamma + R) \cdot R^{N-1}$ and the RDB is

$$RDB = ([N \cdot \Gamma Q^{-1}] R^{-1} + Q^{-1})^{-1} . \tag{3-54}$$

Note that as $N \to \infty$ the RDB is asymptotically equal to

$$RDB \approx \frac{QR}{N\Gamma} . \tag{3-55}$$

3.3.2.4 Nonidentical, Conditionally Independent Scalar Measurements

Suppose that

$$y(1) = x + v(1) \tag{3-56}$$

$$y(2) = x^2 + v(2) \tag{3-57}$$

where v(1), v(2) are independent 0 - mean, Gaussian random variables with variance R. Assume x has 0 mean and variance Q. The variance of the vector measurement $y = (y(1), y(2))^T$ is

$$\Gamma = \begin{bmatrix} Q & 0 \\ 0 & 2Q^2 \end{bmatrix} \tag{3-58}$$

Thus, the RDB for this problem is

$$RDB = ([1 + 2Q + 2Q^2R^{-1}] \cdot R^{-1} + Q^{-1})^{-1} \tag{3-59}$$

Figure 3-6 shows this bound with Q = 1 versus different values of R. Figure 3-6 also shows the mean square error for only one measurement (namely Eq. 3-56).

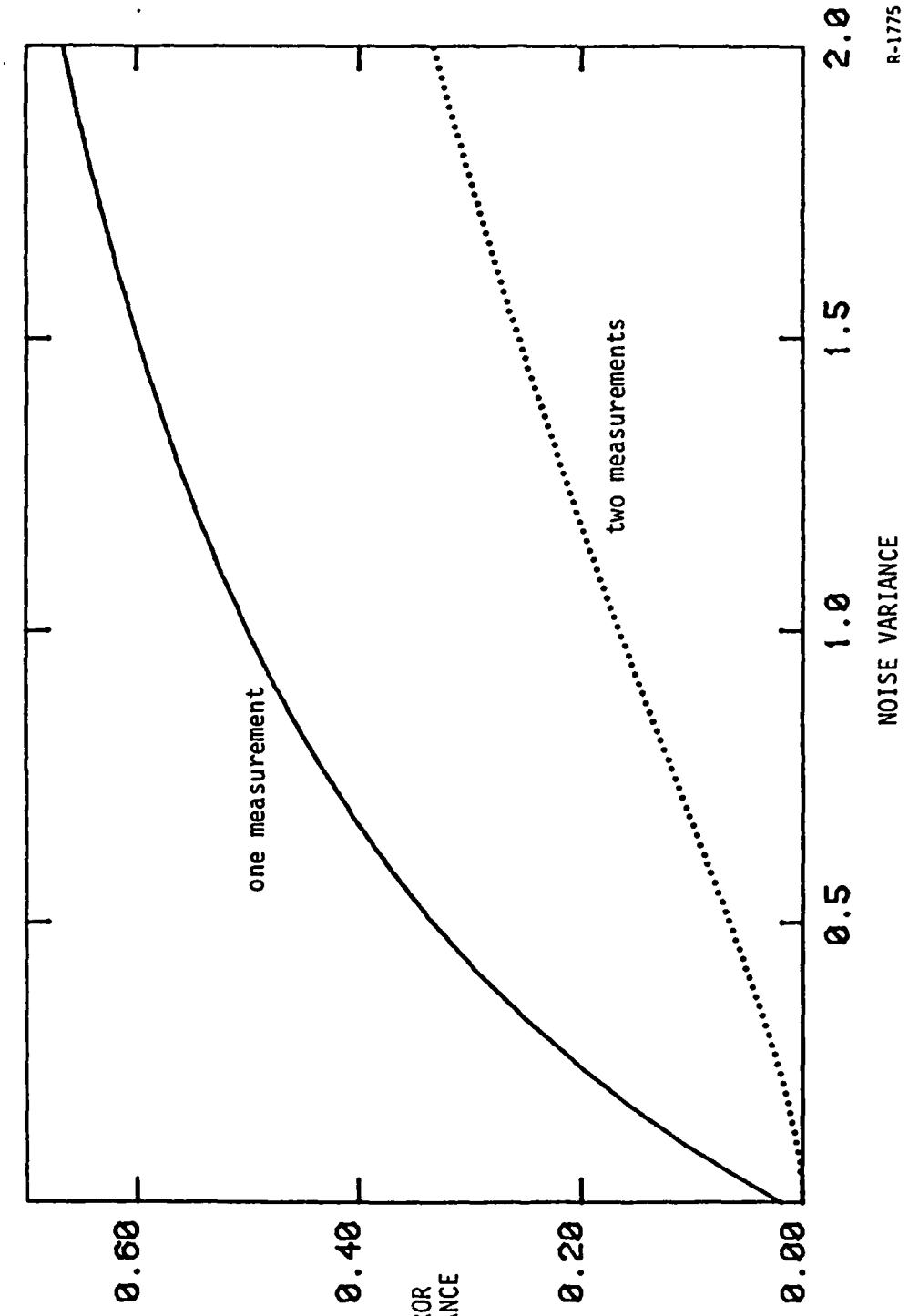

Figure 3-6. Rate Distortion Bounds for One and Two Measurements

3.3.3 Comparison to the Cramer-Rao-Van Trees Bound

3.3.3.1 The Cramer-Rao-Van Trees Bound

Before comparing the Cramer-Rao-Van Trees lower bound (CRVB) to the RDB, let us review what the CRVB is for the static estimation problem formulated above. Van Trees [7] has derived a lower bound on the error convariance of any estimator $\hat{x}(y)$ for the problem in Eq. 3-20. The bound is

$$E([x - \hat{x}(y)]\ [x - \hat{x}(y)]^T) \geq [\Gamma^* + Q^{-1}]^{-1} \tag{3-60}$$

where the inequality is in terms of symmetric matrices, and Γ^* is defined as

$$\Gamma^* = E(\frac{\partial h}{\partial x}(x)^T R^{-1} \frac{\partial h}{\partial x}(x)) \quad . \tag{3-61}$$

If x is a scalar random variable, then Eq. 3-60 gives the following lower bound on the error variance

$$E([x-\hat{x}(y)]^2) \geq [\Gamma^* + Q^{-1}]^{-1} \quad . \tag{3-62}$$

Note that Eq. 3-61 involves computations similar to those required for the RDB. Indeed, if h is a member of the class of functions A_n defined in subsection 3.3.1, then the components of $\frac{\partial h}{\partial x}$ also belong to A_n. In this subsection we will study the relation of the CRVB of Eq. 3-62 to the RDB of Eq. 3-21. Both are lower bounds of the minimum mean square error. Can we determine conditions under which one is a tighter bound than the other?

3.3.3.2 Comparison of Bounds for Scalar Measurements

Let us start by computing the CRVB's corresponding to the examples of subsection 3.3.2.2.

$h(x) = x^n$

The CRVB in this case is

$$CRVB = (C_n Q^{n-1} R^{-1} + Q^{-1})^{-1} \tag{3-63}$$

where

$$C_n = n^2 \cdot \frac{(2[n-1])!}{2^{n-1}\,[n-1]!} \tag{3-64}$$

Figures 3-7a and 3-7b show CRVB and RDB for n = 2,3 versus R with Q = 1.0. Note that RDB > CRVB in these examples. Indeed, one can see that

$$C_n > B_n \tag{3-65}$$

for all n = 1,2,... and therefore CRVB < RDB for all n.

$h(x) = \sin x$ and $h(x) = x - x^3/6$

The CRVB for $h(x) = \sin x$ is found to be

$$CRVB = (\frac{1}{2}\,[1 + e^{-2Q}]R^{-1} + Q^{-1})^{-1} \tag{3-66}$$

and that for $h(x) = x - \frac{x^3}{6}$ is

$$CRVB = ([1 - Q + \frac{3Q^2}{4}]R^{-1} + Q^{-1})^{-1} \quad . \tag{3-67}$$

Figures 3-8a and 3-8b show the CRVB and RDB for these two nonlinear examples (Q = 1.0 and R is varied). Note that the RDB is always tighter (i.e., CRVB < RDB), and in fact one can prove this is true. It is interesting to note that as $Q \to \infty$, Eq. 3-48 predicts (correctly) that the mean square error of an estimate of x given $y = \sin x + v$ blows up. The CRVB Eq. 3-66 predicts (incorrectly) that the error remains bounded.

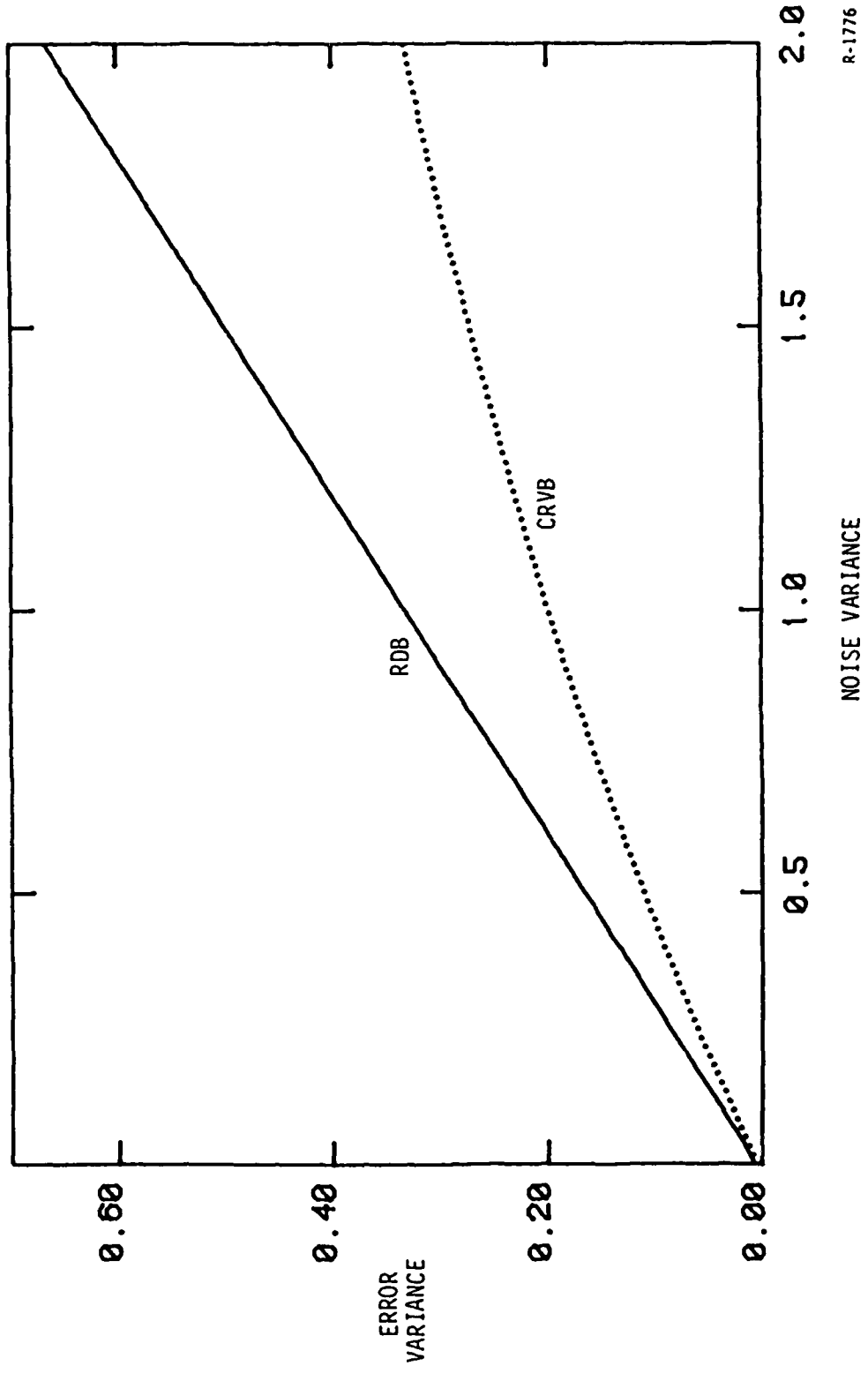

Figure 3-7a. Comparison of Rate Distortion and Cramer-Rao-Van Trees Bounds for $h(x) = x^2$

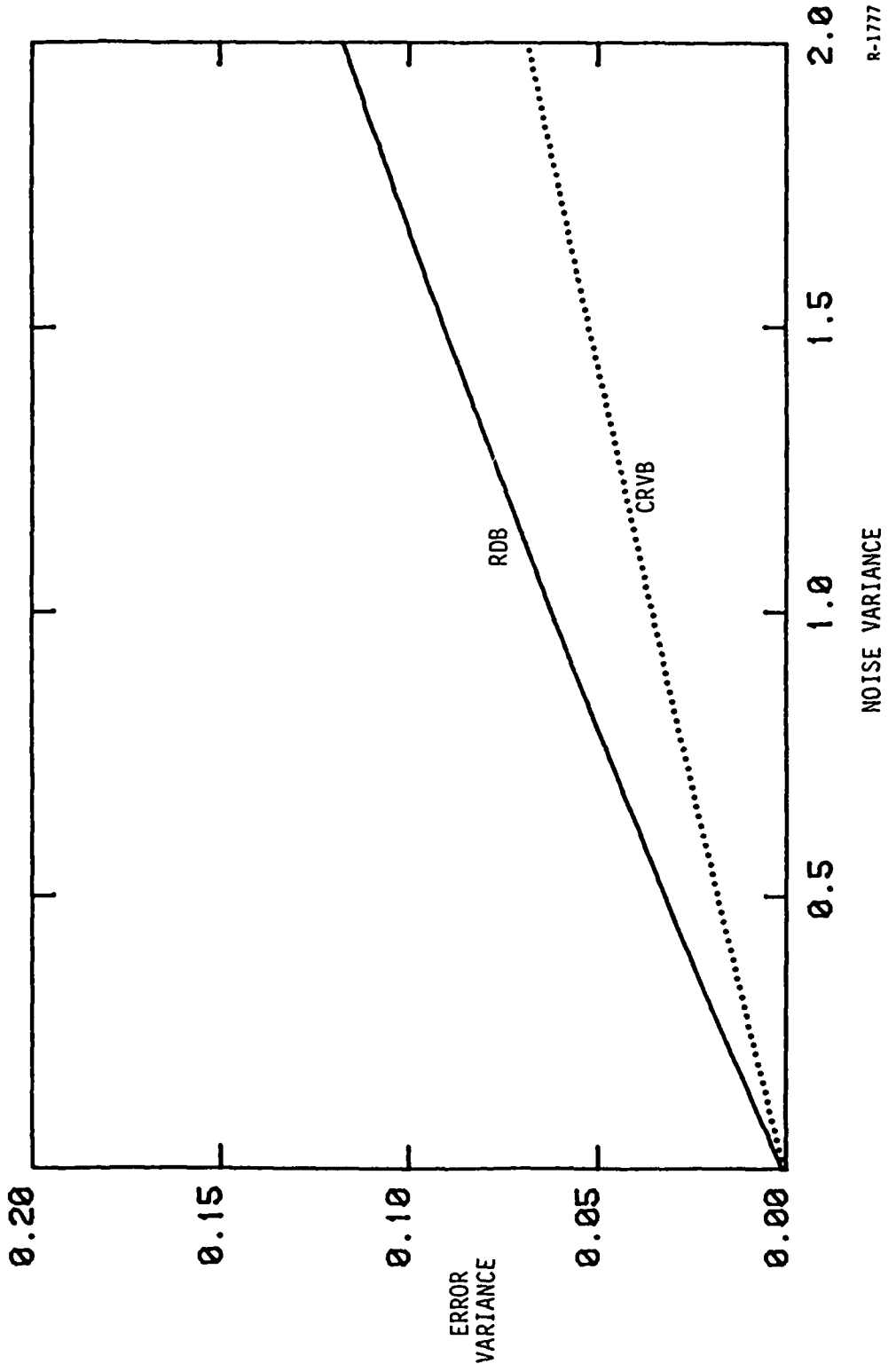

Figure 3-7b. Comparison of Rate Distortion and Cramer-Rao-Van Trees Bounds for $h(x) = x^3$

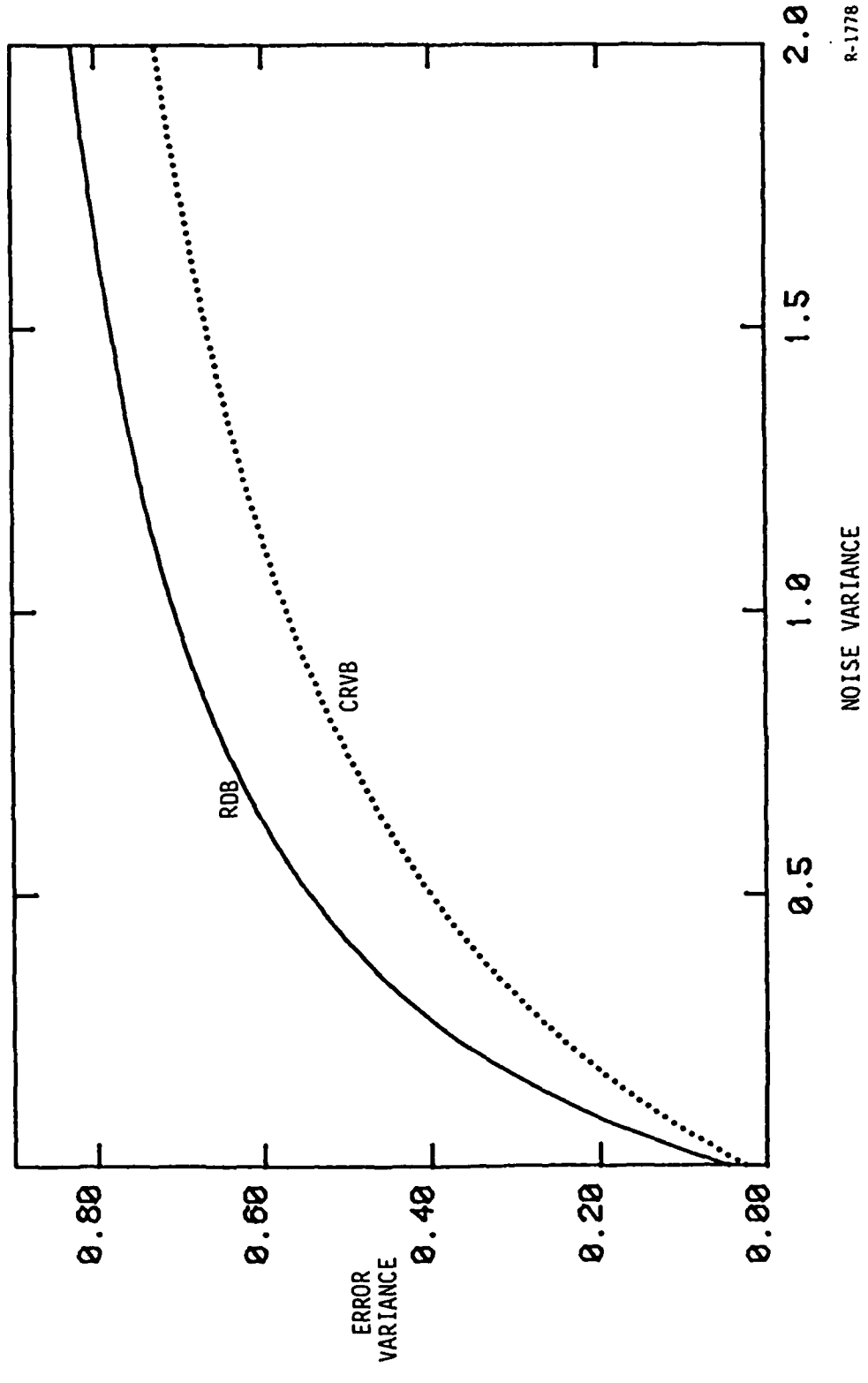

Figure 3-8a. Comparison of Rate Distortion and Cramer-Rao-Van Trees Bounds for $h(x) = x - \frac{x^3}{6}$

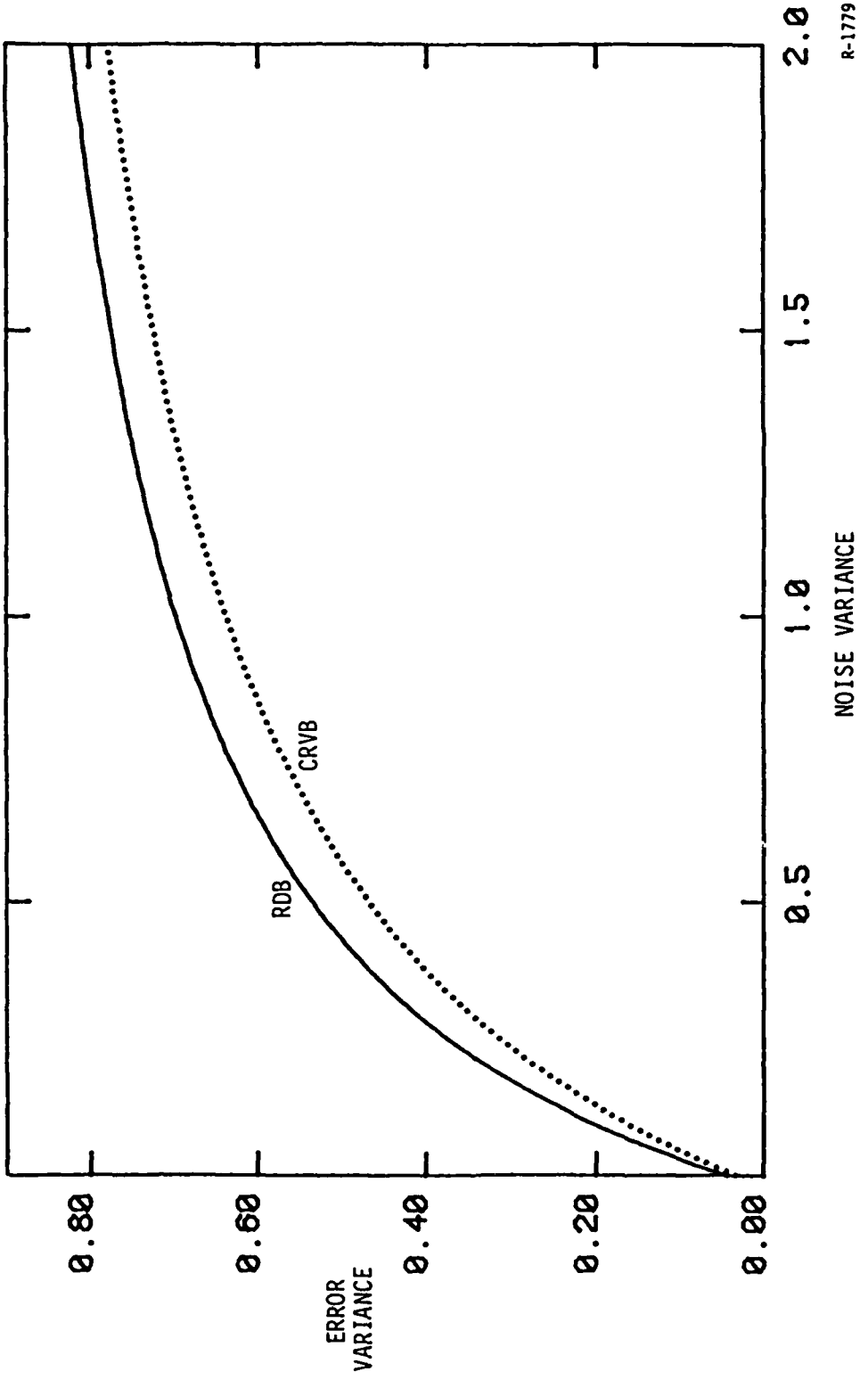

Figure 3-8b. Comparison of Rate Distortion and Cramer-Rao-Van Trees Bounds for h(x) = sin x

General nonlinear h(x)

As one might expect from the examples above, it is possible to show that CRVB ≤ RDB all the time in case of scalar measurements. Furthermore, one can show CRVB = RDB if and only if h(x) is linear. Recall that our underlying assumptions at this point are that x is a scalar Gaussian random variable and y is a scalar measurement. We prove the following theorem:

Theorem. If h(x) is continuously differentiable in x, and the expectations $E(h(x)^2)$, $E([h'(x)]^2)$ are both finite, then

$$CRVB \leq RDB$$

where CRVB = RDB if and only if

$$h(x) = ax + b$$

for constants a,b .

We will prove this theorem in the remainder of the subsection. Assume first that $\bar{x} = 0$ and define

$$\Phi(x) = [h(x) - h(0)]^2 \, x^{-1} \, e^{-\frac{x^2}{2Q}} \tag{3-68}$$

for $x \neq 0$, and

$$\Phi(0) = 0 \quad . \tag{3-69}$$

Note that $\Phi(x)$ is continuously differentiable and

$$\begin{aligned} \Phi'(x) = {} & 2[h(x) - h(0)] \, h'(x) x^{-1} \, e^{-\frac{x^2}{2Q}} \\ & - [h(x) - h(0)]^2 \, x^{-2} \, e^{-\frac{x^2}{2Q}} \\ & - \frac{[h(x) - h(0)]^2}{Q} \cdot e^{-\frac{x^2}{2Q}} \end{aligned} \tag{3-70}$$

for $x \neq 0$, and

$$\Phi'(0) = [h'(0)]^2 \quad . \tag{3-71}$$

Given that $E(h(x)^2)$ and $E(h'(x)^2)$ are finite, we have that

$$\int_{-\infty}^{\infty} \Phi'(x)\, dx = \lim_{x \to \infty} [\Phi(x) - \Phi(-x)] = 0 \tag{3-72}$$

Note that by definition of mathematical expectation,

$$E(f(x)) = \frac{1}{\sqrt{2\pi Q}} \int_{-\infty}^{\infty} f(x)\, e^{-\frac{x^2}{2Q}}\, dx \quad . \tag{3-73}$$

Using Eqs. 3-70 and 3-73 to rewrite Eq. 3-72 gives us

$$E(h'(x)^2) = Q^{-1}\, E([h(x) - h(0)]^2) + E\left([h'(x) - \frac{h(x) - h(0)}{x}]^2\right) \tag{3-74}$$

Let $\bar{h} = E(h(x))$. Then

$$E(h'(x)^2) = Q^{-1}\, E([h(x) - \bar{h}]^2) + Q^{-1}\, [\bar{h} - h(0)]^2 + E\left([h'(x) - \frac{h(x) - h(0)}{x}]^2\right) \tag{3-75}$$

it follows that

$$E(h'(x)^2) \geq Q^{-1}\, E([h(x) - \bar{h}]^2) \tag{3-76}$$

with equality if and only if

$$\bar{h} = h(0) \tag{3-77}$$

and

$$h'(x) = \frac{h(x) - h(0)}{x} \tag{3-78}$$

The Eqs. 3-77 and 3-78 are equivalent to h being of the form

$$h(x) = ax + b \tag{3-79}$$

for constants a, b. Note that Eq. 3-76 is equivalent to

$$\Gamma^* \cdot R \geq \Gamma \cdot Q^{-1} \quad . \tag{3-80}$$

Since

$$CRVB = (\Gamma^* + Q^{-1})^{-1} \quad ,$$

and

$$RDB = (\Gamma Q^{-1} R^{-1} + Q^{-1})^{-1} \quad , \tag{3-81}$$

Eq. 3-80 proves that CRVB $\geq$ RDB, at least for the case $\bar{x} = 0$.

The general case of $\bar{x} \neq 0$ follows easily from the $\bar{x} = 0$ case. Simply apply the earlier results to $x - \bar{x}$ with the measurement function $h(x + \bar{x})$. This problem will yield the same bounds as for x, h(x).

3.3.3.3 Comparison of Bounds for Identically Distributed - Conditionally Independent Measurements

Under the problem assumptions of subsection 3.3.2.3, we can show that CRVB $\leq$ RDB holds for general nonlinear h(x). Recall (Eq. 3-54) that

$$RDB = ([N \cdot \Gamma Q^{-1}] R^{-1} + Q^{-1})^{-1} \tag{3-82}$$

One can easily show that

$$CRB = ([N \cdot \Gamma^* R] R^{-1} + Q^{-1})^{-1} \tag{3-83}$$

We proved that $\Gamma Q^{-1} \leq \Gamma^* R$ in the last subsection. Consequently, we see that CRVB $\leq$ RDB in this case also. Note that CRVB predicts a mean square error that is asymptotic to

$$CRVB \approx \frac{1}{N\Gamma^*} \tag{3-84}$$

as $N \to \infty$. This is in constrast to

$$RDB \approx \frac{QR}{N\Gamma} \quad . \tag{3-85}$$

Thus, we have

$$\frac{CRVB}{RDB} \approx \frac{\Gamma}{QR\Gamma^*} \tag{3-86}$$

asymptotically as $N \to \infty$. For nonlinear $h(x)$ we saw previously that $\Gamma/QR\Gamma^* < 1$. Thus, the CRVB predicts a faster rate of decrease in mean square error than is in fact possible.

3.3.3.4 Comparison of Bounds for Vector Measurements

From the preceding results one might conjecture that CRVB $\leq$ RDB in general. The following example shows that this need not be true. Consider the example of subsection 3.3.2.4. The CRVB for this example is

$$CRVB = ([1 + 4Q]R^{-1} + Q^{-1})^{-1} \tag{3-87}$$

Figure 3-9 shows CRVB and the corresponding RDB of Eq. 3-59, namely

$$RDB = ([1 + 2Q + 2Q^2R^{-1}]R^{-1} + Q^{-1})^{-1} \quad . \tag{3-88}$$

It is easy to see in this example that CRVB $\geq$ RDB if $R \leq Q$ and CRVB $\leq$ RDB if $R \geq Q$. We can show in general that CRVB $\leq$ RDB if R is sufficiently large (i.e., as signal-to-noise ratio approaches 0).

Without loss of generality (by using the same transformation as in subsection 3.3.2.1) we can assume that the measurement noise covariance is a

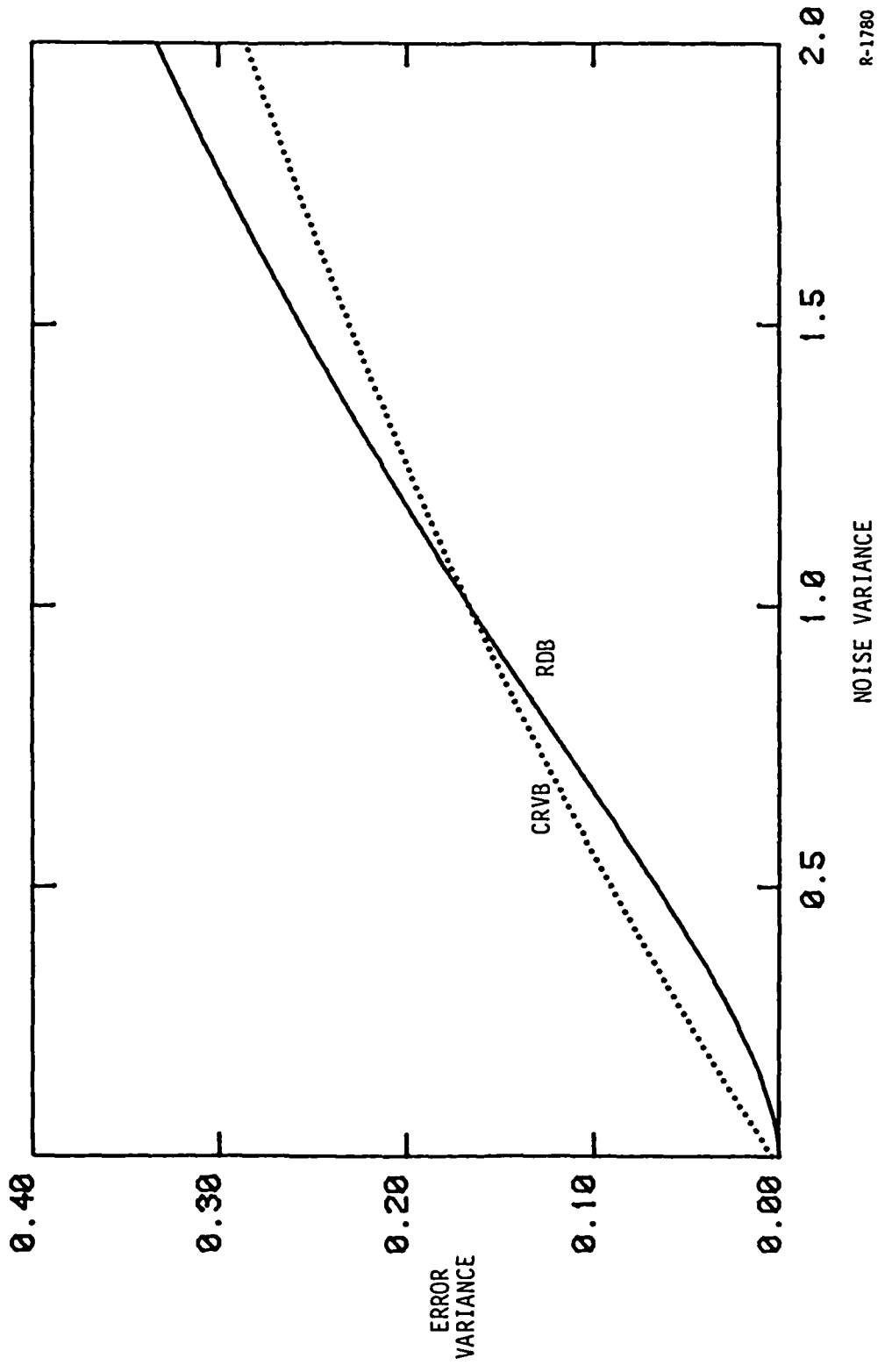

Figure 3-9. Comparison of Distortion Rate and Cramer-Rao-Van Trees Bounds in Vector Measurement Example

scalar constant R multiplied times the mxm identity matrix I_m. Then we have

$$RDB = Q \cdot (\det[I_{mxm} + R^{-1}\ \Gamma])^{-1} \tag{3-89}$$

and

$$CRVB = (\left[\sum_{k=1}^{m} E(h_k'(x)^2)\right]R^{-1} + Q^{-1})^{-1} \tag{3-90}$$

where $h_k(x)$ are the components of h(x). The determinant in Eq. 3-89 can be expanded in powers of R^{-1} so that

$$\det\ (I_{mxm} + R^{-1}\ \Gamma) = 1 + Tr[R^{-1}\Gamma] + O(R^{-2}) \tag{3-91}$$

where $O(R^{-2})$ denotes terms of order R^{-2} or higher powers of R^{-1}. The trace is

$$Tr[R^{-1}\Gamma] = R^{-1} \sum_{k=1}^{n} E([h_k(x) - E(h_k(x))]^2) \tag{3-92}$$

Thus, we see that

$$RDB = (\sum_{k=1}^{n} E([h_k(x) - E(h_k(x))]^2) \cdot Q^{-1}\ R^{-1} + Q^{-1} + O(R^{-2}))^{-1} \tag{3-93}$$

The theorem of subsection 3.3.3.2 implies that

$$E([h_k(x) - E(h_k(x))]^2)\ Q^{-1} \leq E(h_k'(x)^2) \tag{3-94}$$

for each k with equality if and only if h_k is linear. Consequently, if h is not linear, then CRVB < RDB for R suffiently large. If h is linear, then both bounds are equal to the minimum mean square error.

3.4 VECTOR STATE

3.4.1 Rate Distortion Bound for Vector State and Scalar Measurement

Rate distortion theory naturally gives bounds on scalar errors. For vector state estimation problems, however, we need a bound on the error covariance matrix such as the CRVB provides (Eq. 3-60). In this subsection we derive a RDB for vector state estimation problems with scalar measurements.

Suppose that

$$y = h(x_1, x_2) + v \tag{3-95}$$

where v is a 0-mean Gaussian random variable of variance R and x_1, x_2 are jointly Gaussian random variables. We are interested in deriving a lower bound for the mean square error

$$E([x_1 - \hat{x}_1(y)]^2) \tag{3-96}$$

of an estimate $\hat{x}_1(y)$ of x_1 . Suppose x_2 were a fixed, known constant. Then the previous result for a scalar state implies that

$$E([x_1 - \hat{x}_1(y)]^2|x_2) \geq ([\Gamma_1(x_2)Q_1^{-1}]R^{-1} + Q_1^{-1})^{-1} \tag{3-97}$$

where

$$\Gamma_1(x_2) = E([h(x_1,x_2) - E(h(x_1,x_2)|x_2)]^2|x_2) \tag{3-98}$$

and

$$Q_1 = E([x_1 - E(x_1|x_2)]^2|x_2) \quad . \tag{3-99}$$

Note that the conditional variance in Eq. 3-99 does not actually depend on x_2 because x_1 and x_2 are jointly Gaussian.

Equation 3-97 can also be written as

$$E([x_1 - \hat{x}_1(y)]^2|x_2)^{-1} \leq [\Gamma_1(x_2)Q_1^{-1}]R^{-1} + Q_1^{-1} \quad . \tag{3-100}$$

Jensen's inequality states that

$$\phi(E(\xi)) \leq E(\phi(\xi)) \tag{3-101}$$

if ϕ is a convex function [10]. Note that $\phi(\xi) = \xi^{-1}$ is convex if $\xi > 0$. Thus, we can apply Jensen's inequality to obtain

$$E(\xi)^{-1} \leq E(\xi^{-1}) \quad . \tag{3-102}$$

If $\xi = E([x_1 - \hat{x}_1(y)]^2|x_2)$ we obtain

$$E([x_1 - \hat{x}_1(y)]^2)^{-1} \leq [\Gamma_1 \cdot Q_1^{-1}]R^{-1} + Q_1^{-1} \tag{3-103}$$

where

$$\Gamma_1 = E(\Gamma_1(x_2)) \quad . \tag{3-104}$$

This gives the rate distortion bound

$$E([x_1 - \hat{x}_1(y)]^2) \geq ([\Gamma_1 Q_1^{-1}]R^{-1} + Q_1^{-1})^{-1} \tag{3-105}$$

where

$$\Gamma_1 = E([h(x_1,x_2) - E(h(x_1,x_2)|x_2)]^2) \quad . \tag{3-106}$$

Note also that

$$\Gamma_1 = E(h(x_1,x_2)^2) - E([E(h(x_1,x_2)|x_2)]^2) \quad . \tag{3-107}$$

Equation 3-105 is our basic RDB for the vector state, scalar measurement case. Note that x_2 could be a Gaussian random vector. Thus, for

$$y = h(x_1,x_2,\ldots,x_n) + v \tag{3-108}$$

one has the same bound Eq. 3-105 except that

$$\Gamma_1 = E([h(x_1,x_2,\ldots,x_n) - E(h(x_1,x_2,\ldots,x_n)|x_2\ldots x_n)]^2) \quad . \quad (3\text{-}109)$$

3.4.2 Computation of the Rate Distortion Bound

To compute the RDB of the previous subsection it is necessary to compute the expression Γ_1 in Eq. 3-106 and 3-107 (or more generally, Eq. 3-109). It is possible to do this in much the same way as we did in subsection 3.3.1. Specifically, if h belongs to the class A_n of functions defined in subsection 3.3.1 (Eq. 3-13), then we can compute Γ_1 in closed form.

Suppose that x_1 is a random n-dimensional vector, x_2 is a random m-dimensional and x_1,x_2 are jointly Gaussian. Then we know

$$E(x_1,x_2) = a + Bx_2 \quad (3\text{-}110)$$

$$E([x_1-E(x_1|x_2)]\ [x_1 - E(x_1|x_2)]^T|x_2) = C \quad (3\text{-}111)$$

for constant vector a and constant matrices B, C. If

$$\Phi(u,x_1) = \exp(u^T x_1) \quad (3\text{-}112)$$

then

$$E(\Phi(u,x_1)|x_2) = \psi(u,x_2) \quad (3\text{-}113)$$

where

$$\psi(u,x_2) = \exp(u^T a + u^T B x_2 + \frac{1}{2}\, u^T C u) \quad . \quad (3\text{-}114)$$

where u is an n-dimensional vector of complex constants. Note that for any constants a, B, C, u the function $\psi(u,x_2)$ of x_2 belongs to A_n. Thus, if

$$f(x_1) = \sum_{k=1}^{p} C_k\ D_k \Phi(u_k,x_1) \quad (3\text{-}115)$$

as in subsection 3.3.1 (Eqs. 3-32 and 3-34), then

$$E(f(x_1)|x_2) = \sum_{k=1}^{p} C_k D_k \psi(u_k, x_2) \quad . \tag{3-116}$$

In other words, if $f(x_1)$ belongs to A_n, then $E(f(x_1)|x_2)$ belongs to A_m.

Consequently, if $h(x_1, x_2, \ldots x_n)$ belongs to the class A_n of functions, then $E(h(x_1, x_2 \ldots, x_n)|x_2, \ldots x_n)$ belongs to A_{n-1} and so does $[E(h(x_1, x_2, \ldots x_n)|x_2, \ldots x_n)]^2$. Thus Γ_1 in Eqs. 3-106, 3-107, and 3-109 can be computed in closed form.

3.4.3 Examples of the Rate Distortion Bound

3.4.3.1 Linear Measurement

Suppose that $h(x) = h \cdot x$ is linear (h is a row vector and x is a column vector). Suppose that x has been partitioned into a one-dimensional component x_1 (which we want to estimate) and an (n-1) dimensional component x_2.

$$y = h_1 \cdot x_1 + h_2 \cdot x_2 + v \tag{3-117}$$

is the measurement equation. The mean and covariance of x are given by

$$E(x_1) = \bar{x}_1 \tag{3-118}$$

$$E(x_2) = \bar{x}_2 \tag{3-119}$$

$$E([x_1 - \bar{x}_1]^2) = Q_{11} \tag{3-120}$$

$$E([x_1 - \bar{x}_1]\,[x_2 - \bar{x}_2]^T) = Q_{12} \tag{3-121}$$

$$E([x_2 - \bar{x}_2]\,[x_1 - \bar{x}_1]) = Q_{21} \tag{3-122}$$

$$E([x_2 - \bar{x}_2]\,[x_2 - \bar{x}_2]^T) = Q_{22} \tag{3-123}$$

The conditional mean and variance of x_1 given x_2 are

$$E(x_1|x_2) = \bar{x}_1 + Q_{12}\, Q_{22}^{-1}\, [x_2 - \bar{x}_2] \tag{3-124}$$

$$E([x_1 - E(x_1|x_2)]^2|x_2) = Q_{11} - Q_{12}\, Q_{22}^{-1}\, Q_{21} \quad . \tag{3-125}$$

Thus, we find that

$$Q_1 = Q_{11} - Q_{12}\, Q_{22}^{-1}\, Q_{21} \tag{3-126}$$

and

$$\Gamma = \Gamma_1(x_2) = h_1^2 \cdot Q_1 \quad . \tag{3-127}$$

The corresponding bound is

$$RDB = (h_1^2 R^{-1} + Q_1^{-1})^{-1} \tag{3-128}$$

$$= (h_1^2 R^{-1} + [Q_{11} - Q_{12}\, Q_{22}^{-1}\, Q_{21}]^{-1})^{-1} \tag{3-129}$$

Note that the choice of the component x_2 is somewhat arbitrary, and one could try to select it to make RDB as large as possible. For example, one might choose x_2 independent of x_1 so that $Q_{21} = Q_{12}^T = 0$. Thus, the largest RDB bound obtained by choosing x_2 independent of x_1 is in the linear case

$$RDB = (h_1^2 R^{-1} + Q_{11}^{-1})^{-1} \quad . \tag{3-130}$$

This is generally smaller than the minimum mean square error. We will examine this more closely in subsection 3.4.4 where we compare the RDB with the CRVB. Let us remark that it is possible to develop a tighter rate distortion bound that gives the minimum mean square error exactly. However, this bound appears to be difficult to compute in nonlinear problems.

3.4.3.2 Nonlinear Measurement

Consider the simple example

$$y = x_1^2 + x_2 + v \quad , \tag{3-131}$$

where x_1 and x_2 are independent Gaussian random variables with variances Q_{11} and Q_{22} respectively. Then $Q_1 = Q_{11}$, $\Gamma_1 = 2Q_{11}2$ and the RDB is

$$RDB = ([2Q_{11}]R^{-1} + Q_{11}^{-1})^{-1} \quad . \tag{3-132}$$

3.4.4 Comparison to Cramer-Rao Van Trees Bound

3.4.4.1 Examples

The following examples show that neither CRVB < RDB nor RDB < CRVB in general for vector states and scalar measurements. Suppose that x_1 and x_2 are independent Gaussian random variables with respective variances Q_{11} and Q_{22}.

$h(x_1,x_2) = x_1 + x_2$

This is an example of linear measurements. As we found above, the RDB is

$$RDB = (R^{-1} + Q_{11}^{-1})^{-1} \quad . \tag{3-133}$$

The CRVB is also the minimum mean square error for this case and is given by

$$CRVB = (R^{-1} + Q_{11}^{-1} - R^{-2}[Q_{22}^{-1} + R^{-1}]^{-1})^{-1} \quad . \tag{3-134}$$

Thus, in this case we always have CRVB > RDB. Figure 3-10 shows the two bounds versus R for $Q_{11} = Q_{22} = 1.0$.

$h(x_1,x_2) = x_1^2 + x_2$

We computed the RDB above:

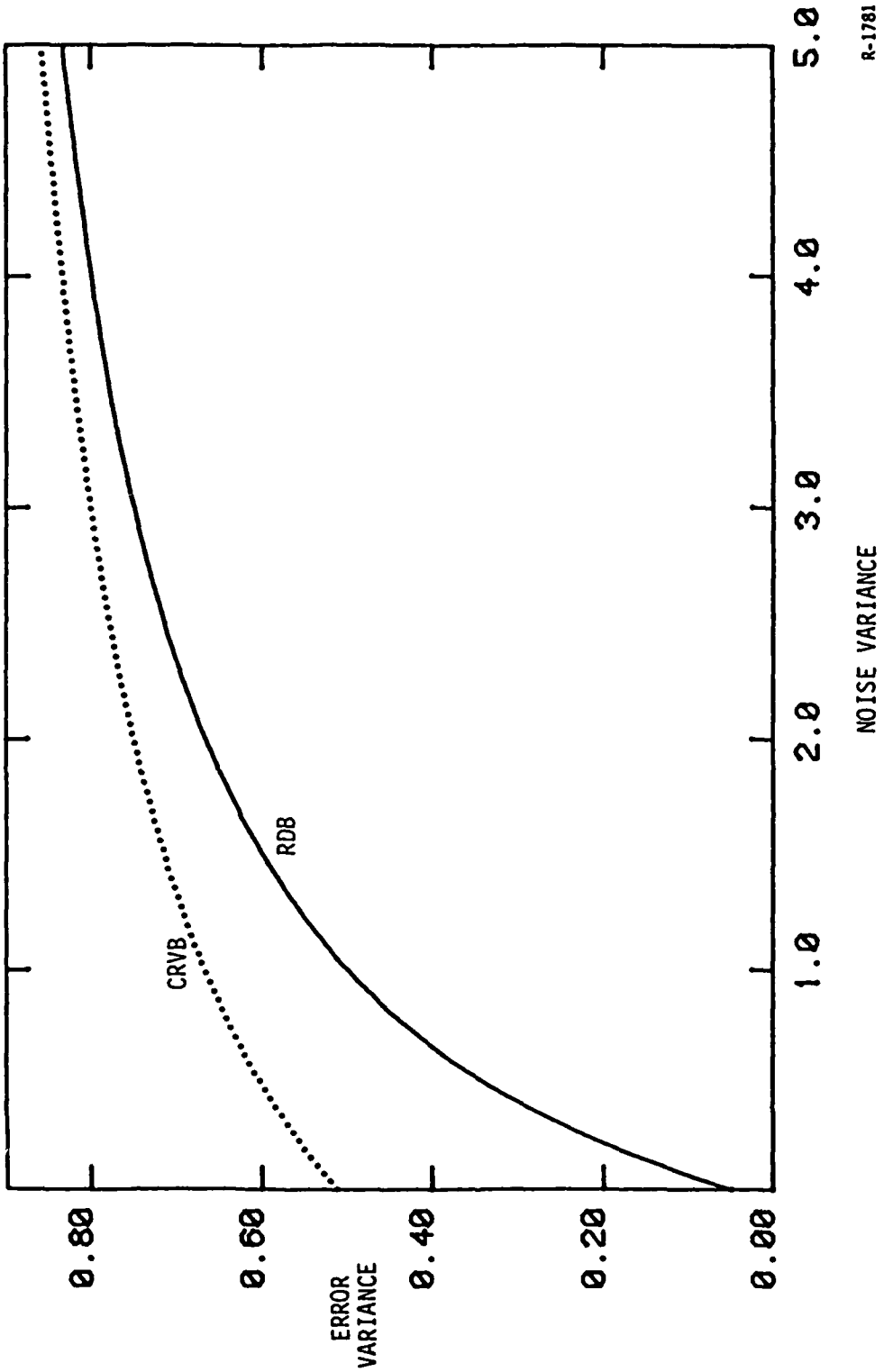

Figure 3-10. Comparison of Rate Distortion and Cramer-Rao-Van Trees Bounds for Vector State With Linear Measurement

$$RDB = ([2Q_{11}]R^{-1} + Q_{11}^{-1})^{-1} \quad . \tag{3-135}$$

The CRVB is easily found to be

$$CRVB = ([4Q_{11}]R^{-1} + Q_{11}^{-1})^{-1} \quad . \tag{3-136}$$

Thus, in this case we always have RDB > CRVB. Figure 3-11 shows the two bounds versus R for $Q_{11} = 1.0$.

3.4.4.2 Comparison at Low Signal-to-Noise Ratios

We can prove a general asymptotic relationship between CRVB and RDB as $R \to \infty$. This relationship is similar to the one we proved in subsection 3.3.3.4. Let x be partitioned into components x_1 and x_2, and define Q_{11}, Q_{12}, Q_{21}, and Q_{22} as in subsection 3.4.2.1. Recall that

$$Q_1 = Q_{11} - Q_{12}\, Q_{22}^{-1}\, Q_{21} \tag{3-137}$$

and

$$\Gamma_1 = E([h(x_1,x_2) - E(h(x_1,x_2)|x_2)]^2) \quad . \tag{3-138}$$

The RDB is simply

$$RDB = ([\Gamma_1 Q_1^{-1}]R^{-1} + Q_1^{-1})^{-1} \quad . \tag{3-139}$$

The CRVB gives a lower bound on the error covariance matrix. This matrix bound is

$$B = (Q^{-1} + R^{-1}\, E(\frac{\partial h^T}{\partial x}\, \frac{\partial h}{\partial x}))^{-1} \tag{3-140}$$

The CRVB for the x_1 estimate is the B_{11} element of the matrix B. For large R we can approximate B by

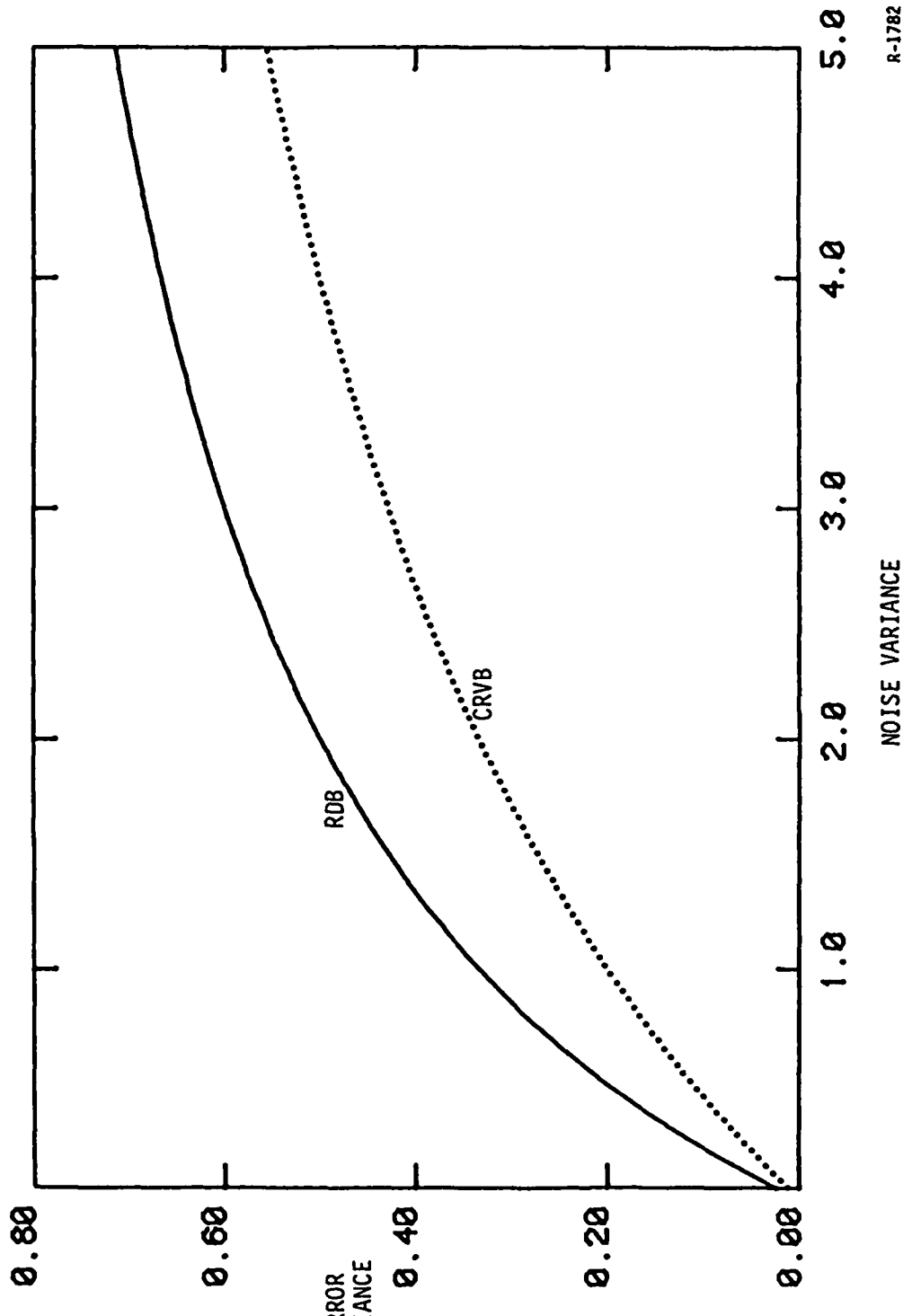

Figure 3-11. Comparison of Rate Distortion and Cramer-Rao-Van Trees Bounds for Vector State With Nonlinear Measurement

$$B = Q - R^{-1}QE\left(\frac{\partial h^T}{\partial x}\frac{\partial h}{\partial x}\right)Q + O(R^{-2}) \quad . \tag{3-141}$$

If $Q_{12} = 0$, $Q_{21} = 0$, then we have to first order in R^{-1}:

$$CRVB = Q_{11} - R^{-1}Q_{11}^{-2}\left(\left[\frac{\partial h}{\partial x_1}\right]^2\right) + O(R^{-2}) \tag{3-142}$$

Equivalently, we have

$$CRVB = \left(\left[E\left(\left[\frac{\partial h}{\partial x_1}\right]^2\right)\right]R^{-1} + Q_{11}^{-1} + O(R^{-2})\right)^{-1} \tag{3-143}$$

to compare with Eq. 3-139. From the scalar state inequality Eq. 3-76 we have

$$Q_1^{-1} \cdot \Gamma_1(x_2) \leq E\left(\left[\frac{\partial h}{\partial x_1}\right]^2 | x_2\right) \tag{3-144}$$

and consequently,

$$Q_1^{-1}\Gamma_1 \leq E\left(\left[\frac{\partial h}{\partial x_1}\right]^2\right) \quad . \tag{3-145}$$

We will assume that the partition x_1, x_2 of x has been chosen so that x_1 and x_2 are independent (i.e., $Q_{12} = 0$, $Q_{21} = 0$).

Then we see that $Q_1 = Q_{11}$ and

$$CRVB \leq RDB + O(R^{-2}) \quad . \tag{3-146}$$

That is, there is a term $O(R^{-2})$ which converges to 0 as fast as R^{-2} when $R \to \infty$, and the CRVB is larger than RDB by at most $O(R^{-2})$. Note that if h depends on x_1 in a nonlinear way, then we must have CRVB < RDB for sufficiently large R.

This is the case in the example $h(x_1,x_2) = x_1^2+x_2$ above. In the linear example $h(x_1,x_2)=x_1+x_2$, one can see from Eqs. 3-133 and 3-144 that CRVB exceeds RDB only by a term of order R^{-2}

3.4.5 Rate Distortion Bound for Vector State and Vector Measurement

If an m dimensional vector measurement is taken, the results of subsection 3.4.1 change as follows. The earlier result Eq. 3-19 for the scalar state case implies

$$E([x_1 - \hat{x}_1(y)]^2|x_2) \geq Q_1 \ (\det(\Gamma_1(x_2)R^{-1} + I_m))^{-1} \qquad (3\text{-}147)$$

where I_m is the mxm identify matrix, Q_1 is given as in Eq. 3-99 and

$$\Gamma_1(x_2) = E([h(x_1,x_2) - E(h(x_1,x_2)|x_2)]\ [h(x_1,x_2) - E(h(x_1,x_2)|x_2)]^T|x_2) \qquad (3\text{-}148)$$

Thus we have

$$E([x_1 - \hat{x}_1(y)]^2) \geq Q_1 \cdot\{E(\det(\Gamma_1(x_2)R^{-1} + I_m))\}^{-1} \quad . \qquad (3\text{-}149)$$

The right-hand-side of Eq. 3-149 is computable in closed form if each component of h belongs to the class A_n. Unfortunately, this computation appears to be difficult in general, and further development is required to make the RDB useful for the general vector state, vector measurement case. However, if the measurement vector consists of N identically distributed, conditionally independent scalar measurements, then RDB is given by

$$RDB = ([N\Gamma_1 Q_1^{-1}]R^{-1} + Q_1^{-1})^{-1} \quad . \qquad (3\text{-}150)$$

3.5 CONCLUDING REMARKS

3.5.1 Summary

In this report we have described how to compute analytically rate distortion bounds of mean square error for static nonlinear estimation problems of the form

$$y = h(x) + v \tag{3-151}$$

where x and v are Gaussian distributed. Specifically, we obtained a lower bound of

$$E([x_1 - \hat{x}_1(y)]^2) \tag{3-152}$$

where x_1 is a scalar component of x. We showed that the rate distortion bound is asymptotically tighter than the Cramer-Rao-Van Trees bound in the limit as the noise covariance R becomes unbounded (i.e., as signal-to-noise ratio approaches 0). We illustrated the rate distortion bound and its comparison to the Cramer-Rao-Van Trees bound using a number of simple examples.

3.5.2 Conclusions

Based on present results, the rate distortion bound offers a better approximation of mean square performance in the high measurement noise regime than the Cramer-Rao-Van Trees bound. Furthermore, the rate distortion bound requires little, if any, more computation than the Cramer-Rao-Van Trees bound. Thus, the rate distortion bound appears to complement the Cramer-Rao-Van Trees method in the nonlinear, high noise regime where the latter bound is known to give overly optimistic approximations of the true mean square error. However, in order to make the rate distortion theory useful for the dynamic nonlinear estimation problems of tracking, we must develop our current results in two significant ways:

1. it is necessary to obtain a simple rate distortion bound in the case of a vector state and a general vector measurement;

2. it is necessary to derive a recursively computable bound for dynamic estimation problems.

3.5.3 Other Work

Zakai and Ziv [11] first applied rate distortion theory to mean square performance analysis of nonlinear filtering problems. The results of [11] were restricted to a special class of continuous-time processes. Galdos [12] extended these results to general vector processes, both in continuous and discrete time. In this section we have derived some preliminary bounds on individual component errors as in Eq. 3-152. The results of [12] give bounds on the sum over all component errors

$$\sum_{k=1}^{n} E(x_k - \hat{x}_k(y)]^2) \quad . \tag{3-153}$$

We believe the approach here, based on our earlier work [13],[14], will yield a more accurate estimate of mean square estimation error. However, until results of this section are extended, we can make no comparisons with [11],[12].

3.5.4 Further Investigation

Other directions for further investigation exist beside the two necessary extensions noted in subsection 3.5.2 above. One direction would extend the bounds to problems for which x is an unknown, non-random parameter (or a mixture of random and non-random parameters). In [1] we found that a large class of tracking problems can be modeled by a state process which consists of an unknown deterministic component and an unknown, Gaussian distributed random component. Rate distortion theory for nonstatistical sources (ε - entropy methods [4] may allow us to derive such results.

Another direction is to study the effect of architecture constraints, such as preprocessing of measurements, on tracking estimation performance. We investigated this problem in [1] using Cramer-Rao-Van Trees methods. A rate distortion approach, based as it is on info ~ation theory, would provide a more general, more accurate method of analyzing architectural constraints.

SECTION 4

AMBIGUITY PERFORMANCE ANALYSIS

4.1 INTRODUCTION

Ambiguity analysis ([7],[15] Chapter 10) is an attempt to understand the global nature of a parameter estimation problem. This is in contrast to Cramer-Rao methods which provide a more local analysis of estimation performance. The Cramer-Rao lower bound on mean square estimation error will be an accurate estimate of true optimal performance provided that it is possible to acquire or maintain an estimate near the unknown parameter at all. The local problem (addressed by the Cramer-Rao method) is to analyze accuracy given acquisition; the global problem (addressed by ambiguity analysis) is to analyze the acquisition performance.

The ambiguity approach can be formulated as follows. Suppose one wishes to estimate an unknown parameter x given a measurement y. Let $\hat{x}$ denote the maximum likelihood estimator of x which depends on y and consider the mean square estimation error

$$E_x\{(x - \hat{x})^2\} = \sum_{k=0}^{n} E_x\{(x - \hat{x})^2 | \hat{x} \epsilon R_k\} \, P_x\{\hat{x} \epsilon R_k\}$$

where $E_x\{\cdot\}$ and $P_x\{\cdot\}$ denote the expectation and probability given that x is the true value of the parameter; and R_0, R_1, ..., R_n are n+1 regions subdividing the x parameter space. Approximate $E_x\{(x - \hat{x})^2 | \hat{x} \epsilon R_k\}$ by ϵ_k^2 and approximate $P_x\{\hat{x} \epsilon R_k\}$ by p_k. Then the mean square error is approximated by

$$E_x\{(x - \hat{x})^2\} \approx \sum_{k=0}^{n} \varepsilon_k^2 \cdot p_k \quad .$$

For example, assume that the true parameter $x \in R_0$ and let ε_0^2 be the Cramer-Rao bound for the problem. If $k \neq 0$, choose a typical $x_k \in R_k$ and let $\varepsilon_k^2 = (x - x_k)^2$. Approximate $P_x\{\hat{x} \in R_k\}$ by the following hypothesis testing problem. Let $\hat{x}_n(y)$ be the x_k that maximizes $P_{x_k}\{y\}$ and let p_k be $P_x\{\hat{x}_n \in R_k\}$.

Can we show rigorously that

$$\sum_{k=0}^{n} \varepsilon_k^2 \cdot p_k \longrightarrow E_x\{(x - \hat{x})^2\}$$

as the number n+1 of regions increases and the size of the regions decreases? Can we estimate the size of the error for a given n and choice of regions R_k?

In this section we provide detailed convergence analysis for a particular sequence of approximations for the calculation of the error variance in a maximum likelihood estimation problem. We restrict our attention here to a scalar problem. While several of the detailed calculations we perform do use the scalar nature of the problem to allow us to write down very explicit formulae, the general nature of the analysis can be extended (this would, however, involve the determination of several additional estimates to replace the closed-form expressions available in the scalar case).

4.2 PROBLEM FORMULATION

We consider the problem of estimating a scalar parameter x which is known to take values on the interval [0,1]. We have available the scalar measurement

$$y = h(x) + \nu \qquad (4\text{-}1)$$

where ν is a Gaussian random variable with mean 0 and variance 1. We also assume

$$h(0) > 0 \tag{4-2a}$$

$$0 < h'(x) \leq M < \infty \quad \text{for all } x\varepsilon[0,1] \tag{4-2b}$$

and h(x) can be expanded in a series around any point $\alpha\varepsilon[0,1]$:

$$h(x) = h(\alpha) + \frac{dh}{dx}(\alpha)[x - \alpha] + R(x - \alpha) \tag{4-3}$$

where $R(x - x_0) = O((x - x_0)^2)$. Note that Eq. 4-2a is a trivial assumption since we can always add a constant to h. Also note that the monotonicity assumption (Eq. 4-2b) simply avoids the possibility that $h(x_1) = h(x_2)$ for any $x_1, x_2\varepsilon[0,1]$.

The problem with which we are concerned is the following. Suppose that the true value of x is x_0. We wish to calculate (or more precisely to obtain a sequence of approximations to)

$$E[(\hat{x} - x_0)^2 | x = x_0]$$

where $\hat{x}$ is the maximum likelihood estimate. That is, let

$$\ell(x) = yh(x) - \frac{1}{2} h(x)^2 \tag{4-4}$$

Then

$$\hat{x} = \arg\max_x \ell(x) \tag{4-5}$$

We begin with several preliminary calculations.

Computation of the Distribution Function for $\hat{x}$

Let us rewrite Eq. 4-4 using Eq. 4-1 and the fact that $x = x_0$:

$$\ell(x) = h(x_0)\, h(x) + \nu\, h(x) - \frac{1}{2} h(x)^2 \tag{4-6}$$

Consider the derivative of Eq. 4-6

$$\ell'(x) = [h(x_0) + \nu - h(x)]h'(x) \tag{4-7}$$

Note that, thanks to Eq. 4-2b $\ell'(x) = 0$ if and only if

$$\nu = h(x) - h(x_0) \tag{4-8}$$

Thus, again thanks to Eq. 4-2 we see that

$$\ell'(x) > 0 \quad \text{for all } x\varepsilon[0,1] \quad \text{if} \quad \nu > h(1) - h(x_0) \tag{4-9a}$$

$$\ell'(x) < 0 \quad \text{for all } x\varepsilon[0,1] \quad \text{if} \quad \nu < h(0) - h(x_0) \tag{4-9b}$$

Thus

$$\text{Prob}(\hat{x} = 0 | x = x_0) = \text{Prob}(\nu < h(0) - h(x_0)) \tag{4-10a}$$

$$\text{Prob}(\hat{x} = 1 | x = x_0) = \text{Prob}(\nu > h(1) - h(x_0)) \tag{4-10b}$$

If $\nu\varepsilon(h(0) - h(x_0), h(1) - h(x_0))$, $\hat{x}$ will be the value of x for which $\ell'(x) = 0$, i.e., the value for which Eq. 4-8 is satisfied. Thus,

$$\text{Prob}(0 < \hat{x} < \alpha | x = x_0) = \text{Prob}(h(0) - h(x_0) < \nu < h(\alpha) - h(x_0))$$

$$= \int_{h(0)-h(x_0)}^{h(\alpha)-h(x_0)} N(\nu;\ 0,1)\ d\nu \tag{4-11}$$

where

$$N(\nu;\ 0,1) = \frac{1}{\sqrt{2\pi}}\ e^{-\nu^2/2} \tag{4-12}$$

Thus the probability density function for $\hat{x}$ on [0,1] is

$$P_{\hat{x}}(\alpha) = \frac{d}{d\alpha} \text{Prob}(0 < \hat{x} < \alpha | x = x_0)$$
$$= N(h(\alpha) - h(x_0); 0,1)h'(\alpha) \tag{4-13}$$

Note that in this case we obtain a formula for the error variance

$$E[(\hat{x} - x_0)^2 | x = x_0] = x_0^2 \text{ Prob}(\nu < h(0) - h(x_0))$$
$$+ (1 - x_0)^2 \text{ Prob}(\nu > h(1) - h(x_0))$$
$$+ \int_0^1 (x_0 - \alpha)^2 \frac{h'(\alpha)}{\sqrt{2\pi}} \exp\left\{-\frac{1}{2}(h(\alpha) - h(x_0))^2\right\} d\alpha$$

In the sequel we develop a sequence of approximations to this quantity motivated by our desire to develop methods that can be applied to more complex problems.

The Cramer-Rao Bound and the Ambiguity Function

For this problem

$$p(y|x) = \frac{1}{\sqrt{2\pi}} \exp\left\{-\frac{1}{2}(y - h(x))^2\right\} \tag{4-14}$$

and it is a straightforward computation to verify that the Cramer-Rao Bound is

$$\text{CRB}(x_0) = -\left\{E\left(\frac{\partial^2 \ell n\, p(y|x_0)}{\partial x^2} \,\middle|\, x = x_0\right)\right\}^{-1} = \frac{1}{\left(\frac{dh(x_0)}{dx}\right)^2} \tag{4-15}$$

The ambiguity function in this problem is

$$A(x_1, x_2) = h(x_1)h(x_2) \tag{4-16}$$

Note that

$$E\left[\ell(x)\,|\,x_0 = x\right] = A(x,x_0) - \frac{1}{2}A(x,x) \tag{4-17}$$

$$\text{Cov}\left[\ell(x_1),\ell(x_2)\right] = A(x_1,x_2) \tag{4-18}$$

and

$$-\left\{\frac{\partial^2}{\partial x^2}\left[A(x,x_0) - \frac{1}{2}A(x,x)\right]\Bigg|_{x = x_0}\right\}^{-1} = \text{CRB}\,(x_0) \tag{4-19}$$

Thus the Cramer-Rao bound is seen to depend explicitly on the curvature of $E[\ell(x)|x = x_0]$ at the location of its peak, i.e., at $x = x_0$.

4.3 CONVERGENCE ANALYSIS

We now construct a sequence of approximations indexed by the integer N. Essentially what we will do is to divide the interval [0,1] into subintervals, most of which will be of length 1/N. There will, however, be one interval centered at the true value x_0 that will be larger. Specifically, let

$$I_c^N = \left(x_0 - \frac{1}{\sqrt{N}}\ ,\ x_0 + \frac{1}{\sqrt{N}}\right) \cap [0,1] \tag{4-20}$$

Assuming that N is large enough so that $x_0 - 1/\sqrt{N} > 0$, define

$$I_{L,-1}^N = \{0\} \tag{4-21a}$$

$$I_{L,i}^N = \left(\frac{i}{N}\ ,\ \frac{i+1}{N} \wedge \left(x_0 - \frac{1}{\sqrt{N}}\right)\right]\ ,\quad i = 0,\ 1,\ \ldots,\ L(N) \tag{4-21b}$$

where $a \wedge b$ indicates minimum of a and b and where

$$L(N) = \left\lceil Nx_0 - \sqrt{N} - 1 \right\rceil \tag{4-21c}$$

(Here $\lceil z \rceil$ is the smallest integer greater than or equal z). Note that $L(N) = O(N)$. Similarly assuming that $x_0 + 1/\sqrt{N} < 1$, define

$$I_{R,-1}^N = \{1\} \tag{4-22a}$$

$$I_{R,i}^N = \left[\left(x_0 + \frac{1}{\sqrt{N}} \right) \vee \frac{N-i-1}{N}, \frac{N-i}{N} \right) \quad , \quad i = 0, 1, \ldots, R(N) \tag{4-22b}$$

where a V b indicates maximum of a and b and where

$$R(N) = \left\lceil N - 1 - Nx_0 - \sqrt{N} \right\rceil \tag{4-22c}$$

Again $R(N) = O(N)$. What we have done is to partition [0,1] into disjoint sets. There is one, larger central set I_c^N, and the two endpoints $I_{L,-1}^N$ and $I_{R,-1}^N$. The remaining sets to the left of I_c^N are of the form $(i/N, i+1/N]$ except for the one bordering on I_c^N which is clipped off so that it doesn't overlap. Similarly the sets to the right of I_c^N are of the form $[i/N, i+1/N)$ except for the one bordering on I_c^N which is clipped off so that it doesn't overlap.

Since these sets don't overlap, we have the following equality

$$\begin{aligned} E[(\hat{x} - x_0)^2 | \alpha = x_0] = & \sum_{i=-1}^{L(N)} E[(\hat{x} - x_0)^2 | x = x_0, \hat{x} \epsilon I_{Li}^N] Pr(\hat{x} \epsilon I_{Li}^N | x = x_0) \\ & + \sum_{i=-1}^{R(N)} E[(\hat{x} - x_0)^2 | x = x_0, \hat{x} \epsilon I_{Ri}^N] Pr(\hat{x} \epsilon I_{Ri} | x = x_0) \\ & + E[(\hat{x} - x_0)^2 | x = x_0, x \epsilon I_c^N] Pr(\hat{x} \epsilon I_c^N | x = x_0) \end{aligned} \tag{4-23}$$

Our approximate method for evaluating the left-hand side of Eq. 4-23 is based on obtaining approximations for each of the terms on the right-hand side. To do this, we proceed by defining the following discrete set of points

$$\begin{aligned}
&\delta_{-1}^N = 0 \\
&\delta_i^N = \text{center point of } I_{L,i}^N \quad , \quad i = 0, \ldots, L(N) \\
&x_0 \\
&\gamma_{-1}^N = 1 \\
&\gamma_i^N = \text{center point of } I_{R,i}^N \quad , \quad i = 0, \ldots, R(N)
\end{aligned} \tag{4-24}$$

Note that

$$\begin{aligned}
&\delta_0^N - \delta_{-1}^N = \frac{1}{2N} \\
&\delta_{i+1}^N - \delta_i^N = \frac{1}{N} \quad , \quad i = 0, \ldots, L(N) - 2 \\
&\delta_{i+1}^N - \delta_i^N = O\left(\frac{1}{N}\right) \quad , \quad i = L(N) - 1 \\
&x_0 - \delta_{L(N)}^N = O\left(\frac{1}{\sqrt{N}}\right) \\
&\gamma_{R(N)}^N - x_0 = O\left(\frac{1}{\sqrt{N}}\right) \\
&\gamma_i^N - \gamma_{i+1}^N = O\left(\frac{1}{N}\right) \quad , \quad i = R(N) - 1 \\
&\gamma_i^N - \gamma_{i+1}^N = \frac{1}{N} \quad , \quad i = 0, \ldots, R(N) - 2 \\
&\gamma_{-1}^N - \gamma_0^N = \frac{1}{2N}
\end{aligned} \tag{4-25}$$

Consider the hypothesis testing problem in which we assume that we know that x takes on one of the finite set of values in Eq. 4-24, and suppose that we use the maximum likelihood criterion for choosing our estimate from this finite set. Let

$$\rho_{Li}^{N}(x_0) = \text{Prob}(\text{choose } \delta_i^N | x = x_0) \quad , \quad i = -1, \ldots, L(N) \tag{4-26a}$$

$$\rho_{c}^{N}(x_0) = \text{Prob}(\text{choose } x_0 | x = x_0) \tag{4-26b}$$

$$\rho_{Ri}^{N}(x_0) = \text{Prob}(\text{choose } \gamma_i^N | x = x_0) \quad , \quad i = -1, \ldots, R(N) \tag{4-26c}$$

Then our approximation to Eq. 4-23 is

$$\begin{aligned} E\left[(\hat{x} - x_0)^2 | x = x_0\right] \approx & \sum_{i=-1}^{L(N)} (\delta_i^N - x_0)^2 \, \rho_{LI}^{N}(x_0) \\ & + \sum_{i=-1}^{R(N)} (\gamma_i^N - x_0)^2 \, \rho_{Ri}^{N}(x_0) \\ & + \text{CRB}(x_0) P(N) \, \rho_c^N(x_0) \triangleq \hat{V}(x_0) \end{aligned} \tag{4-27}$$

where

$$P(N) = E\left[\nu^2 \left| |\nu| \leq \frac{1}{\sqrt{N}} \frac{dh}{dx}(x_0)\right.\right] \tag{4-28}$$

We now proceed to estimate the errors in the various terms and to show that Eq. 4-27 converges to $E[(\hat{x} - x_0)^2 | x = x_0]$ as $N \to \infty$.

The Terms $E[(\hat{x} - x_0)^2 | x = x_0, \hat{x} \epsilon I_{L,i}^N]$ and $E[(\hat{x} - x_0)^2 | x = x_0, \hat{x} \epsilon I_{R,i}^N]$

Note first that

$$E[(\hat{x} - x_0)^2 | x = x_0, \hat{x} \epsilon I_{L,-1}^N] = (\delta_{-1}^N - x_0)^2 \tag{4-29a}$$

$$E[(\hat{x} - x_0)^2 | x = x_0, \hat{x} \epsilon I_{R,-1}^N] = (\gamma_{-1}^N - x_0)^2 \tag{4-29b}$$

Furthermore for $i > 0$

$$E[(\hat{x} - x_0)^2 | x = x_0, \hat{x} \epsilon I_{Li}^N] \tag{4-30}$$

$$= \int_{I_{Li}^N} (\alpha - x_0)^2 \, p_{\hat{x}}(\alpha | x = x_0, \hat{x} \epsilon I_{Li}^N) \, d\alpha$$

where

$$p_{\hat{x}}(\alpha | x = x_0, \hat{x} \epsilon I_{Li}^N) = \frac{p_{\hat{x}}(\alpha | x = x_0)}{\int_{I_{Li}^N} p_{\hat{x}}(\alpha | x = x_0)} \tag{4-31}$$

and $p_{\hat{x}}(\alpha | x = x_0)$ is given in Eq. 4-13. We now see that the integral in Eq. 4-30 is sufficiently smooth over the entire interval, so that we may approximate it as

$$(\delta_i^N - x_0)^2 \, p_{\hat{x}}(\delta_i^N | x = x_0, \hat{x} \epsilon I_{Li}^N) \times \text{Length}(I_{Li}^N) \tag{4-32}$$

The error introduced in this approximation is $O\left(\frac{1}{N^2}\right)$. To see this, examine Fig. 4-1.

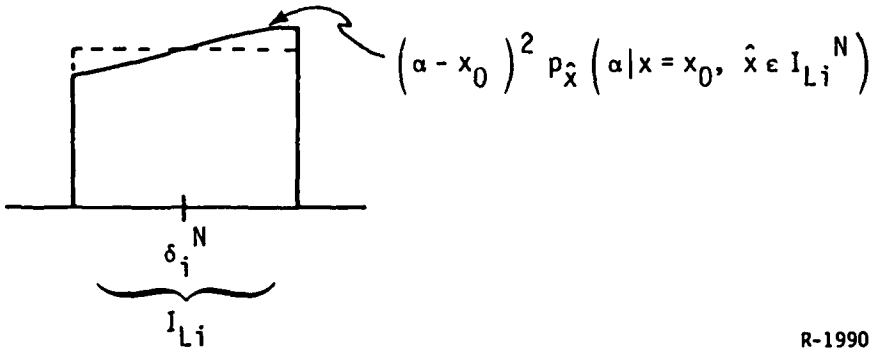

Figure 4-1. $O\left(\frac{1}{N^2}\right)$ Approximation Error

The integral to be evaluated is the area under the solid curve, while Eq. 4-32 equals the area under the dotted curve. Let

$$K = \sup_i \sup_\alpha \left| \frac{d}{d\alpha} \left[(\alpha - x_0)^2 \, p_{\hat{x}}(\alpha | x = x_0, \hat{x} \epsilon I_{Li}^N) \right] \right|$$

It is easy to see that $K < \infty$ and that the magnitude of the difference between the areas under the solid and dashed curves in Fig. 4-1 is bounded above by

$$\frac{K}{2} \left[\text{Length}(I_{Li}^N) \right]^2$$

which, from Eq. 4-21 is $O\left(\frac{1}{N^2}\right)$. Finally we note that by the same type of argument

$$\begin{aligned} 1 &= \int_{I_{Li}} p_{\hat{x}}(\alpha | x = x_0, \hat{x} \epsilon I_{Li}^N) \, d\alpha \\ &= p_{\hat{x}}(\delta_i^N | x = x_0, \hat{x} \epsilon I_{Li}^N) \times \text{Length}(I_{Li}^N) + O\left(\frac{1}{N^2}\right) \end{aligned} \tag{4-33}$$

Combining Eqs. 4-30 through 4-33 we see that

$$E[(\hat{x} - x_0)^2 | x = x_0, \hat{x} \epsilon I_{Li}^N] = (\delta_i^N - x_0)^2 + o\left(\frac{1}{N^2}\right) \qquad i = 0, \ldots, L(N) \tag{4-34}$$

In an analogous fashion we can show that

$$E[(\hat{x} - x_0)^2 | x = x_0, \hat{x} \epsilon I_{Ri}^N] = (\gamma_i^N - x_0)^2 + o\left(\frac{1}{N^2}\right) \qquad i = 0, \ldots, R(N) \tag{4-35}$$

The Term $E[(\hat{x} - x_0)^2 | x = x_0, \hat{x} \epsilon I_c^N]$

Substituting Eq. 4-3 into Eq. 4-6 we obtain

$$\ell(x) = \frac{1}{2} h(x_0)^2 - \frac{1}{2}\left(\frac{dh}{dx}(x_0)\right)^2 [x - x_0]^2 - \frac{dh}{dx}(x_0)[x - x_0] R(x - x_0) - \frac{1}{2}\left[R(x - x_0)\right]^2 + \nu\, h(x_0) + \nu \frac{dh}{dx}[x - x_0] + \nu\, R(x - x_0) \tag{4-36}$$

Assuming that $\hat{x} \epsilon I_c^N$ we have that

$$0 = \frac{d\ell(\hat{x})}{dx} = -\left(\frac{dh}{dx}(x_0)\right)^2 [\hat{x} - x_0] + \nu \frac{dh}{dx}(x_0) + \Delta_1(\hat{x}) + \nu \Delta_2(\hat{x}) \tag{4-37}$$

where

$$\Delta_1(\hat{x}) = -\frac{dh}{dx}(x_0)[R(\hat{x} - x_0) + (\hat{x} - x_0)\frac{d}{dx} R(\hat{x} - x_0)] - R(\hat{x} - x_0)\frac{d}{dx} R(\hat{x} - x_0) \tag{4-38a}$$

$$\Delta_2(\hat{x}) = \frac{d}{dx} R(\hat{x} - x_0) \tag{4-38b}$$

and

$$\sup_{\hat{x}\epsilon I_c^N} |\Delta_1(\hat{x})| = O\left(\frac{1}{N}\right) \tag{4-39a}$$

$$\sup_{\hat{x}\epsilon I_c^N} |\Delta_2(\hat{x})| = O\left(\frac{1}{\sqrt{N}}\right) \tag{4-39b}$$

From Eq. 4-37 we see that

$$\hat{x} - x_0 = \left[\frac{dh}{dx}(x_0)\right]^{-1} \nu + \left[\frac{dh}{dx}(x_0)\right]^{-2} \left[\Delta_1(\hat{x}) + \nu\Delta_2(\hat{x})\right] \tag{4-40}$$

Also we are assuming

$$|\hat{x} - x_0| < \frac{1}{\sqrt{N}}$$

Combining Eqs. 4-39 and Eq. 4-40 we can deduce that the implied constraint on ν is

$$|\nu| < \frac{1}{\sqrt{N}} \frac{dh}{dx}(x_0) + O\left(\frac{1}{N}\right) \tag{4-41}$$

Thus

$$\begin{aligned} E\left[\nu^2 | x = x_0,\ \hat{x}\epsilon I_c^N\right] &= E\left[\nu^2 \left| |\nu| < \frac{1}{\sqrt{N}} \frac{dh}{dx}(x_0)\right.\right] + O\left(\frac{1}{N^{5/2}}\right) \\ &= P(N) + O\left(\frac{1}{N^{5/2}}\right) \end{aligned} \tag{4-42}$$

The $O\left(\frac{1}{N^{5/2}}\right)$ comes from the $O\left(\frac{1}{N}\right)$ term in Eq. 4-41 which implies that the actual limits on ν can differ by a term of order 1/N. Thus the probability mass in the interval between

$$\frac{1}{\sqrt{N}} \frac{dh}{dx}(x_0)$$

and the right-hand side of Eq. 4-41 is $O\left(\frac{1}{N}\right)$, and

$$\left[\frac{1}{\sqrt{N}} \frac{dh}{dx}(x_0) + O\left(\frac{1}{N}\right)\right]^2 - \left[\frac{1}{\sqrt{N}} \frac{dh}{dx}(x_0)\right]^2 = O\left(\frac{1}{N^{3/2}}\right) \tag{4-43}$$

Finally, using Eqs. 4-39, 4-40, and 4-42 we obtain

$$E\left[(\hat{x} - x_0)^2 | x = x_0, \hat{x} \epsilon I_c^N\right] = P(N)\left[\frac{dh}{dx}(x_0)\right]^{-2} + O\left(\frac{1}{N^{3/2}}\right) \tag{4-44}$$

The Probabilities in Eq. 4-23

Under the assumption that x is one of the points in Eq. 4-23, the maximum likelihood decision rule is to choose x corresponding to the largest among the values $\ell(x)$ evaluated at these points. Note next that under the assumption that $x_0 = x$

$$\begin{aligned} \ell(\delta_{i+1}^N) - \ell(\delta_i^N) = h(x_0)\left[h(\delta_{i+1}^N) - h(\delta_i^N)\right] \\ - \frac{1}{2}\left[h(\delta_{i+1}^N)^2 - h(\delta_i^N)\right]^2 \\ + \nu\left[h(\delta_{i+1}^N) - h(\delta_i^N)\right] \end{aligned} \tag{4-45}$$

Thus using Eq. 4-2b we see that the sign of $\ell(\delta_{i+1}^N) - \ell(\delta_i^N)$ is the same as the sign of

$$h(x_0) - \frac{1}{2}\left[h(\delta_{i+1}^N) + h(\delta_i^N)\right] + \nu \triangleq -\mu_{Li}^N + \nu \qquad (4\text{-}46a)$$

Similarly the signs of $\ell(x_0) - \ell(\delta_{L(N)}^N)$, $\ell(\gamma_{R(N)}^N) - \ell(x_0)$, and $\ell(\gamma_i^N) - \ell(\gamma_{i+1}^N)$ are the same as the signs of

$$h(x_0) - \frac{1}{2}\left[h(x_0) + h(\delta_{L(N)}^N)\right] + \nu \triangleq -\mu_{c1}^N + \nu \qquad (4\text{-}46b)$$

$$h(x_0) - \frac{1}{2}\left[h(\gamma_{R(N)}^N) + h(x_0)\right] + \nu \triangleq -\mu_{c2}^N + \nu \qquad (4\text{-}46c)$$

$$h(x_0) - \frac{1}{2}\left[h(\gamma_i^N) + h(\gamma_{i+1}^N)\right] + \nu \triangleq -\mu_{Ri}^N + \nu \qquad (4\text{-}46d)$$

Again using Eq. 4-2b) we have that

$$\mu_{L,-1}^N < \mu_{L,0}^N < \ldots < \mu_{L,L(N)-1}^N < \mu_{c1}^N < \mu_{c2}^N < \mu_{R,R(N)-1}^N < \ldots < \mu_{R,-1}^N \qquad (4\text{-}46e)$$

and from this we can deduce that the quantities in Eq. 4-46 are as follows:

$$\rho_{L,-1}^N(x_0) = \text{Prob}(\nu < \mu_{L,-1}^N) \qquad (4\text{-}47a)$$

$$\rho_{L,i}^N(x_0) = \text{Prob}(\mu_{L,i-1}^N < \nu < \mu_{L,i}^N) \qquad (4\text{-}47b)$$

$$i = 0, 1, \ldots, L(N) - 1$$

$$\rho_{L,L(N)}^N(x_0) = \text{Prob}(\mu_{L,L(N)-1}^N < \nu < \mu_{c1}^N) \qquad (4\text{-}47c)$$

$$\rho_c^N(x_0) = \text{Prob}(\mu_{c1}^N < \nu < \mu_{c2}^N) \qquad (4\text{-}47d)$$

$$\rho_{R,R(N)}^N = \text{Prob}(\mu_{c2}^N < \nu < \mu_{R,R(N)-1}^N) \qquad (4\text{-}47e)$$

$$\rho_{R,i}^{N} = \text{Prob}(\mu_{R,i}^{N} < \nu < \mu_{R,i-1}^{N}) \qquad (4\text{-}47f)$$

$$i = 0, \ldots, R(N) - 1$$

$$\rho_{R,-1} = = \text{Prob}(\nu > \mu_{R,-1}^{N}) \qquad (4\text{-}47g)$$

We now compare these terms to the terms to which they correspond in Eq. 4-23. First, note that

$$\rho_{L,-1}^{N}(x_0) = \text{Prob}(\text{choose } 0 | x = x_0) = \text{Prob}\left(\nu < \frac{1}{2}\left[h\left(\frac{1}{2N}\right) + h(0)\right] - h(x_0)\right) \qquad (4\text{-}48a)$$

while

$$\text{Prob}(\hat{x} \epsilon I_{L,-1}^{N} | x = x_0) = \text{Prob}(\nu < h(0) - h(x_0)) \qquad (4\text{-}48b)$$

Given Eq. 4-2b we have

$$\text{Prob}(\hat{x} \epsilon I_{L,-1}^{N} | x = x_0) = \rho_{L,-1}^{N} + O\left(\frac{1}{N}\right) \qquad (4\text{-}49)$$

Similarly

$$\text{Prob}(\hat{x} \epsilon I_{R,-1}^{N} | x = x\ ) = \rho_{R,-1}^{N} + O\left(\frac{1}{N}\right) \qquad (4\text{-}50)$$

Next note that for $i = 0, 1, \ldots, L(N) - 2$

$$\rho_{L,i}^{N}(x_0) = \int_{\mu_{L,i}^{N}}^{\frac{1}{2}\left[\left(\frac{i+3/2}{N}\right) + h\left(\frac{i+1/2}{N}\right)\right] - h(x_0)} N(\nu;\ 0,1)\, d\nu = \int_{\mu_{L,i-1}^{N}}^{\frac{1}{2}\left[\left(\frac{i+1/2}{N}\right) + h\left(\frac{i-1/2}{N}\right)\right] - h(x_0)} N(\nu;\ 0,1)\, d\nu \qquad (4\text{-}51)$$

while from Eq. 4-11 for i = 0, 1, ..., L(N) - 2

$$\text{Prob}\left(\hat{x}\epsilon I_{L,i}^{N} | x = x_0\right) = \int_{h\left(\frac{i}{N}\right)-h(x_0)}^{h\left(\frac{i+1}{N}\right)-h(x_0)} N(\nu;\, 0,1)\, d\nu \qquad (4\text{-}52)$$

Using Eq. 4-3 (with $\alpha = i/N$) we have that

$$\frac{1}{2}\left[h\left(\frac{i + 1/2}{N}\right) + h\left(\frac{i - 1/2}{N}\right)\right] = h\left(\frac{i}{N}\right) + O\left(\frac{1}{N^2}\right) \qquad (4\text{-}53a)$$

$$\frac{1}{2}\left[h\left(\frac{i + 3/2}{N}\right) + h\left(\frac{i + 1/2}{N}\right)\right] = h\left(\frac{i + 1}{N}\right) + O\left(\frac{1}{N^2}\right) \qquad (4\text{-}53b)$$

Thus

$$\text{Prob}\left(\hat{x}\epsilon I_{L,i}^{N} | x = x_0\right) = \rho_{L,i}^{N}(x_0) + O\left(\frac{1}{N^2}\right) \quad , \quad i = 0, 1, \ldots, L(N) - 2 \qquad (4\text{-}54)$$

Similarly

$$\text{Prob}\left(\hat{x}\epsilon I_{R,i}^{N} | x = x_0\right) = \rho_{R,i}^{N}(x_0) + O\left(\frac{1}{N^2}\right) \quad , \quad i = 0, 1, \ldots, R(N) - 2 \qquad (4\text{-}55)$$

Now for i = L(N) - 1

$$\rho_{L,L(N)-1}^{N}(x_0) = \int_{\frac{1}{2}\left[h\left(\frac{L(N)-3/2}{N}\right)+h\left(\frac{L(N)-1/2}{N}\right)\right]-h(x_0)}^{\frac{1}{2}\left[h\left(\delta_{L(N)}^{N}\right)+h\left(\frac{L(N)-1/2}{N}\right)\right]-h(x_0)} N(\nu;\, 0,1)\, d\nu \qquad (4\text{-}56a)$$

while

$$\text{Prob}\left(\hat{x}\epsilon I_{L,L(N)-1}{}^{N} | x = x_0\right) = \int_{h\left(\frac{L(N)-1}{N}\right)-h(x_0)}^{h\left(\frac{L(N)}{N}\right)-h(x_0)} N(\nu;\, 0,1)\, d\nu \qquad (4\text{-}56b)$$

and furthermore

$$\delta_{L(N)}{}^{N} = \frac{1}{2}\left[\frac{L(N)}{N} + \left(x_0 - \frac{1}{\sqrt{N}}\right)\right] \qquad (4\text{-}57)$$

Using Eq. 4-3 we have

$$\frac{1}{2}\left[h\left(\delta_{L(N)}{}^{N}\right) + h\left(\frac{L(N) - 1/2}{N}\right)\right] = h\left(\frac{L(N)}{N}\right) + O\left(\frac{1}{N}\right) \qquad (4\text{-}58)$$

so that

$$\text{Prob}\left(\hat{x}\epsilon I_{L,L(N)-1}{}^{N} | x = x_0\right) = \rho_{L,L(N)-1}{}^{N}(x_0) + O\left(\frac{1}{N}\right) \qquad (4\text{-}59)$$

and similarly

$$\text{Prob}\left(\hat{x}\epsilon I_{R,R(N)-1}{}^{N} | x = x_0\right) = \rho_{R,R(N)-1}(x_0) + O\left(\frac{1}{N}\right) \qquad (4\text{-}60)$$

Next we have that

$$\rho_{L,L(N)}{}^{N}(x_0) = \int_{\frac{1}{2}\left[h\left(\delta_{L(N)}{}^{N}\right) + h\left(\frac{L(N) - 1/2}{N}\right)\right]-h(x_0)}^{\frac{1}{2}\left[h(x_0)+h\left(\delta_{L(N)}{}^{N}\right)\right]-h(x_0)} N(\nu;\, 0,1)\, d\nu \qquad (4\text{-}61)$$

and

$$\text{Prob}\left(\hat{x}\epsilon I_{L,L(N)^N} \middle| x = x_0\right) = \int_{h\left(x_0 - \frac{1}{\sqrt{N}}\right)-h(x_0)}^{h\left(\frac{L(N)}{N}\right)-h(x_0)} N(\nu;\, 0,1)\, d\nu \qquad (4\text{-}62)$$

A similar argument to the preceding ones yields

$$\text{Prob}\left(\hat{x}\epsilon I_{L,L(N)^N} \middle| x = x_0\right) = \rho_{L,L(N)^N}(x_0) + O\left(\frac{1}{\sqrt{N}}\right) \qquad (4\text{-}63)$$

and similarly

$$\text{Prob}\left(\hat{x}\epsilon I_{R,R(N)^N} \middle| x = x_0\right) = \rho_{R,R(N)^N}(x_0) + O\left(\frac{1}{\sqrt{N}}\right) \qquad (4\text{-}64)$$

Finally

$$\rho_c{}^N(x_0) = \int_{\frac{1}{2}\left[h(x_0)+h\left(\gamma_{R(N)^N}\right)\right]-h(x_0)}^{\frac{1}{2}\left[h(x_0)+h\left(\delta_{L(N)^N}\right)\right]-h(x_0)} N(\nu;\, 0,1)\, d\nu \qquad (4\text{-}65)$$

and

$$\text{Prob}\left(\hat{x}\epsilon I_c{}^N \middle| x\epsilon x_0\right) = \int_{h\left(x_0 - \frac{1}{\sqrt{N}}\right)-h(x_0)}^{h\left(x_0 + \frac{1}{\sqrt{N}}\right)-h(x_0)} N(\nu;\, 0,1)\, d\nu \qquad (4\text{-}66)$$

Using Eq. 4-57, the corresponding expression for $\gamma_{R(N)}{}^N$ and Eq. 4-3 we find that

$$\frac{1}{2}\left[h(x_0) + h(\delta_{L(N)}{}^N)\right] = h\left(x_0 - \frac{1}{\sqrt{N}}\right) + O\left(\frac{1}{\sqrt{N}}\right) \qquad (4\text{-}67)$$

$$\frac{1}{2}\left[h(x_0) + h(\gamma_{R(N)}{}^N)\right] = h\left(x_0 + \frac{1}{\sqrt{N}}\right) + O\left(\frac{1}{\sqrt{N}}\right) \qquad (4\text{-}68)$$

and thus

$$\text{Prob}(\hat{x}\epsilon I_C{}^N | x = x_0) = \rho_C{}^N(x_0) + O\left(\frac{1}{\sqrt{N}}\right) \qquad (4\text{-}69)$$

Combining the estimates 4-35, 4-44, 4-49, 4-50, 4-54, 4-55, 4-59, 4-60, 4-63, 4-64, 4-69, and the facts that $P(N) = O\left(\frac{1}{\sqrt{N}}\right)$ and

$$E\left[(\hat{x} - x_0)^2 | x = x_0, \hat{x}\epsilon I_{L(N)}{}^N\right] = O\left(\frac{1}{N}\right) \qquad (4\text{-}70a)$$

$$E\left[(\hat{x} - x_0)^2 | x = x_0, \hat{x}\epsilon I_{R(N)}{}^N\right] = O\left(\frac{1}{N}\right) \qquad (4\text{-}70b)$$

we conclude that

$$E\left[(\hat{x} - x_0)^2 | x_0 = \alpha\right] = \hat{V}(x_0) + O\left(\frac{1}{N}\right) \qquad (4\text{-}71)$$

where $\hat{V}(x_0)$ is the approximation in Eq. 4-27.

4.4 CONCLUSION

In this section we have studied the ambiguity analysis method of approximating mean square estimation error for a simple nonlinear parameter estimation problem given by Eq. 4-1. We saw that the method outlined in subsection 4.1 converges to the true mean square error of the maximum likelihood estimator and that the error is inversely proportional to the number of regions used to subdivide the parameter space. Note that the central region R_0 for which the Cramer-Rao bound was used to estimate $E_x\{(\hat{x}_0-x)^2|\hat{x}\epsilon R_0\}$ was proportional to $(\sqrt{N^{-1}})$ in size. The remaining regions were proportional to N^{-1} in size. For large N this means that N is of the order of the number n of regions subdividing the parameter space. Thus, the approximation error $O\left(\frac{1}{N}\right)$ is also $O\left(\frac{1}{n}\right)$.

Further work is required to determine how the magnitude of the measurement noise (or equivalently, the signal-to-noise ratio) enters into the approximation error. This result will clarify how large the number of regions needs to be for a given signal-to-noise ratio. The convergence analysis also needs to be extended to the general case of vector states and measurements and to the case where a measurement process is observed. The order of the approximation error is expected to remain the same in these generalizations but a more precise idea of the size of this error would help us understand the computational feasibility of applying the ambiguity analysis method to analyze the performance of complex estimation problems.

SECTION 5

CONCLUDING REMARKS

5.1 GENERAL SUMMARY

The research described in this report has investigated methods for predicting performance in passive tracking problems. Our objective has been to develop performance prediction methods that are computationally efficient, applicable to realistic passive tracking models, and accurate. In our previous work [1] we developed a Cramer-Rao method to obtain a method that was computationally efficient and applicable to a large class of mathematical models. In Section 2 of this report we have shown that this method is easy to apply to more realistic models than the ones used in [1]. Specifically, we have used the method to study the effect of uncertain, unstable source frequency and the effect of the presence of a broadband source component on tracking accuracy.

In some nonlinear estimation problems of low signal-to-noise ratio, Cramer-Rao methods may predict performance much better than the optimal processing algorithm can actually achieve. This disadvantage of Cramer-Rao methods motivated us to investigate performance prediction methods which would be more accurate when the signal-to-noise ratio was low, but which are still efficiently computable for a large class of realistic models. Sections 3 and 4 focused on this problem.

Section 3 investigated an analytical (i.e., not requiring simulation) method based on rate distortion theory [4]. This method shows great promise because it is efficient to compute for a large class of nonlinear problems and it is better than the Cramer-Rao method when signal-to-noise ratio is low. However, the method requires further development to make it applicable to realistic dynamic problems.

Section 5 investigated a numerical method of performance prediction often described as ambiguity analysis [7],[15]. This method is essentially based on numerical computations rather than on analytical formulas. The method can give an accurate performance prediction provided sufficient computational resources are available. Our investigation studied the relationship between prediction accuracy and computational complexity for this method. Further work remains to determine the precise effect of signal-to-noise ratio on the relationship between prediction accuracy and computational complexity.

5.2 CRAMER-RAO PERFORMANCE ANALYSIS OF FREQUENCY INSTABILITY AND BROADBAND SIGNALS

The method developed in [1] was used to study two effects: the effect of an initially uncertain and randomly unstable source frequency, and the effect of a broadband component of the source frequency. The random frequency was parameterized by two variables, initial root-mean-square uncertainty and rate of variation. The rate of variation (studied for .01 to 1.0 Hz/min) appeared to have negligible effect on both position and velocity tracking error. Initial uncertainty had little effect on position tracking error, but it did have a significant effect on velocity tracking error. When the initial source frequency uncertainty reaches 1 Hz, the initial velocity

tracking error is not substantially reduced until the source passes through the sonobuoy field. This indicates that initial uncertainty concerning source frequency can make the velocity tracking performance sensitive to source-sensor geometry (i.e., good velocity tracking will depend more crucially on good geometry).

The broadband source component was modeled as a simple stationary first-order Markov process. The bandwidth of this process was fixed at 200 Hz and the ratio of broadband to narrowband power was varied from 10^{-5} to 10^{4}. Increasing this ratio increases the total source power, and the position and velocity tracking error decrease as a consequence. The decrease in tracking error is comparable to the decrease in error with increased narrowband source signal power studied in [1]. This indicates that broadband source energy is comparable in value to narrowband source energy, and that the broadband component of the source signal can be profitably exploited by an acoustic signal processing system.

Many other realistic models can be analyzed using the methods of Section 2. However, before analyzing the performance of other realistic models of passive acoustic tracking problems, we need to determine the degree of optimism inherent in the performance prediction of Section 2. Sections 3 and 4 present one approach to doing this, namely by trying to develop more accurate performance predictions with which to compare the methods of Section 2. It is also desirable to compare these performance predictions to the performance of actual algorithms. The methods of Section 2 suggest a processing algorithm architecture that might realize the performance prediction in some cases (see [1] for discussion).

5.3 RATE DISTORTION PERFORMANCE ANALYSIS

In Section 3 we showed how to compute analytically rate distortion bounds of mean square error for static nonlinear estimation problems with a Gaussian distributed state vector and additive Gaussian noise. Specifically, we obtained a lower bound of the mean square estimation error for any specified component of the state vector. We showed that the rate distortion bound is asymptotically tighter than the Cramer-Rao bound in the limit of low signal-to-noise ratio.

Based on these results we conclude that rate distortion offers a better approximation of mean square performance in the low signal-to-noise regime than the Cramer-Rao bound. Furthermore, our rate distortion bound requires little, if any, more computation than the Cramer-Rao bound for the special class of estimation problems of interest. Thus, the rate distortion bound appears to complement the Cramer-Rao method in the nonlinear, low signal-to-noise ratio cases where the latter bound is believed to give overly optimistic performance predictions.

In order to make the rate distortion bound useful for dynamic nonlinear estimation problems of tracking, we must develop our current results to simplify the computations for large dimensional state and measurement vectors and to obtain recursively computable formulas for dynamic estimation problems.

5.4 AMBIGUITY PERFORMANCE ANALYSIS

In Section 4 we analyzed the mean square parameter estimation error of the maximum likelihood method using the ambiguity analysis method. We showed that this numerical method converges to the exact mean square error as the

number of discretization regions increases, and the approximation error is inversely proportional to the number of regions used to subdivide the parameter space.

Further work is required to determine how the signal-to-noise ratio quantitatively affects the approximation error. This result would clarify how large the number of discretization regions need to be for a given signal-to-noise ratio. The convergence analysis also needs to be extended to the general case of vector states and measurements and to the case where a measurement process is observed. The order of the approximation error is expected to remain the same in these generalizations, but a more precise idea of the size of this error would help us understand the computational feasibility of applying the ambiguity analysis method to estimation problems.

REFERENCES

1. Washburn, R.B., "Unified Theory for Airborne Acoustic ASW Processing and Tracking," Technical Report TR-161, ALPHATECH, Inc., Burlington, Massachusetts, 1983.

2. Jazwinski, A.H., Stochastic Processes and Filtering Theory, Academic Press, New York, 1970.

3. Doob, J.L., Stochastic Processes, John Wiley, New York, 1953.

4. Berger, T., Rate Distortion Theory, Prentice-Hall, Englewood Cliffs, New Jersey, 1971.

5. Shannon, C.E. and W. Weaver, "A Mathematical Theory of Communication," Bell Systems Technical Journal, Volume 27, pp. 379-423, 623-656, 1948.

6. Shannon, C.E., "Coding Theorems for a Discrete Source with Fidelity Criterion," IRE National Conv. Rec., Part 4, pp. 142-163, 1959.

7. Van Trees, H.L., Detection, Estimation, and Modulation Theory, Part I, Wiley, New York, 1968.

8. Snyder, D.L., and I.B. Rhodes, "Filtering and Control Performance Bounds with Implications on Asymptotic Separation," Automatica, Volume 8, pp. 747-753, 1972.

9. Bobrovsky, B.Z. and M. Zakai, "A Lower Bound on the Estimation Error for Certain Diffusion Processes," IEEE Transactions on Information Theory, Volume IT-22, pp. 45-52, 1976.

10. Breiman, L., Probability, Addison Wesley, Reading, Massachusetts, 1968.

11. Zakai, M. and J. Ziv, "Lower and Upper Bounds on the Optimal Filtering Error of Certain Diffusion Processes," IEEE Transactions on Information Theory, Volume IT-18, pp. 325-331, May 1972.

12. Galdos, J.I., "A Lower Bound on Filtering Error with Application to Phase Demodulation," IEEE Transactions on Information Theory, Volume IT-25, pp. 452-462, July 1979.

13. Teneketzis, D., "Communication in Decentralized Control," Ph.D. Thesis, Massachusetts Institute of Technology, Cambridge, Massachusetts, September 1979.

14. Teneketzis, D., N.R. Sandell, L.C. Kramer, and M. Athans, "Information Flow in Event-Driven Large-Scale Systems," Interim Report TR-127, ALPHATECH, Inc., Burlington, Massachusetts, September 1981.

15. Van Trees, H.L., Detection, Estimation and Modulation Theory, Part III, John Wiley, New York, 1971.